Title
Negative regulation of the receptor protein tyrosine phosphatase CD45 by dimerization is mediated by an inhibitory structural wedge

Author
Majeti, Ravindra,

Publication Date
2000

Peer reviewed|Thesis/dissertation

Negative Regulation of the Receptor Protein Tyrosine Phosphatase CD45 by Dimerization is Mediated by an Inhibitory Structural Wedge

by

Ravindra Majeti

DISSERTATION

Submitted in partial satisfaction of the requirements for the degree of

DOCTOR OF PHILOSOPHY

in

Biomedical Sciences

in the

GRADUATE DIVISION

of the

UNIVERSITY OF CALIFORNIA SAN FRANCISCO

Date University Librarian

Degree Conferred: .....

To my parents Vimala and Satya, and my wife Jiangwen,

for all your love and support

PREFACE

There are many people I would like to acknowledge, but none more so than my parents, Vimala and Satya. Their constant support and efforts have made it possible for me to focus on my education without major distractions. More importantly, they have always helped me through difficult times, placing my needs ahead of their own. Personally and professionally, my parents are the only role models I ever needed. Their dedication to their education, careers, and family has always been an inspiration and motivation for me. Perhaps the most important lesson I have learned from them is the need for balance in one's life. I hope to achieve the same level of success in all areas of my life as they have in theirs.

My wife Jiangwen deserves a special acknowledgement. She has brought balance into my life by reminding me that I shouldn't be waiting for life to start; it's passing by everyday. Her love and support make it so much easier to face the long training process still ahead of me. Most importantly, she accommodates and understands my sometimes overzealous pursuit of work and training. I am truly fortunate to have her in my life.

Now at the completion of graduate school, I have a good idea of the perfect graduate advisor - he would be just like Art Weiss. My accomplishments in graduate school and development as a scientist are the direct result of mentoring by Art. He has provided an excellent environment and all the resources necessary to learn and succeed. More importantly he has invested his energy and efforts into making me a better scientist, through numerous discussions both formal and informal. His enthusiasm for science is contagious and I hope to have the same spirit at that point in my career. Art's greatest

asset is that he takes the role of mentor seriously by looking out for the interests of his students and post-docs. Art has sought out opportunities for me to present my research, interact with other scientists, and receive recognition for my work. I am truly grateful to Art for all that he has done for me.

One person who requires a special acknowledgement is Nigel Killeen. It is safe to say that this thesis project could not have been accomplished without his help. Nigel has been so giving of his time and energy, personally assisting me in the generation of the mouse and having an open door for consultation, when he was under no obligation to do anything for me. Nigel is the most giving scientist I have ever met and I am very grateful for all his help.

This acknowledgement would not be complete without mention of members of the Weiss lab. Collectively, they have generated a stimulating and fun environment to work in, but most importantly they have provided an extremely collaborative environment making it easy to learn. I would like to thank Nicolai van Oers, David Chu, and Ginny Shapiro for helping me get started in the lab by spending time to teach me basic techniques. David, in particular, requires special thanks for sharing his bench with me in the "kiddie corner". I would also like to acknowledge Nigel Killeen and Henry Bourne for serving on my thesis committee. Finally, I would like to acknowledge the wonderful research community at UCSF for generating an open environment that allowed me to easily get input from various experts on my project.

In the course of carrying out the experiments presented in this thesis, I was assisted by numerous individuals. First, Dr. Arthur Weiss served as the principal investigator supporting this work. Second, the data presented in Chapter 2 and most of the text was presented in the following publication:

Majeti, R., Bilwes, A.M., Noel, J.P., Hunter, T. and Weiss, A. (1998). Dimerization-induced inhibition of receptor protein tyrosine phosphatase function through an inhibitory wedge. Science. 279: 88-91.

The coauthors Alexandrine Bilwes, Joseph Noel, and Tony Hunter provided information prior to publication and performed the structural modeling of CD45. The data presented in Chapter 3 was mostly generated by myself with assistance from the following people: Nigel Killeen assisted in generating the "knock-in" mice, Tris Parslow and Jean Olson helped with pathological analysis of tissues, and David Daikh performed the anti-dsDNA ELISA assay. I performed the experiments presented in the Appendices.

ABSTRACT

Negative Regulation of the Receptor Protein Tyrosine Phosphatase CD45 by Dimerization is Mediated by an Inhibitory Structural Wedge

Ravindra Majeti

The receptor-like transmembrane protein tyrosine phosphatases (RPTPs) constitute a family of signaling molecules whose function and regulation are poorly characterized. CD45 is a RPTP expressed on all nucleated hematopoietic cells, where it is required for signal transduction through antigen receptors. The consequences of dimerization on CD45 function were examined with a chimeric EGFR-CD45 molecule, which restored TCR-mediated signal transduction in a CD45-deficient T cell line. Strikingly, EGF-induced dimerization of EGFR-CD45 inhibited TCR-mediated signaling, suggesting that CD45 is negatively regulated by dimerization. A potential molecular explanation for this negative regulation was provided by the crystal structure of phosphatase domain 1 of RPTPα, which forms a symmetrical dimer in which the catalytic site of one molecule is blocked by specific contacts with a structural wedge from the membrane-proximal region of the other; amino acid residues forming this wedge are conserved in RPTPs, including CD45. These observations suggest a model for the regulation of CD45, and other RPTPs, in which dimerization inhibits phosphatase activity and function, through symmetrical interactions between the catalytic site and the structural wedge. The experiments presented in this thesis were designed both to test this model and to examine the

physiological role of negative regulation of CD45 by dimerization. Here I provide functional evidence for this model by demonstrating that a glutamatic acid residue in the wedge is required for ligand-induced negative regulation of CD45 function in TCR signal transduction in vitro. One prediction from this result is that mutation of the wedge in vivo will lead to inappropriate CD45 activation under normal dimerizing conditions, with potentially pathological consequences. Here I report the phenotype of mice with an inactivating point mutation, glutamate 613 to arginine, in the wedge of CD45. CD45 E613R mice appear normal during the first few months of life; however, they subsequently develop a lymphoproliferative syndrome with apparent polyclonal T and B lymphocyte activation, and severe autoimmune nephritis with autoantibody production, leading to premature death. The dramatic phenotype of CD45 E613R mice demonstrates the in vivo importance of negative regulation of CD45 by dimerization, strongly supporting the model for regulation of CD45, and RPTPs in general.

TABLE OF CONTENTS

LIST OF FIGURES

CHAPTER 1: THE FUNCTION AND REGULATION OF THE RECEPTOR PROTEIN TYROSINE PHOSPHATASE CD45 IN T CELL RECEPTOR SIGNAL TRANSDUCTION

CHAPTER 2: A POINT MUTATION IN THE PUTATIVE INHIBITORY WEDGE OF CD45 ELIMINATES NEGATIVE REGULATION BY DIMERIZATION IN VITRO

CHAPTER 3: A POINT MUTATION IN THE PUTATIVE INHIBITORY WEDGE OF CD45 ELIMINATES NEGATIVE REGULATION BY DIMERIZATION IN VIVO

CHAPTER 1

THE FUNCTION AND REGULATION OF THE RECEPTOR PROTEIN TYROSINE PHOSPHATASE CD45 IN T CELL RECEPTOR SIGNAL TRANSDUCTION

Summary

Numerous cellular signal transduction cascades utilize protein tyrosine phosphorylation to transmit extracellular stimuli into cellular responses. Protein tyrosine phosphorylation is regulated by two families of enzymes: (1) protein tyrosine kinases, which catalyze phosphate transfer, and (2) protein tyrosine phosphatases, which catalyze phosphate hydrolysis. The phosphorylation state of a given tyrosine is determined by the balance of specific kinase and phosphatase activities. Signal transduction through the T cell receptor employs protein tyrosine phosphorylation to stimulate cellular pathways that result in T cell activation. Src-family protein tyrosine kinases are critical for initiation of T cell signal transduction, and they in turn are regulated by tyrosine phosphorylation, both positively and negatively. Thus, a complex set of phosphorylation and dephosphorylation events is essential for the proper regulation of T cell signal transduction. In this introductory chapter, I briefly review the initial events of T cell activation, discuss the regulation of src-kinases by tyrosine phosphorylation, focusing on Lck, and detail the role of the protein tyrosine phosphatase CD45 in antigen receptor signal transduction. I conclude the chapter by describing negative regulation of CD45 by dimerization and a potentially novel molecular mechanism for this regulation.

T cell receptor signal transduction: an overview

Binding of the appropriate MHC/peptide complex to the T cell antigen receptor (TCR) initiates a signal transduction cascade leading to new gene transcription, cytoskeletal reorganization, cytokine production, and proliferation, collectively referred to as T cell activation. Much is known about the intracellular events involved in transducing this external stimulus into cellular responses, especially the importance of tyrosine phosphorylation; increased protein tyrosine phosphorylation is detected within seconds following TCR stimulation (*1*).

The TCR consists of a ligand-recognition complex composed of a TCRα/TCRβ heterodimer and a signal transducing complex composed of the CD3 chains ($\alpha,\gamma,\delta,\zeta_2$). Following TCR stimulation, the CD3 chains become phosphorylated on tyrosine residues contained within immunoreceptor tyrosine-based activation motifs (ITAMs) in their cytoplasmic domains. This phosphorylation is catalyzed primarily by the tyrosine kinase Lck, found noncovalently associated with the CD4/CD8 co-receptors. Thus, during a productive TCR-MHC/peptide interaction, binding of CD4/CD8 to conserved regions of the MHC ligand recruits Lck to the TCR complex. Through a poorly understood mechanism, recruitment of Lck results in its activation and subsequent phosphorylation of the CD3 ITAMs. The ITAMs consist of a $YxxLx_{(6-8)}YxxL$ core consensus sequence; when phosphorylated on both tyrosine residues, ITAMs serve as a ligand for the tandem SH2-domains of the ZAP-70 tyrosine kinase, recruiting it to the TCR complex. Subsequent phosphorylation by Lck activates ZAP-70, which in turn phosphorylates downstream substrates propagating signals resulting in T cell activation (Figure 1).

Figure 1: Initial events upon TCR signal transduction

Binding of the appropriate MHC/peptide complex to the T cell antigen receptor initiates a signal transduction cascade leading to T cell activation. Simultaneous binding of CD4/CD8 to conserved regions of the MHC ligand recruits Lck to the TCR complex, resulting in Lck activation and subsequent phosphorylation of the CD3 ITAMs. The phosphorylated ITAMs serve as a ligand for the tandem SH2 domains of ZAP-70, recruiting it to the TCR complex. Subsequent phosphorylation by Lck activates ZAP-70, which in turn phosphorylates downstream substrates propagating signals resulting in T cell activation.

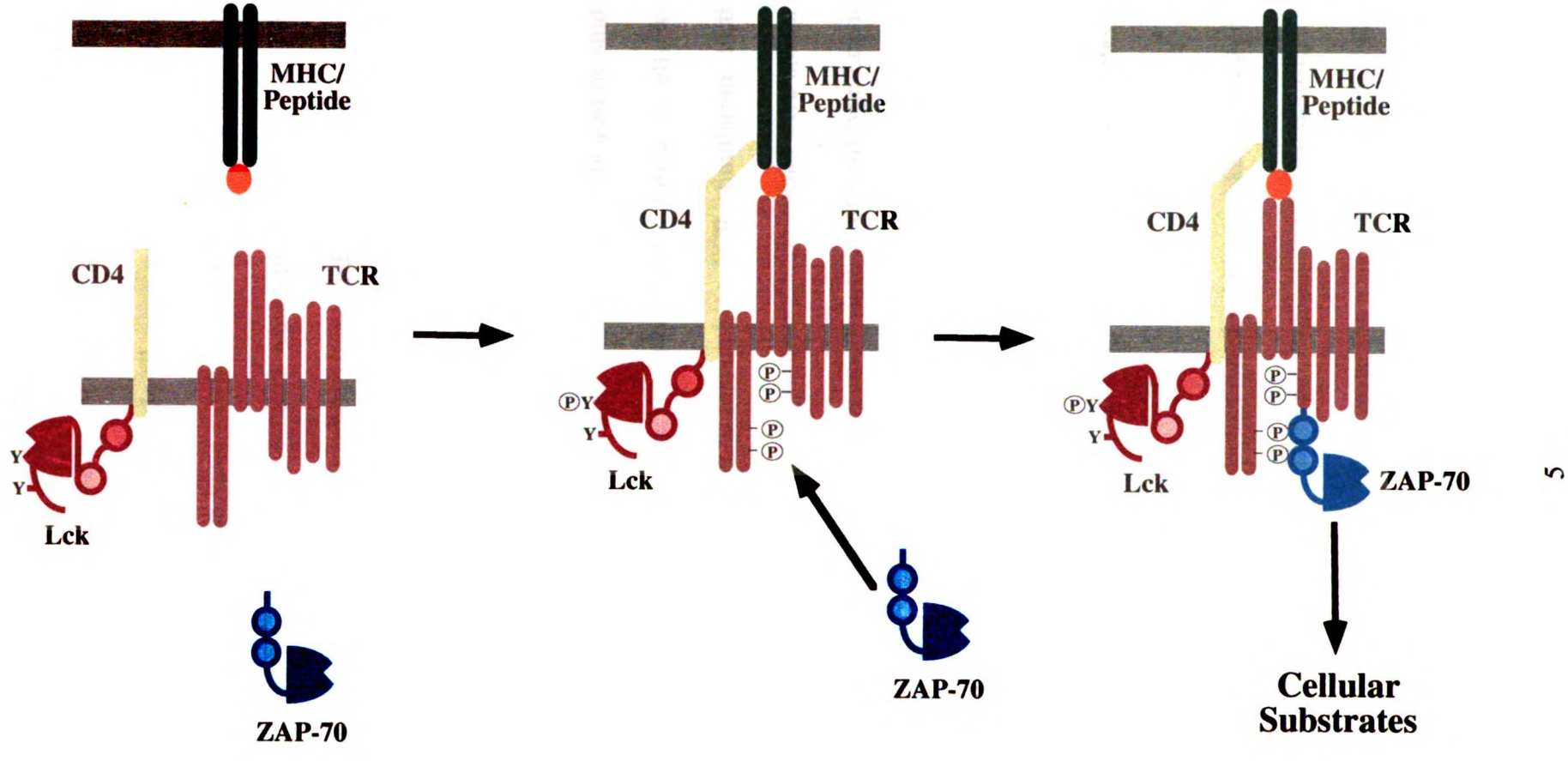
MHC/
Peptide
CD4
TCR
Y
Y
Lck
ZAP-70
MHC/
Peptide
CD4
TCR
PY
Y
Lck
P
P
P
P
ZAP-70
MHC/
Peptide
CD4
TCR
PY
Y
Lck
P
P
P
P
ZAP-70
Cellular
Substrates

ITAMs have been identified in a number of immune receptor complexes including the B cell antigen receptor (BCR), Fc antigen receptors (FcR), NK cell receptors, and several virally encoded molecules. In all cases, while the actual molecules involved may differ, signaling proceeds via a similar mechanism as in T cells: ligand binding to the receptor activates src-family kinases which phosphorylate the ITAMs resulting in the recruitment of a Syk/ZAP-70 family kinase and subsequent activation of downstream pathways.

Dynamic regulation of Lck by tyrosine phosphorylation

A critical requirement for Lck in TCR signal transduction is indicated by studies of Lck-deficient T cells and Lck-deficient mice. Lck-deficient Jurkat T cells were identified by their inability to flux calcium in response to TCR stimulation; further analysis indicated that most downstream tyrosine phosphorylation events were absent in these cells (*2,3*). These defects were corrected by reintroduction of wild type Lck into these cells, demonstrating the requirement for Lck in TCR signaling. Lck-deficient mice have a profound defect in T cell development such that only 5% of the normal number of peripheral T cells are detected (*4*). Thymocytes are arrested at the pre-TCR checkpoint, the first developmental stage requiring TCR signaling; Lck-deficient thymocytes are unable to provide this signal.

Lck is a member of the src-family of protein tyrosine kinases; like all members of this family, Lck consists of several different domains: a unique N-terminal domain, SH3 domain, SH2 domain, linker region, catalytic domain, and a C-terminal tail (*5*). These different regions serve to direct subcellular localization, mediate protein-protein

interactions, and regulate catalytic activity. Lck is itself regulated by tyrosine phosphorylation on two residues, Y394 and Y505 (*5-7*). Y394 is found within the activation loop of the kinase domain, where its phosphorylation is required for full activation. Y505 is found within the C-terminal tail; phosphorylated Y505 inactivates Lck by forming an intramolecular interaction with the SH2 domain which forces the catalytic domain into an inactive conformation. Lck in which neither site is phosphorylated is not fully active and is considered "primed" for activation by phosphorylation at Y394.

How is the phosphorylation state of Lck Y394 and Y505 controlled? In general, the opposing actions of protein tyrosine kinases (PTKs) and protein tyrosine phosphatases (PTPs) control tyrosine phosphorylation. The phosphorylation status of Y505 is dependent on the activities of the Csk (C-terminal src kinase) tyrosine kinase and the CD45 protein tyrosine phosphatase; Csk is able to phosphorylate Lck Y505, while CD45 mediates dephosphorylation of Y505 (*6,8,9*). The phosphorylation status of Y394 is also dependent on the activities of a PTK and PTP(s). However, the molecular identities are less well established than for Y505. Lck autophosphorylation may mediate phosphorylation of Y394, while a number of PTPs including CD45 and PEP may be responsible for dephosphorylating Y394.

During the course of stimulation of resting T cells and subsequent recovery, the activity of Lck is dynamically controlled by phosphorylation of Y394 and Y505 (Figure 2). In resting T cells, CD45 activity predominates over that of Csk so that most Lck is unphosphorylated and in its "primed" conformation. Upon TCR stimulation, full activation of Lck occurs through phosphorylation of Y394. The molecular details of this

Figure 2: Dynamic regulation of Lck by tyrosine phosphorylation

Lck is dynamically regulated by tyrosine phosphorylation on two residues, Y394 in the activation loop of the kinase domain, and Y505 in the C-terminal tail. Csk-mediated phosphorylation of Y505 inactivates Lck by forming an intramolecular phospho-Y505/SH2 domain interaction which forces the catalytic domain into an inactive conformation. Dephosphorylation of Y505 by CD45 allows Lck to adopt the open, 'primed" conformation, which predominates in resting T cells. Upon TCR stimulation, full activation of Lck occurs through phosphorylation of Y394. Following stimulation, Lck activity is inihibited through dephosphorylation of Y394 by PTPs and phosphorylation of Y505 by Csk.

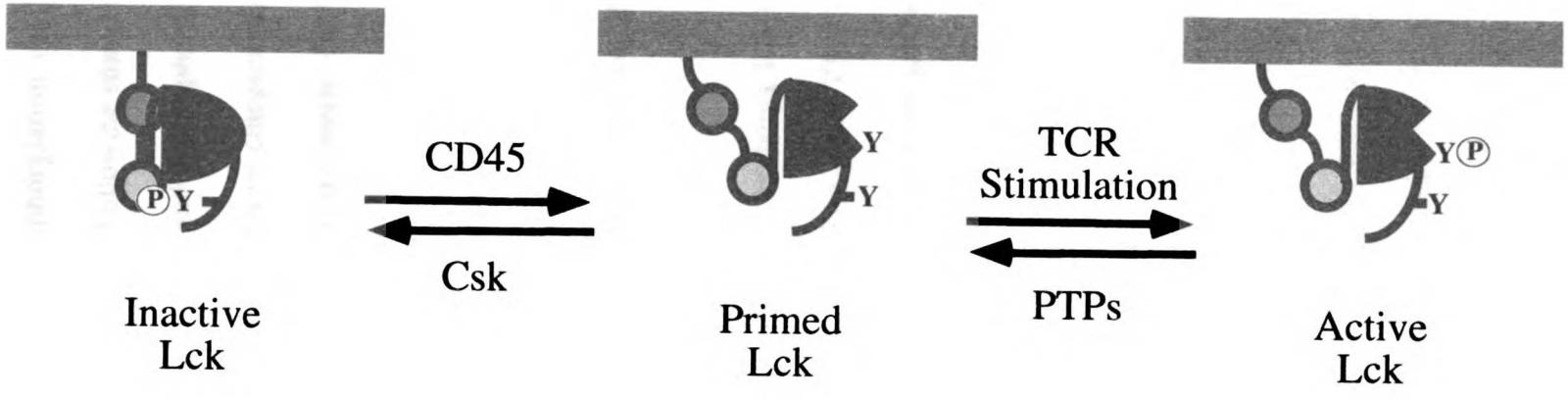
CD45
Csk
TCR
Stimulation
PTPs
Y
Y
Y
Y
P
Inactive
Lck
Primed
Lck
Active
Lck

phosphorylation are not well characterized; however, the prevailing model is that aggregation of "primed" Lck results in transphosphorylation on Y394 leading to increased activity and further Y394 phosphorylation. Following stimulation, Lck activity is inhibited through phosphorylation of Y505 by Csk and dephosphorylation of Y394 by PTPs. It has been shown that Csk exists in a constitutive complex with the PTP PEP; evidence suggests that Csk phosphorylates Lck Y505 while PEP simultaneously dephosphorylates Y394 causing rapid inhibition of Lck activity (*10*). However, additional evidence suggests that CD45 is also able to dephosphorylate Y394 (*7,11-13*). It may be that multiple PTPs dephosphorylate Y394 and act coordinately to reduce the activity of Lck. Finally, the subsequent action of CD45 on Y505 would return Lck to its unphosphorylated, "primed" state.

The importance of tyrosine phosphorylation in regulating Lck activity has been demonstrated in transgenic mice expressing Lck Y505F, in which Y505 has been mutated to phenylalanine (*14*). These mice display evidence of hyperactivated T cells and develop thymomas in a transgene dose-dependent manner; furthermore, Lck in these transgenic T cells is more heavily phosphorylated at Y394, consistent with the roles of these two sites of regulatory tyrosine phosphorylation.

The src-kinase family consists of nine members many of which are exclusively expressed in cells of the immune system (*15,16*). Like Lck, all of these molecules are regulated by tyrosine phosphorylation on two residues, one in the activation loop and one in the C-terminal tail. The consequences of phosphorylation are the same as in Lck; in fact, the original v-Src was found to be lacking the C-terminal site of tyrosine phosphorylation contributing to its oncogenicty. Csk is responsible for phosphorylation

of the C-terminal tyrosine in these kinases; however, it may not be the only kinase as several related molecules have recently been identified. CD45 dephosphorylates the C-terminal tyrosine of all src-kinases expressed in hematopoietic cells; other PTPs, such as RPTPα, may perform this function outside of the immune system.

CD45: the prototypical receptor-like protein tyrosine phosphatase

CD45 is a protein tyrosine phosphatase expressed on all nucleated hematopoietic cells, and was originally identified as a group of transmembrane proteins on the surface of white blood cells, termed leukocyte common antigen (LCA) (*6,17-20*). CD45 is a transmembrane protein consisting of a large extracellular domain, a single transmembrane domain, and a catalytic cytoplasmic domain, classifying it as a receptor-like protein tyrosine phosphatase (RPTP) (Figure 3).

CD45 is required for antigen receptor signal transduction

CD45 is required for signal transduction through receptor complexes which signal through ITAMs (TCR, BCR, FcR, and others). The requirement for CD45 has been demonstrated by studies of (1) numerous CD45-deficient T and B cell lines, (2) CD45-deficient mice, and (3) CD45-deficient humans.

CD45-deficient T cells lines have been isolated by several investigators (*21-23*). These cells are unresponsive to TCR stimulation indicated by a failure to flux calcium, increase protein tyrosine phosphorylation, and produce cytokines. Re-introduction of CD45 cDNA is able to rescue these defects indicating the critical role played by CD45 in

Figure 3: Schematic representation of CD45

CD45 is a group of transmembrane proteins expressed on all nucleated hematopoietic cells. Distinct isoforms are expressed in a cell- and activation-specific manner due to alternative splicing of exons 4, 5, and 6 in the extracellular domain. The cytoplasmic domain consists of tandemly duplicate protein tyrosine phosphatase domains, of which only the first has activity. CD45 is the prototypic member of the family of receptor-like protein tyrosine phosphatases.

CD45

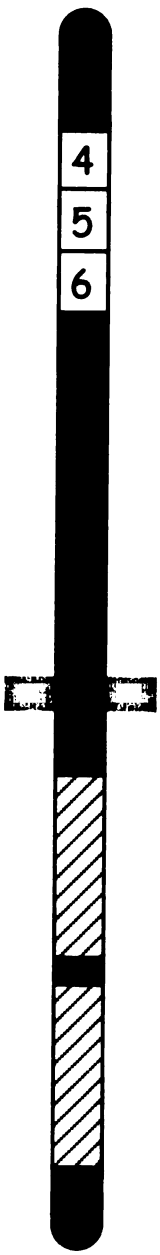

TCR signaling. Similar observations were made with CD45-deficient B cells, which are unable to flux calcium in response to BCR stimulation (*24*).

CD45-deficient mice have been generated using homologous recombination by two different investigators (*25,26*). Both independently-derived lines show a similar phenotype characterized by severe combined immunodeficiency (SCID), due to deficits in T and B cell function. Thymocyte development is partially arrested at the pre-TCR checkpoint and at the double positive to single positive transition, resulting in the production of approximately 5% of the normal number of peripheral T cells. Those T cells which do develop are unresponsive to TCR stimulation, failing to proliferate and produce cytokines, similar to the CD45-deficient T cell lines. B cells are found in these mice in normal numbers; however, their surface phenotype suggests that they are less mature than those from wild type mice. Furthermore, CD45-deficient B cells are unresponsive to BCR stimulation, again similar to the CD45-deficient B cell lines. CD45 heterozygous mice were found to be indistinguishable from wild type mice.

CD45-deficient human patients have also been identified; these patients have a SCID phenotype similar to that observed in the CD45-deficient mice, requiring medical attention as a consequence of repeated infections at a young age (*27,28*). As with the mice, heterozygous humans are unaffected.

The biochemical functions of CD45

The main function of CD45 in these pathways is to dephosphorylate the C-terminal site of negative regulatory tyrosine phosphorylation in src-kinases, maintaining them in the "primed" state (Figure 4). In vitro, CD45 is able to dephosphorylate peptides

Figure 4: CD45 positively regulates TCR signal transduction by dephosphorylating the negative regulatory tyrosine in Lck

In resting T cells, CD45 activity predominates over that of Csk to dephosphorylate the C-terminal site of negative regulatory tyrosine phosphorylation in Lck. Lck remains in its primed conformation until the TCR is stimulated, causing Lck activation. Active Lck phosphorylates the CD3 ITAMs, leading to recruitment of ZAP-70.

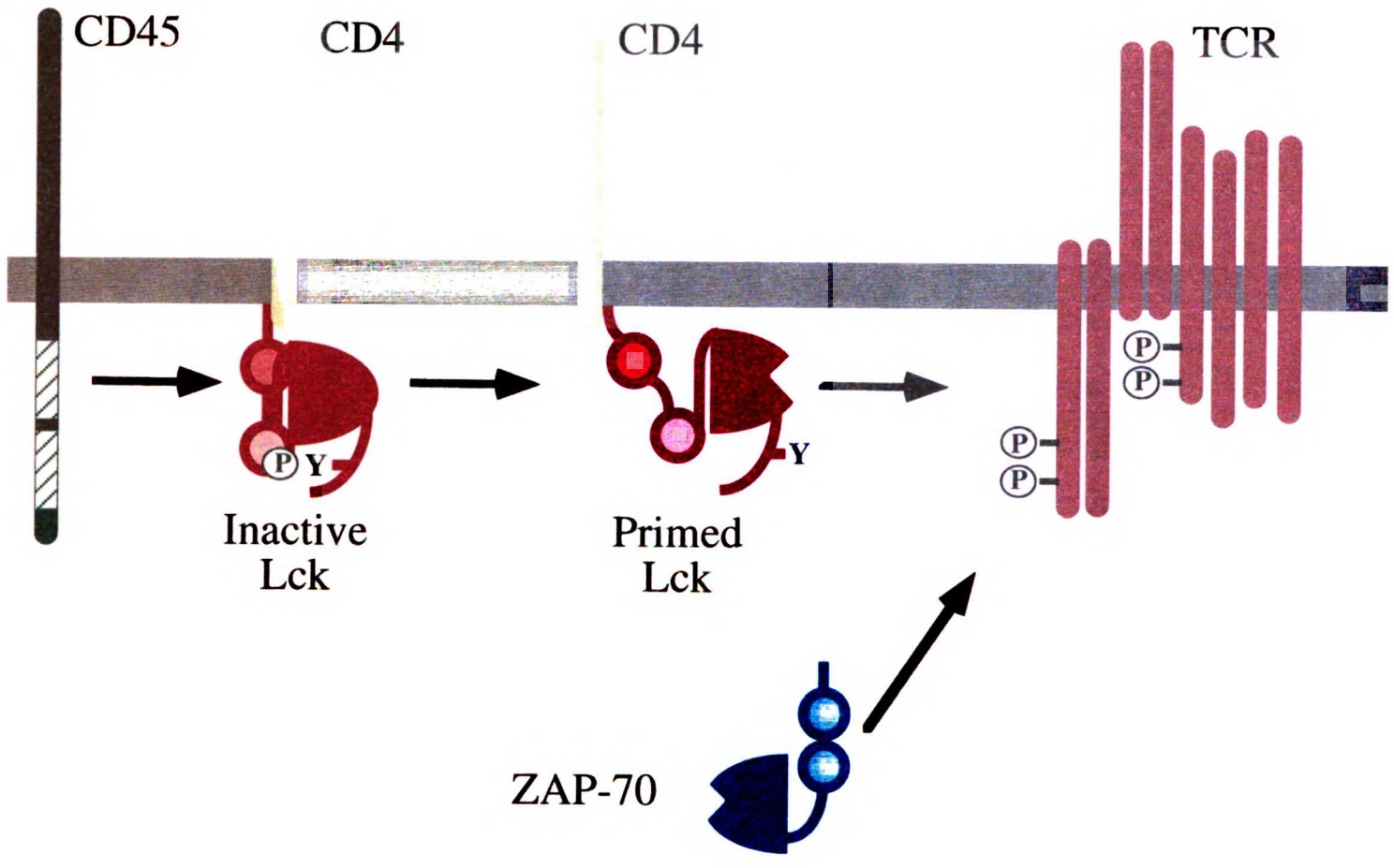
CD45
CD4
CD4
TCR
P
Y
Inactive
Lck
Primed
Lck
ZAP-70

containing the phosphorylated C-terminal tyrosines of Lck and Fyn (*29*). However, CD45, and most PTPs, lack substrate specificity in vitro; in fact, CD45 will efficiently dephosphorylate most phosphotyrosine containing substrates in vitro. More conclusive data comes from in vivo studies; Lck from CD45-deficient T cells was found to be inactive, hypophosphorylated at Y394, and hyperphosphorylated at Y505 (*29-32*). Additionally, peptide binding studies indicate that the SH2 domain of Lck is inaccessible in CD45-deficient T cells, presumably due to the intramolecular interaction with phosphorylated Y505 (*33*). Finally, the Lck Y505F transgene is able to recover T cell development in CD45-deficient mice demonstrating that the main in vivo function of CD45 is to "prime" src-kinases (*34*).

These data do not rule out other substrates and functions for CD45. Accumulating evidence suggests that CD45 is also able to dephosphorylate the activation loop tyrosine of src-kinases (Y394 in Lck) (*7,11,12*). As such, CD45 may serve to reduce src-kinase activity by returning these molecules to their "primed" conformations following receptor stimulation. That src-kinases can be activated and inactivated by the same molecule indicates that regulation of src-kinases by CD45 is more complex than originally appreciated. One recently proposed model suggests that membrane subdomains may be a critical factor in the proper regulation of src-kinases by CD45 (*13*).

Structure/function analysis of CD45

Analysis of the primary sequence of CD45 indicates that it consists of a large extracellular domain with multiple sites for glycosylation, a transmembrane domain, and a cytoplasmic domain consisting of two tandemly duplicated PTP domains (Figure 3).

The essential signaling component of CD45 was mapped to the cytoplasmic domain by independent studies in which the extracellular domain of CD45 was either removed or replaced with heterologous sequences and the subsequent chimeric molecule was able to reconstitute TCR signaling in CD45-deficient T cells (*35-37*). Thus, at least in cell lines, the extracellular domain of CD45 is dispensable for function.

The cytoplasmic domain of CD45 consists of two canonical PTP domains. All PTPs utilize the same catalytic mechanism which employs a cysteine residue for nucleophilic attack on the substrate phosphotyrosine (*38,39*). Two other residues, an aspartic acid and aginine, are also essential for catalysis. Examination of the primary sequence of CD45 indicates that these three residues are present in the membrane-proximal PTP domain (D1), but not in the C-terminal PTP domain (D2), suggesting that only D1 contributes to the phosphatase active of CD45. This is indeed the case as analysis of recombinant proteins in vitro shows that mutation of the D1 cysteine eliminates all PTP activity, while mutation of the D2 cysteine has no effect (*40,41*). Recent analysis of recombinant proteins consisting of the individual domains confirms that D1 has activity while D2 does not (*42*). In vivo, mutation of the D1 cysteine eliminated the ability of CD45 to reconstitute CD45-deficient T cells, while mutation of the D2 cysteine had no effect (*43*). Thus, the essential catalytic function of CD45 is performed by PTP D1. The function of the inactive PTP D2 is unknown, but it is believed to play a regulatory role, perhaps by facilitating substrate interactions or by mediating intramolecular interactions.

CD45 isoforms and alternative splicing

CD45 exists as multiple distinct isoforms as a result of alternative splicing of exons 4, 5, and 6 in the extracellular domain (Figure 3) (*18*). By convention, inclusion of exon 4 is denoted by RA, exon 5 by RB, and exon 6 by RC; the isoform lacking all 3 is denoted R0. These isoforms are expressed in a cell- and activation-specific manner. B cells express only the RABC isoform, containing all 3 exons; T cells express RA^+ isoforms prior to stimulation and subsequently switch to expression of CD45R0. The alternatively spliced exons encode multiple sites of O-linked glycosylation so that the extracellular domain of $CD45RA^+$ isoforms differs in structure and overall charge from CD45R0 (*44*).

Numerous experiments have investigated functional differences between different CD45 isoforms. Phosphatase activity was compared using immunoprecipitated proteins and found to be similar between the different isoforms. Both RABC and R0 are able to reconstitute CD45-deficient T cells with no major differences observed between the two; however, one group observed some differences when using a peptide-specific CD45-deficient T cell clone (*45*). This group went on to demonstrate that different isoforms of CD45 may differentially interact with the TCR itself, accounting for some of the functional differences (*46*). In vivo transgenic experiments to re-express individual CD45 isoforms in CD45-deficient mice have been uninformative as expression levels have not approached those of wild type CD45 (*47*). Collectively, there is little data supporting major differences in function between the different CD45 isoforms.

Negative regulation of CD45 by dimerization

Dimerization is an important regulatory mechanism for many signal transduction molecules, in particular transmembrane receptor proteins (*48,49*). Extensive studies have established that ligand-induced dimerization (or oligomerization) is critical for the activation of receptor tyrosine kinases, antigen receptors, cytokine receptors, TGF-β family receptors, and others. In most cases, dimerization activates receptor kinase activity, either endogenous or associated, by trans-autophosphorylation.

The RPTPs constitute another family of transmembrane proteins involved in signal transduction pathways; however, the mechanism(s) involved in regulating RPTP activity and function are unknown (*50,51*). These molecules often possess extracellular motifs common to receptor proteins, but in most cases ligands have not been identified (Figure 5). In general, the physiological roles and biochemical substrates of most RPTPs are poorly characterized.

CD45 is one RPTP for whom its physiological roles and biochemical functions are well characterized; however, the manner in which CD45 is regulated (if at all) is not known, nor has any ligand been identified for CD45. One early strategy to explore this issue involved examining the functional consequences of treating T cells with anti-CD45 antibodies; some antibodies enhanced T cell signaling, while others were inhibitory (*52-54*). While not conclusive, these studies suggest that CD45 may be regulated by dimerization (or aggregation). Subsequent studies of T cell lines biochemically identified homodimeric forms of CD45 through chemical crosslinking and sucrose gradient centrifugation (*55*); however, the manner in which dimer formation is regulated was not determined. Attempts by numerous investigators have failed to definitively identify any ligand for CD45, although it does appear that CD45 makes an adhesive interaction with

Figure 5: Schematic representation of members of the receptor-like protein tyrosine phosphatase family

RPTPs constitute a large family of transmembrane proteins involved in diverse signal transduction pathways. These molecules possess different extracellular motifs including fibronectin type III repeats, immunoglobulin-like domains, and cysteine rich motifs found in other receptors. The cytoplasmic domains usually consist of tandemly duplicated phosphatase domains (red) of which only the first one is active. The region of RPTPα used for crystallization is highlighted in orange (see below).

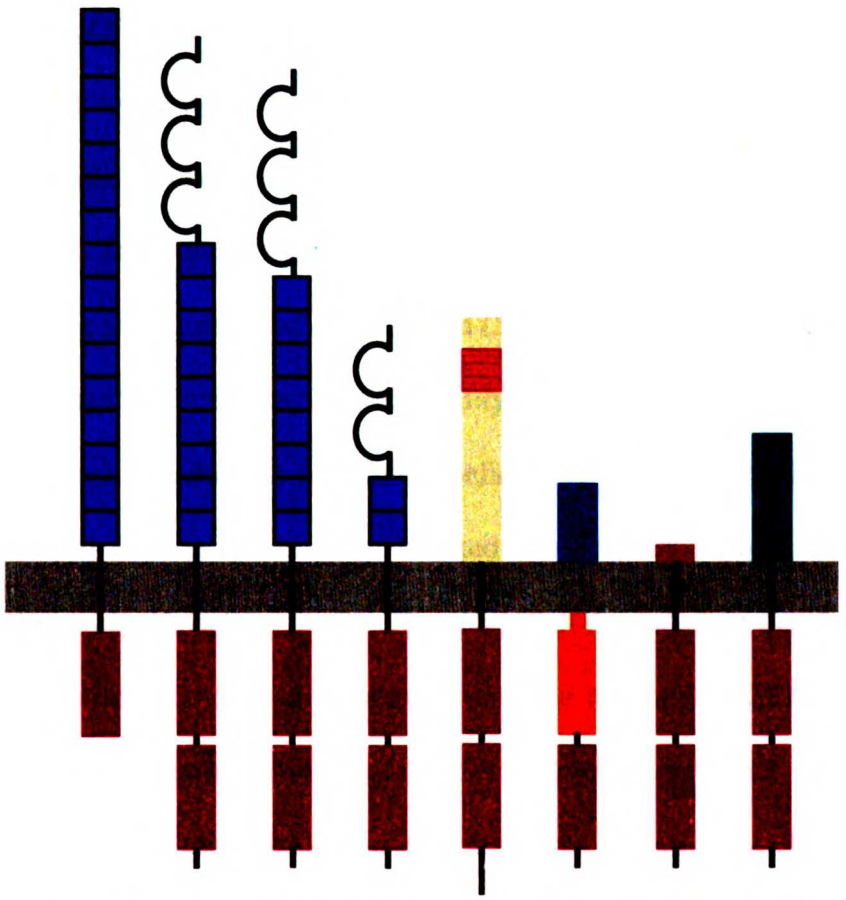

CD22 (*18*). Collectively, these data suggest that CD45 may form dimers in vivo, with functional consequences for signal transduction.

The consequences of dimerization on CD45 function were examined with a chimeric molecule consisting of the extracellular and transmembrane domains of the EGF receptor fused to the cytoplasmic domain of CD45 (EGFR-CD45) (*36*). The EGFR is a receptor tyrosine kinase activated by EGF, its soluble dimerizing ligand; evidence indicates that only the extracellular and transmembrane domains of the EGFR are required for ligand binding and dimerization (*56-58*). Thus, soluble EGF should dimerize the EGFR-CD45 chimeric molecule. Stably transfected EGFR-CD45 restored TCR-mediated signal transduction in a CD45-deficient T cell line. Strikingly, treatment of these cells with EGF inhibited TCR-mediated signal transduction, both calcium flux and inducible tyrosine phosphorylation. This inhibition depended on the dimerization of the CD45 cytoplasmic domain as co-expression of a truncated EGFR, consisting of the extracellular and transmembrane domains alone, reversed the effect. Thus, in contrast to the activating role of dimerization for other receptors, ligand-induced dimerization seems to negatively regulate CD45 function in TCR signal transduction (Figure 6).

Analysis of TCR-induced protein tyrosine phosphorylation in cells inhibited by EGF revealed reduced phosphorylation of the CD3 zeta chain and ZAP-70, indicating a very proximal block in the TCR signal transduction cascade; furthermore, as these molecules are substrates of Lck, their reduced phosphorylation suggests that Lck activity is inhibited. These data are consistent with dimerization-mediated inhibition of CD45 activity, or at least accessibility to its substrate Lck Y505.

Figure 6: An EGFR-CD45 chimera is negatively regulated by ligand-induced dimerization

A chimeric molecule composed of the extracellular and transmembrane domains of the EGFR fused to the cytoplasmic domain of CD45 is able to reconstitute TCR signal transduction in a CD45-deficient T cell line (left). Dimerization of the chimeric molecule with the soluble ligand EGF, inhibits TCR signal transduction, most likely through inhibition of CD45 (right).

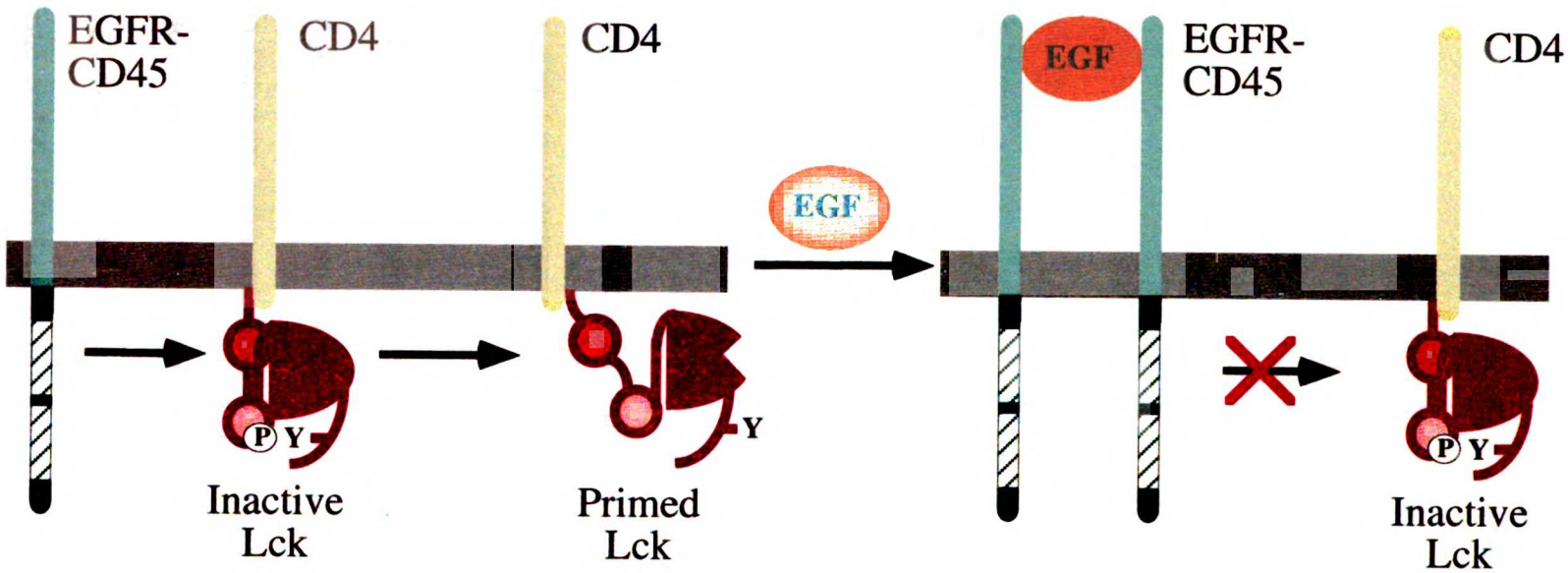
EGFR-
CD45
CD4
CD4
EGF
EGF
EGFR-
CD45
CD4
P
Y
Y
P
Y
Inactive
Lck
Primed
Lck
Inactive
Lck

What is the mechanism for dimerization-mediated negative regulation of CD45? Several possibilities exist, including: (1) inactivating trans-dephosphorylation, although there is little evidence that CD45 is itself tyrosine phosphorylated, (2) internalization of CD45 sequestering it from Lck, although reduced surface expression of EGFR-CD45 was not detected after addition of EGF, (3) non-specific steric hindrance caused by bringing two large CD45 cytoplasmic domains together, preventing access of the catalytic site to Lck Y505, (4) a specific inhibitory interaction mediated across the dimer interface to reduce CD45 catalytic activity, and others.

A potential molecular mechanism for dimerization-mediated negative regulation of CD45 was provided by the crystal structure of the membrane-proximal region and PTP domain 1 of RPTPα, another member of the RPTP family (*59*). In two different crystal packing space groups, this protein fragment formed a symmetrical dimer in which the catalytic site of one molecule is blocked by specific contacts with a structural wedge from the membrane-proximal region of the other (Figure 7). Not only was the active site sterically occluded, but an aspartic acid in the tip of the wedge was observed to make a hydrogen bonding contact with the "mobile loop" of the catalytic site, constraining it away from the active site (Figure 8). PTP catalysis requires this loop to fold into the active site upon substrate binding (*39*). Thus, the wedge interaction with the mobile loop would generate an inactive PTP.

Amino acid residues forming the wedge, including acidic residues at the tip, are conserved within the membrane-proximal regions of RPTPs, including CD45, suggesting a conserved structure and function (Figure 9) (*59*). Moreover, sequences within this region of CD45 are conserved phylogenetically from shark to human, also implying an

Figure 7: The membrane proximal region and phosphatase domain 1 of RPTPα crystallizes as a dimer

RPTPα is another member of the receptor-like protein tyrosine phosphatase family. This crystal structure demonstrates the formation of a symmetrical dimer in which the phosphatase domain 1 catalytic site of one molecule is blocked by specific contacts with a structural wedge from the membrane-proximal region of the other. Note the wedge of the blue molecule occupying the active site of the red molecule, whose active site cysteine is indicated in blue.

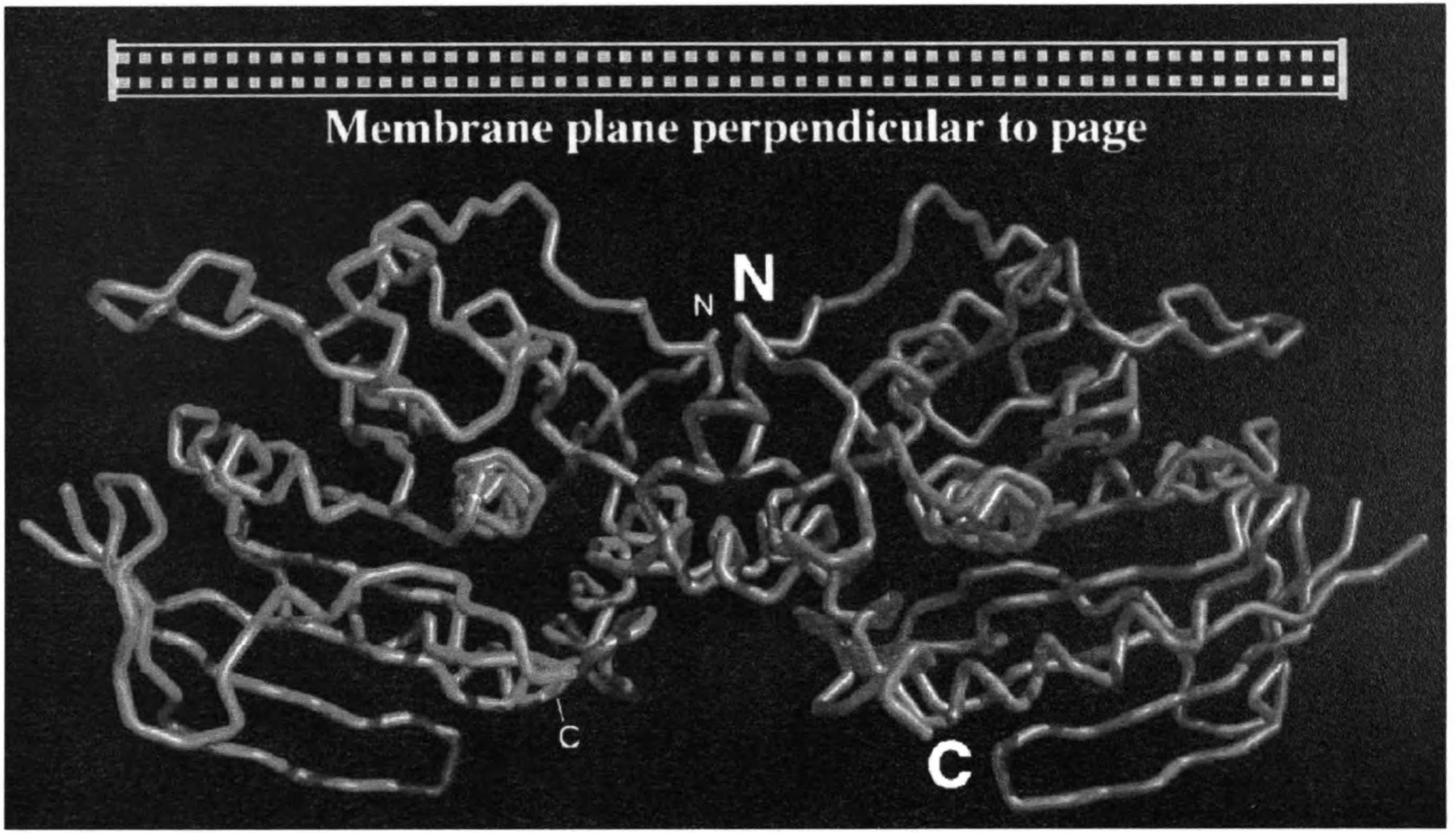

From Bilwes et al., Nature 382: 555 (1996)

Figure 8: Detailed view of the interaction between the structural wedge and the catalytic site in the RPTPα crystal

Hydrogen bonding interactions are detected between multiple residues in the wedge (yellow) and the opposing catalytic site (blue). Aspartic acid 228 is observed to form a hydrogen bond with the "mobile loop" of the catalytic site; this interaction constrains the loop away from the active site. As PTP catalysis requires this loop to fold into the active site upon substrate binding, this interaction would generate an inactive PTP enzyme.

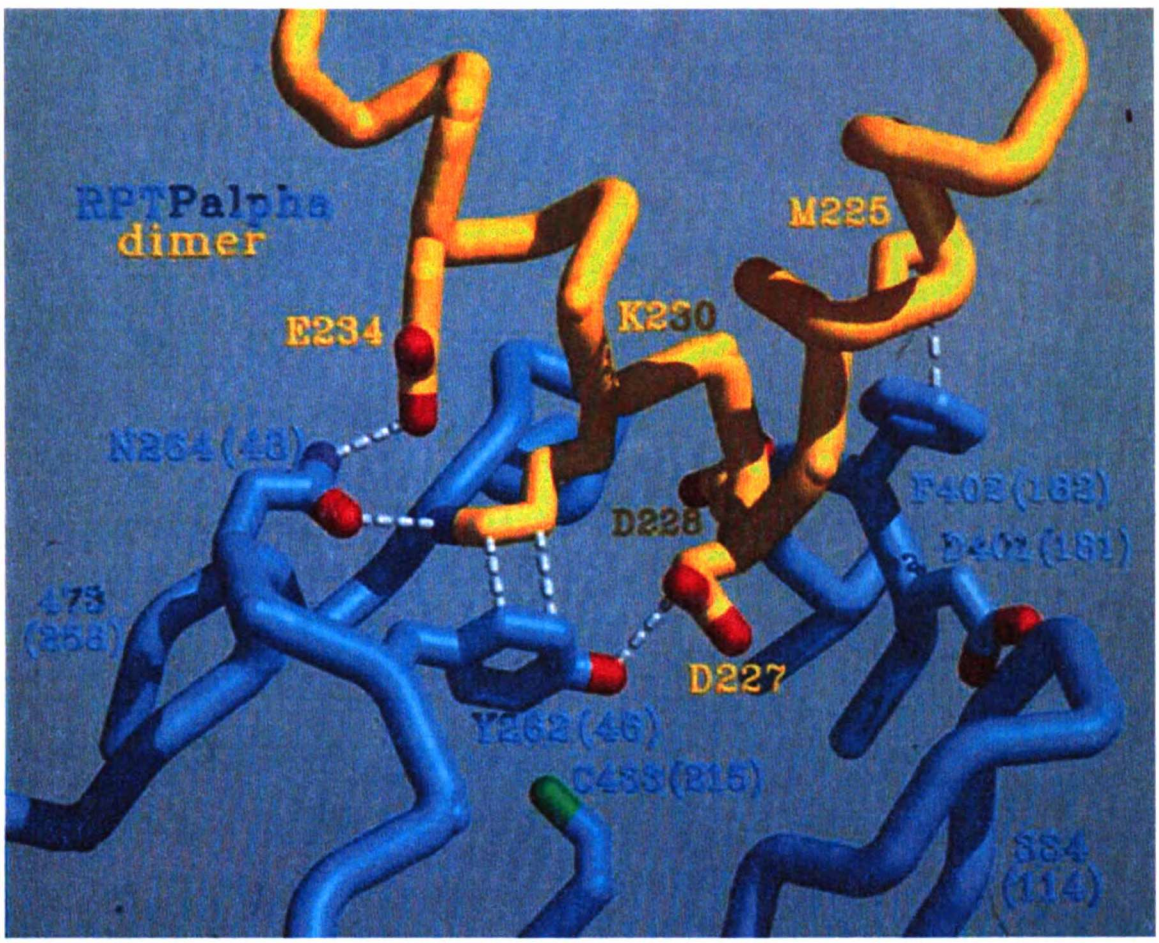

From Bilwes et al., Nature 382: 555 (1996)

Figure 9: Sequence conservation of the inhibitory wedge in the membrane-proximal region of RPTPs

Database screening with a consensus sequence for the structural wedge identified all RPTP domain 1 sequences, and no RPTP domain 2 or non-receptor PTP sequences. Identical residues are highlighted; the sequence of human CD45 is outlined in red. The high degree of conservation suggests a conserved structure and function. Note the conservation of acidic residues at the tip of the wedge, particularly in CD45, aspartate 623 and glutamate 624.

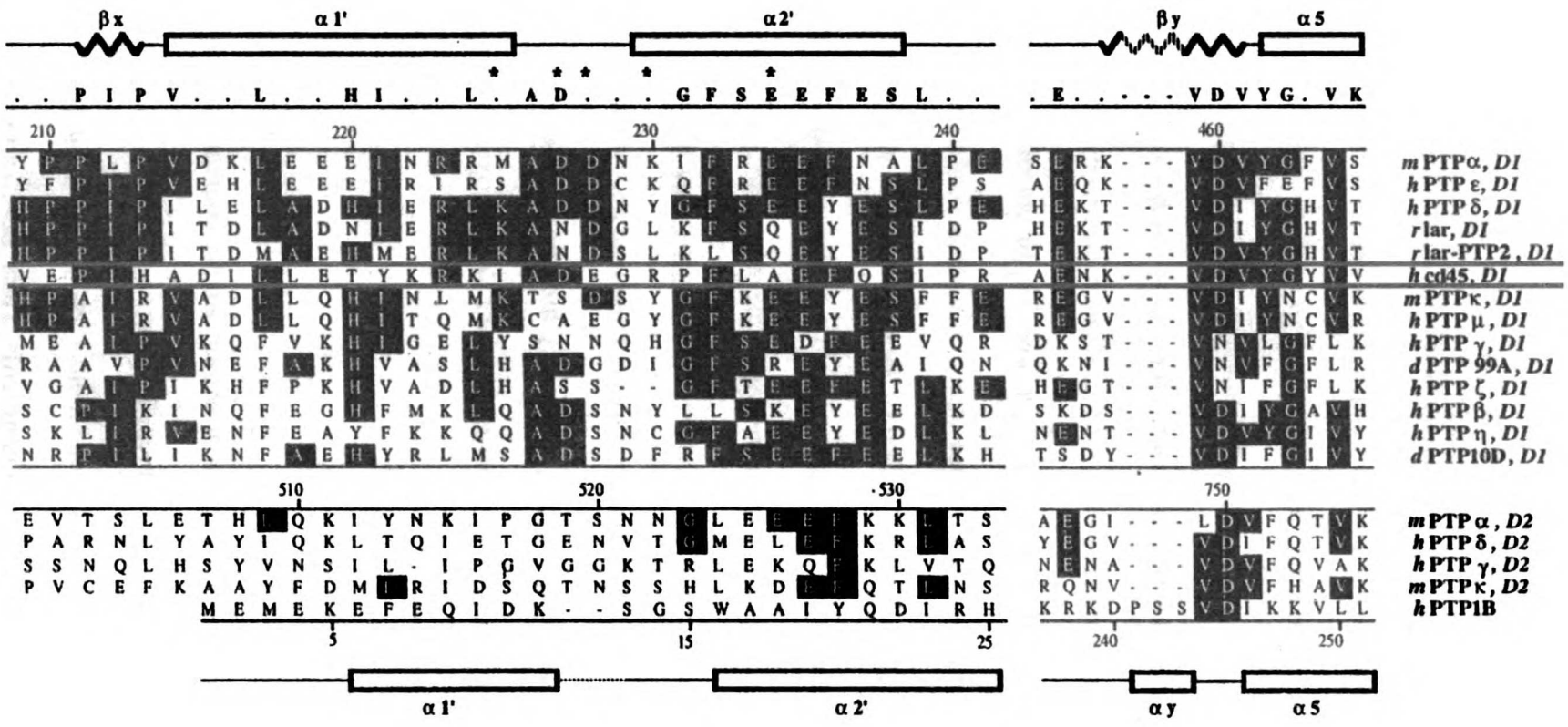

From Bilwes et al., Nature 382: 555 (1996)

important conserved structure and function (Figure 10). These observations suggest a model for the regulation of CD45, and by homology other RPTPs, in which dimerization inhibits phosphatase activity, and consequently function, through symmetrical interactions between the catalytic site and the structural wedge containing the acidic residues (Figure 11).

General organization of the thesis

Negative regulation of the EGFR-CD45 chimeric molecule by dimerization in T cells provides a system to test this model. In Chapter 2, I provide functional evidence supporting the model by demonstrating that mutation of glutamate 624 in the inhibitory wedge of human CD45 eliminates negative regulation of EGFR-CD45 in T cell signal transduction. This result directly predicts that mutation of the homologous residue in the murine genome will generate mice expressing CD45 no longer subject to negative regulation by dimerization, with potentially pathological outcomes. In Chapter 3, I present the phenotype of such "knock-in" mice which develop a lymphoproliferative syndrome and autoimmune nephritis similar to that observed in human patients with systemic lupus erythematosis. This phenotype further supports the model and illustrates the in vivo significance of this regulation for CD45. In Chapter 4, I discuss these results with a particular emphasis on a model for the regulation of CD45 by dimerization during T cell activation. I also discuss the regulation of other RPTPs with an emphasis on recent experiments analyzing the role of the wedge. Finally, I conclude with a discussion of future directions based on this work. The Appendices include experiments designed to

Figure 10: Phylogenetic comparison of the primary sequence of the inhibitory wedge of CD45

Alignment of the primary sequences of CD45 from mouse, rat, human, chicken, and shark indicates strong sequence conservation in the membrane-proximal region of the cytoplasmic domain encoding the wedge (red box). Note in particular, the conservation of glutamate 624 (human) in all species (*). The sequences of murine RPTPα and PTP1B are also indicated for comparison.

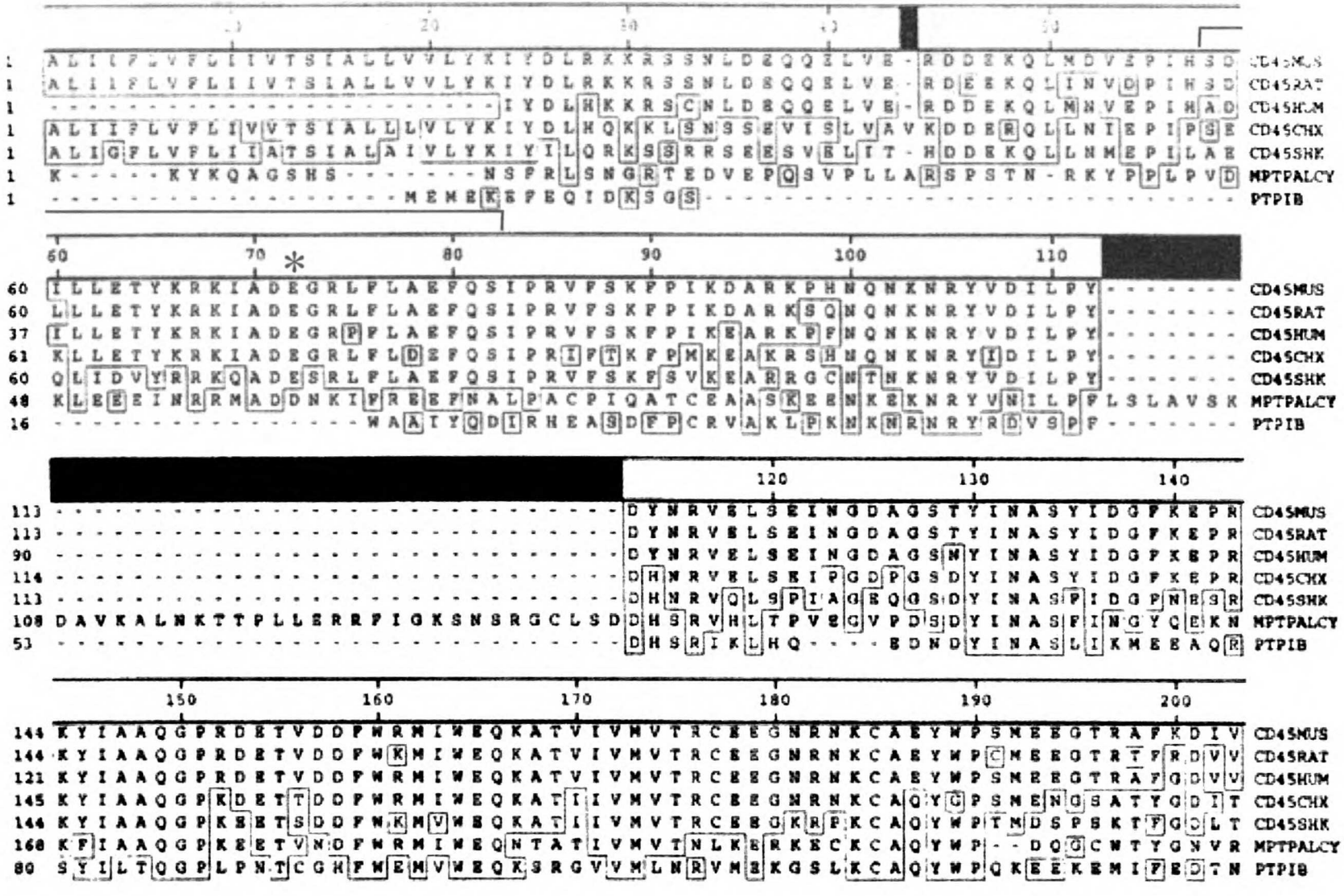
CD45MUS
CD45RAT
CD45HUM
CD45CHX
CD45SHK
MPTPALCY
PTPIB

Figure 11: Model for negative regulation of CD45 by the inhibitory wedge

In the monomeric state, CD45 is active and "primes" Lck by dephosphorylating Y505. Dimerization of CD45, by a ligand or through other means, inactivates CD45 though the symmetrical interactions between the catalytic site of phosphatase domain 1 and the inhibitory structural wedge. Csk activity predominates in phosphorylating Lck Y505, placing it in its inactive conformation and inhibiting T cell signal transduction.

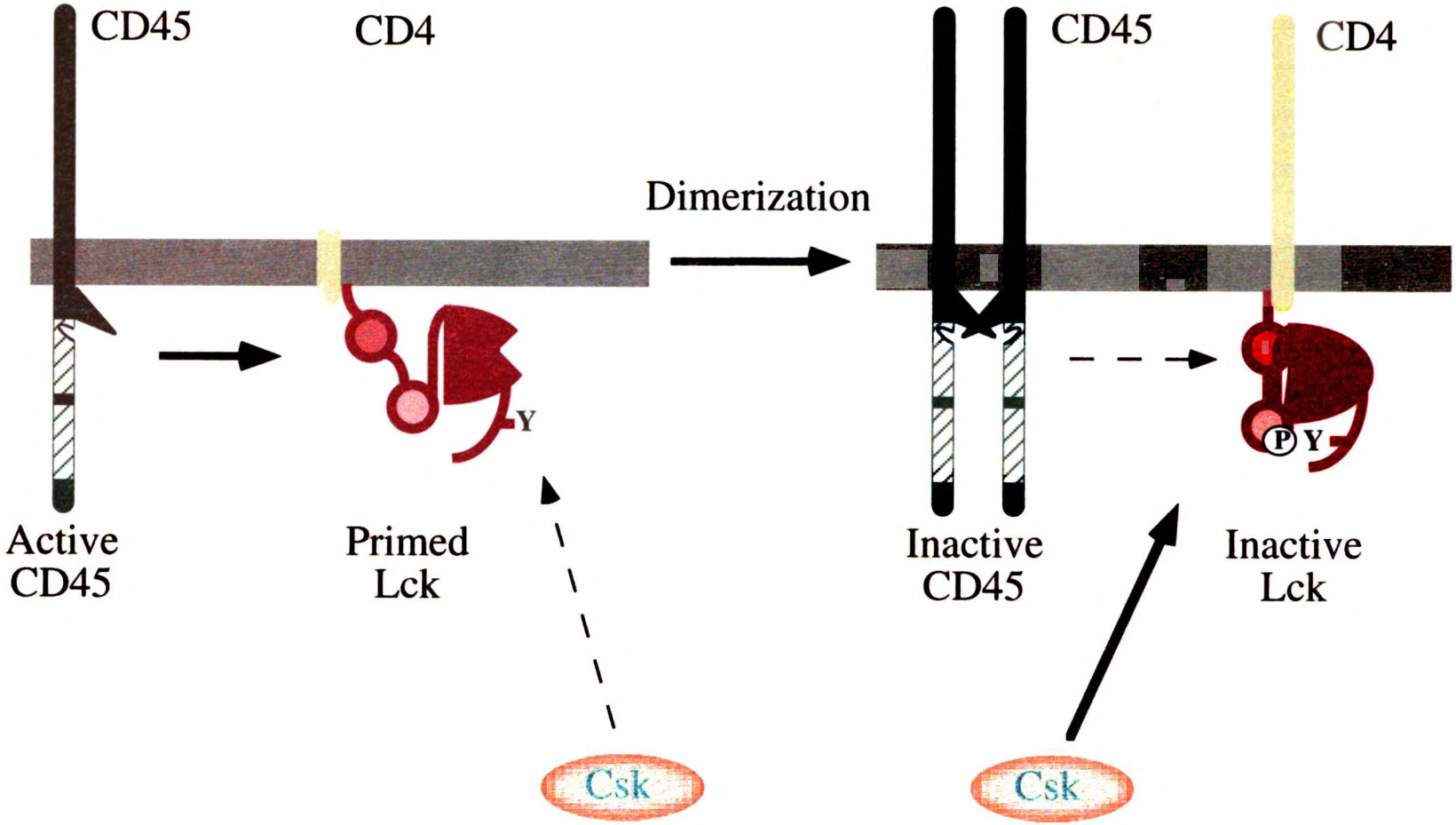
CD45
CD4
Dimerization
CD45
CD4
Y
P
Y
Active
CD45
Primed
Lck
Inactive
CD45
Inactive
Lck
Csk
Csk

examine inhibition of CD45 phosphatase activity by dimerization both in vitro using purified recombinant proteins and in transfection assays.

CHAPTER 2

A POINT MUTATION IN THE PUTATIVE INHIBITORY WEDGE OF CD45 ELIMINATES NEGATIVE REGULATION BY DIMERIZATION IN VITRO

Summary

The receptor-like transmembrane protein tyrosine phosphatases (RPTPs) constitute a family of signaling molecules whose function and regulation are poorly characterized. In T cells, the RPTP CD45 is required for signal transduction through the T cell receptor. Previously, we demonstrated that a chimeric EGFR-CD45 molecule could reconstitute a CD45-deficient T cell line; furthermore, treatment of these cells with EGF blocked TCR-mediated signaling, suggesting that CD45 is negatively regulated by ligand-induced dimerization. A possible molecular explanation for this negative regulation comes from the crystal structure of the membrane-proximal region and phosphatase domain 1 of RPTPα, another RPTP family member, which forms a symmetrical dimer such that the catalytic site of one molecule is blocked by specific contacts with a structural wedge from the other. Notably, sequences comprising this putative inhibitory wedge, including two acidic residues found near the tip, are conserved within CD45 and other RPTPs, implying a general model for the regulation of RPTPs. Here we provide functional evidence for this model by demonstrating that one of these acidic residues, glutamate 624 of CD45, is required for ligand-induced negative regulation of EGFR-CD45 function in TCR signal transduction.

Introduction

The RPTPs constitute a family of signaling molecules whose function and regulation are not well understood (*50,60*). In T cells, the RPTP CD45 is required for T cell development (*25,26*) and T cell receptor (TCR) signal transduction (*18,21,22*), presumably by dephosphorylating the negative regulatory COOH-terminal tyrosine in the Src-family kinase Lck (*30,32,33,61*). A chimeric EGFR-CD45 molecule restores TCR-mediated signal transduction in a CD45-deficient T cell line; furthermore, treatment of these cells with EGF blocks TCR-mediated signaling, suggesting that CD45 is negatively regulated by ligand-induced dimerization (*36*). A possible explanation for this negative regulation comes from the crystal structure of the membrane-proximal phosphatase domain of the RPTP, RPTPα, which revealed a putative inhibitory wedge in symmetrical dimers (*59*). Sequences comprising this putative inhibitory wedge, including two acidic residues found near the tip, are conserved in CD45 and other RPTPs (*59*). Thus, ligand induced-dimerization may result in inhibition of phosphatase activity, and consequently signaling function, through specific interactions between the catalytic site and the wedge containing the acidic residues.

Results

The sequence homology in the membrane-proximal region encoding the structural wedge of RPTPα and the corresponding region of CD45 suggests that CD45 may also form a structural wedge that can make an inhibitory dimeric interaction with the catalytic site of phosphatase domain 1 (*59*). To examine this possibility, the structure of a potential wedge/domain 1 interaction in CD45 was modeled based on the crystal structure of RPTPα (Figure 1). This analysis indicates that it is energetically possible for CD45 to form a structural wedge, and for this wedge to occlude the catalytic site of PTP domain 1 similar to RPTPα. Significantly, glutamic acid 624 in human CD45 is observed to form a hydrogen bond with the "mobile loop" of the catalytic site, analagous to aspartic acid 228 of RPTPα, constraining the loop away from the catalytic pocket. Thus, this interaction would generate an inactive PTP domain 1 of CD45.

To test this model, we stably reconstituted a CD45-deficient T cell line, H45.01 (*22*), with EGFR-CD45 chimeric molecules in which glutamate 624, analogous to aspartate 228 in the RPTPα wedge (*59*), was mutated to alanine or arginine. Subsequently, we assessed the ability of EGF to negatively regulate TCR signal transduction in these cells. Stable reconstitution of this CD45-deficient cell line with the wild-type EGFR-CD45 chimera restored normal TCR-mediated signal transduction (Figure 2) (*36*). Wild-type and mutant reconstituted cell lines expressed comparable amounts of the EGFR-CD45 chimera and comparable amounts of the TCR/CD3 complex as determined by flow cytometry (Figure 2A). Mutation of glutamate 624 appeared not to result in a global defect in the function of CD45 because in H45.01 cells reconstituted

Figure 1: Structural model of the potential wedge/domain 1 interaction in CD45

The structure of a potential wedge/domain 1 interaction in CD45 was modeled based on the crystal structure of RPTPα. CD45 can form a structural wedge, and in dimeric forms of CD45 this wedge can occlude the catalytic site of PTP domain 1 similar to RPTPα. Note that glutamic acid 624 in human CD45 is observed to form a hydrogen bond with the "mobile loop" of the catalytic site constraining the loop away from the catalytic pocket. This interaction would generate an inactive PTP domain 1 of CD45.

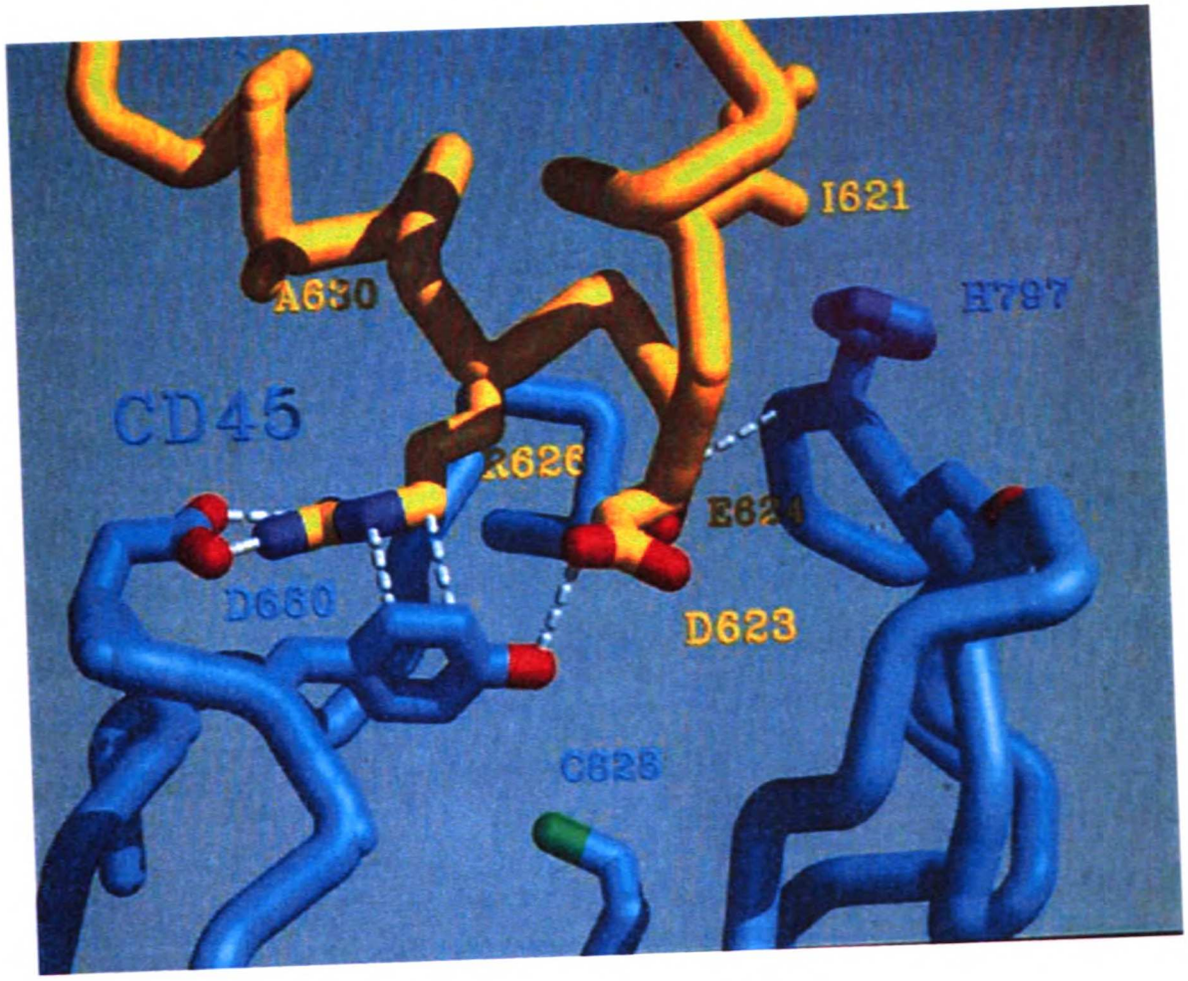

Figure 2: Reconstitution of CD45-deficient T cells with wild-type or E624-mutant EGFR-CD45 chimeric molecules

(A) Cell surface expression of the EGFR-CD45 chimera, CD45, and the TCR on cell lines as determined by immunofluorescence and flow cytometry. Cells were stained with a control Ab (solid line), anti-EGFR (bold line), anti-CD45 (dotted line), and anti-TCR/CD3 (dashed line).

(B) TCR-mediated calcium mobilization. CD45-deficient cells (panel 1) stably reconstituted with EGFR-CD45 wild-type (panel 2), EGFR-CD45/E624A (panel 3), or EGFR-CD45/E624R (panel 4) chimeric molecules were treated at the indicated times with antibody to the TCR (anti-TCR). Similar results were obtained with multiple independently isolated stable clones expressing the E624A or E624R mutant chimeras (data not shown). CD45-deficient cells responded to ionomycin with detectable calcium mobilization (data not shown).

(C and D) Restoration of TCR-mediated ZAP-70 phosphorylation and MAPK phosphorylation. Wild-type CD45-expressing cells (lanes 1 and 2), CD45-deficient cells (lanes 3 and 4), EGFR-CD45 wild-type (lanes 5 and 6), EGFR-CD45/E624R (lanes 7 and 8), and EGFR-CD45/E624A (lanes 9 and 10) reconstituted cells were stimulated 2 min with antibody to the TCR. **(C)** ZAP-70 tyrosine phosphorylation was assessed by immunoprecipitation and immunoblotting with antibody to phosphotyrosine (top panel); the same blot was stripped and reprobed with antibody to ZAP-70 (bottom panel). **(D)** MAPK phosphorylation was assessed by blotting a portion of the whole cell lysate with antibody specific for phosphorylated MAPK (top panel); the same blot was stripped and reprobed with antibody to MAPK (bottom panel). ERK1 (top) and ERK2 (bottom) are detected. Similar results were obtained with multiple independently isolated stable clones (data not shown).

A

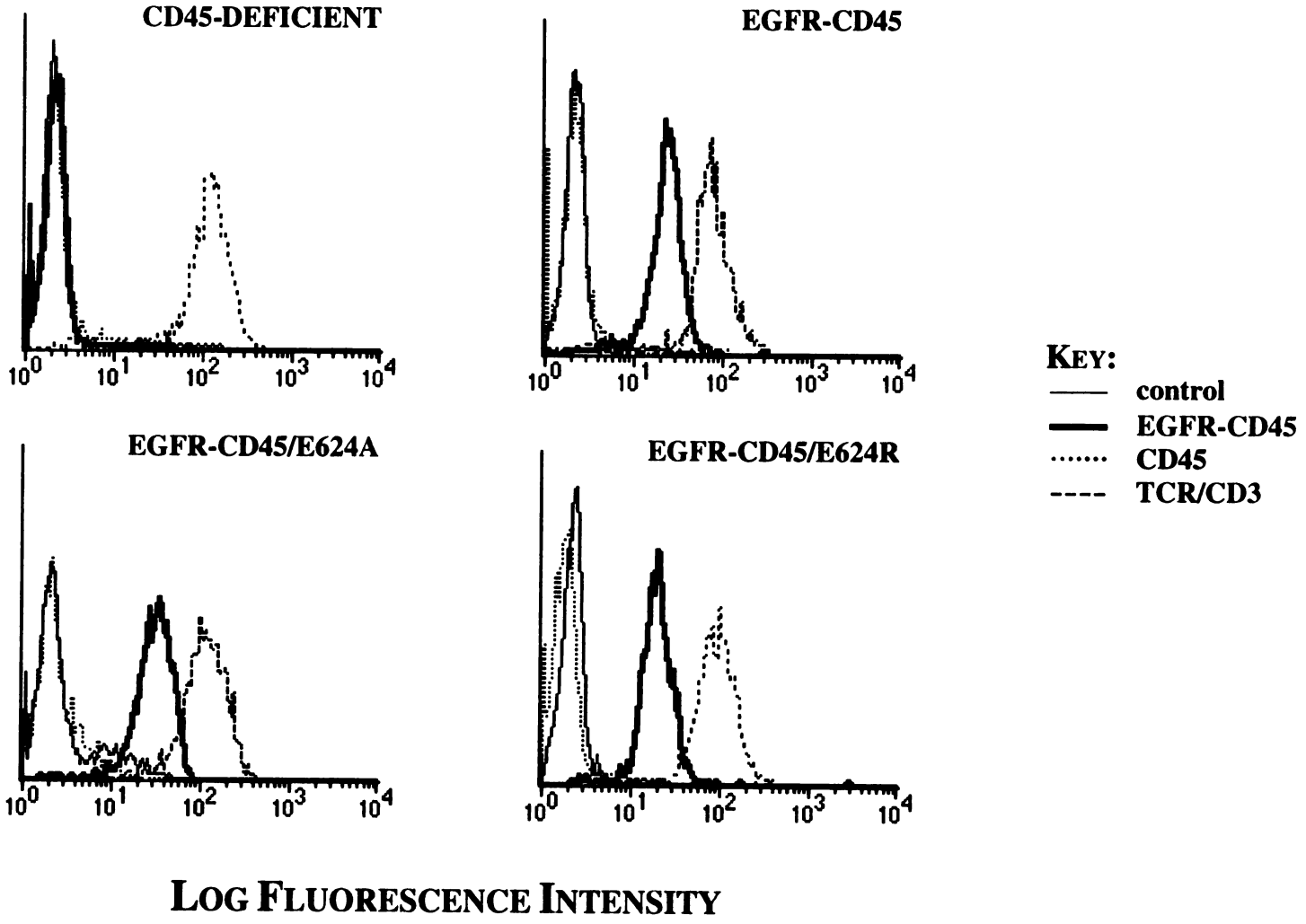
CD45-DEFICIENT
EGFR-CD45
EGFR-CD45/E624A
EGFR-CD45/E624R
10^0 10^1 10^2 10^3 10^4
RELATIVE CELL NUMBER
LOG FLUORESCENCE INTENSITY
KEY:
control
EGFR-CD45
CD45
TCR/CD3

B

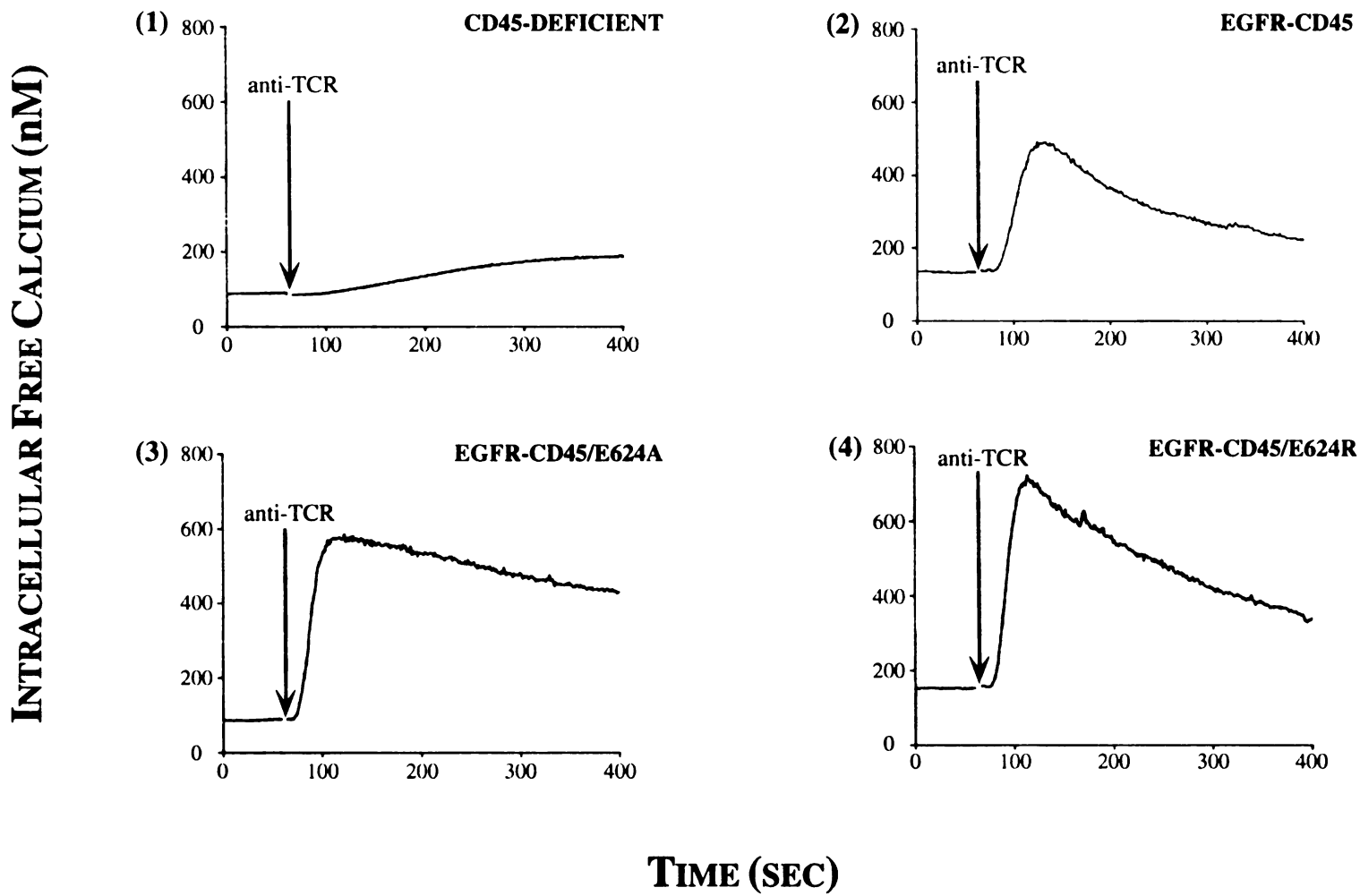
(1) CD45-DEFICIENT
(2) EGFR-CD45
(3) EGFR-CD45/E624A
(4) EGFR-CD45/E624R
anti-TCR
800
600
400
200
0
0
100
200
300
400
INTRACELLULAR FREE CALCIUM (nM)
TIME (SEC)

C

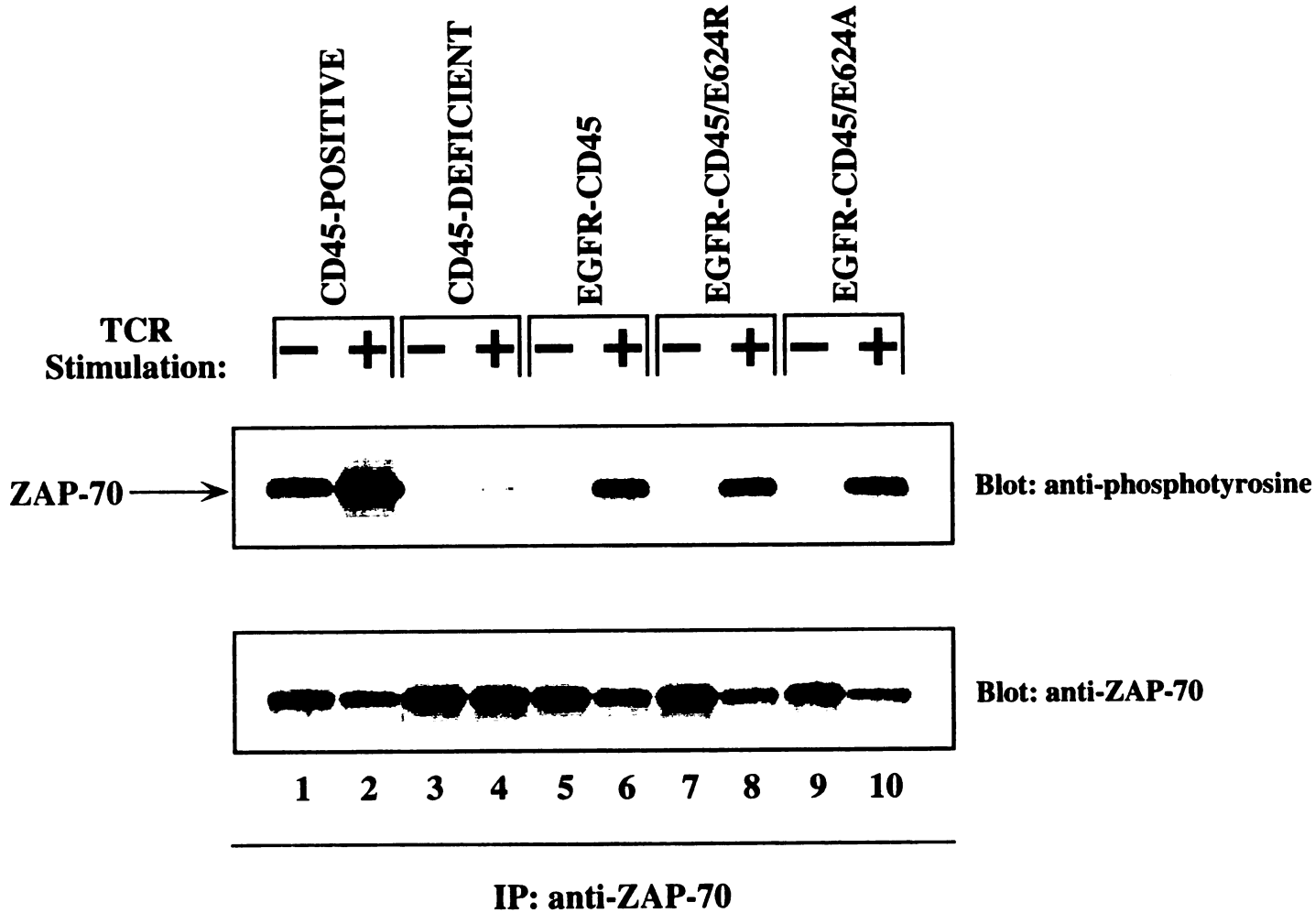

D

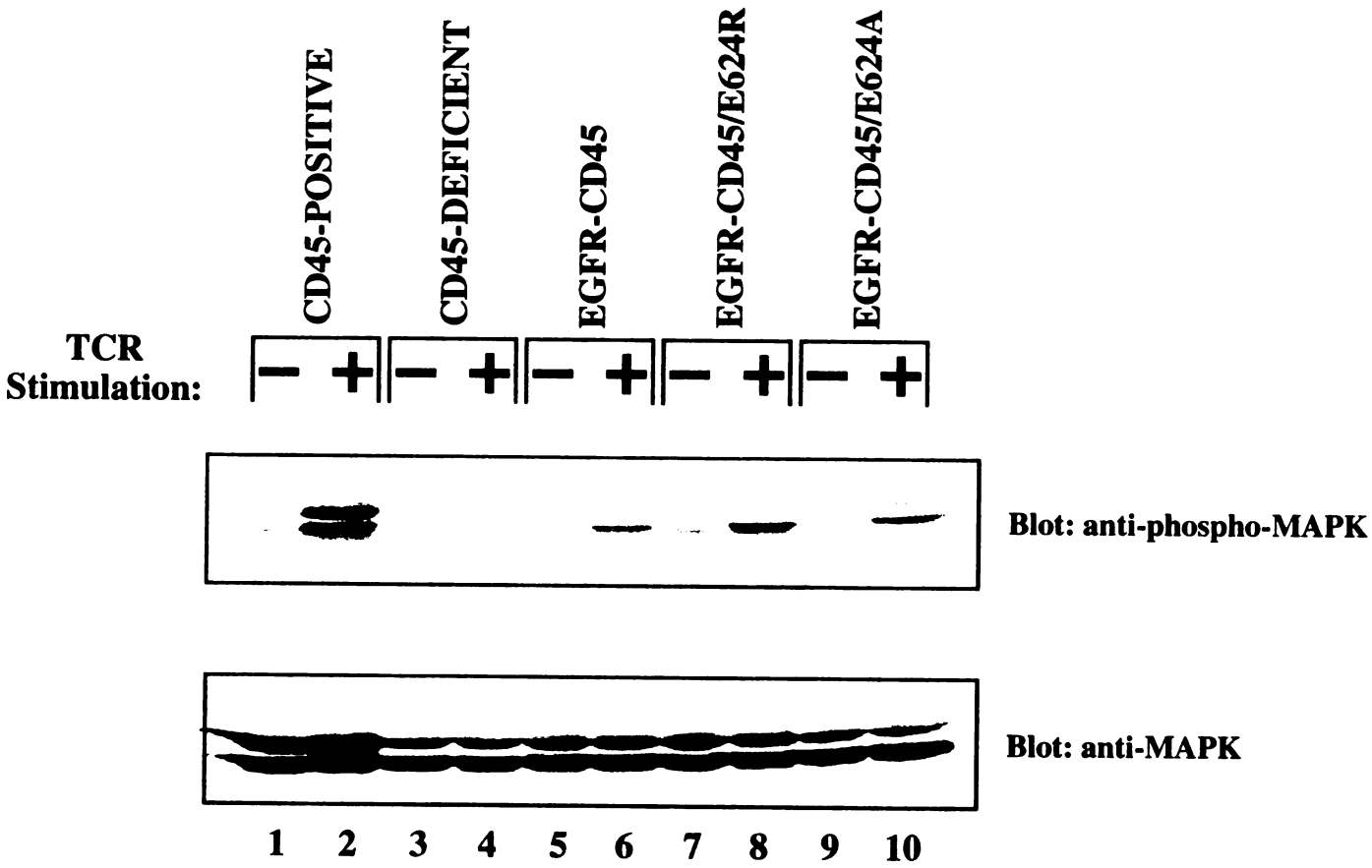
CD45-POSITIVE
CD45-DEFICIENT
EGFR-CD45
EGFR-CD45/E624R
EGFR-CD45/E624A
TCR Stimulation:
− + − + − + − + − +
Blot: anti-phospho-MAPK
Blot: anti-MAPK
1 2 3 4 5 6 7 8 9 10

with E624A or E624R mutant chimeras, mobilization of calcium (Figure 2B) and increased phosphorylation of the protein tyrosine kinase ZAP-70 and mitogen-activated protein kinase (MAPK) (Figure 2C,D) in response to TCR stimulation were similar to those responses in cells reconstituted with the wild-type chimera. Tyrosine phosphatase activity of the mutant CD45 cytoplasmic domains expressed in *E. coli* was similar to that of the wild-type protein (data not shown). It is unlikely that these mutations affect EGF binding to the chimeric receptor because the extracellular portion of all three chimeras consists entirely of the wild-type EGFR extracellular domain, and these cell lines displayed similar specific binding of radioiodinated EGF (data not shown). As observed with the wild-type EGFR-CD45 chimera (*43*), no internalization of the mutant EGFR-CD45 chimeras was detected in cells treated with EGF for up to 30 min (data not shown).

Stable expression of the wild-type EGFR-CD45 chimera in H45.01 cells restored normal amplitude and time course of Ca^{2+} mobilization in response to TCR stimulation (Figure 3A) (*36*). This Ca^{2+} flux was inhibited upon addition of EGF (Figure 3B) (*36*). H45.01 cells stably expressing the EGFR-CD45/E624A mutant chimera also mobilized Ca^{2+} in response to TCR stimulation with a similar amplitude and time course (Figure 3D); however, this Ca^{2+} flux was less effectively inhibited by EGF (Figure 3E). A similar lack of responsiveness to EGF was observed with H45.01 cells stably expressing the EGFR-CD45/E624R mutant chimera (Figure 3G,H). Treating cells expressing the wild-type chimera with EGF before TCR stimulation inhibited Ca^{2+} mobilization (Figure 3C) (*36*). No such inhibition was evident in cells expressing either of the mutant chimeras (Figure 3F,I). Similar effects of EGF both before and after TCR stimulation were obtained when up to 10-fold more EGF was used (data not shown). Thus, upon

Figure 3: Mutation of E624 eliminates inhibition of calcium flux caused by dimerization of the EGFR-CD45 chimera

The effects of EGF on TCR-mediated calcium mobilization in CD45-deficient T cells expressing EGFR-CD45 wild-type (A, B, and C), EGFR-CD45/E624A (D, E, and F), or EGFR-CD45/E624R (G, H, and I) are demonstrated. Cells were treated at the indicated times with either antibody to the TCR or EGF. Similar results were obtained with multiple independently isolated stable clones (data not shown).

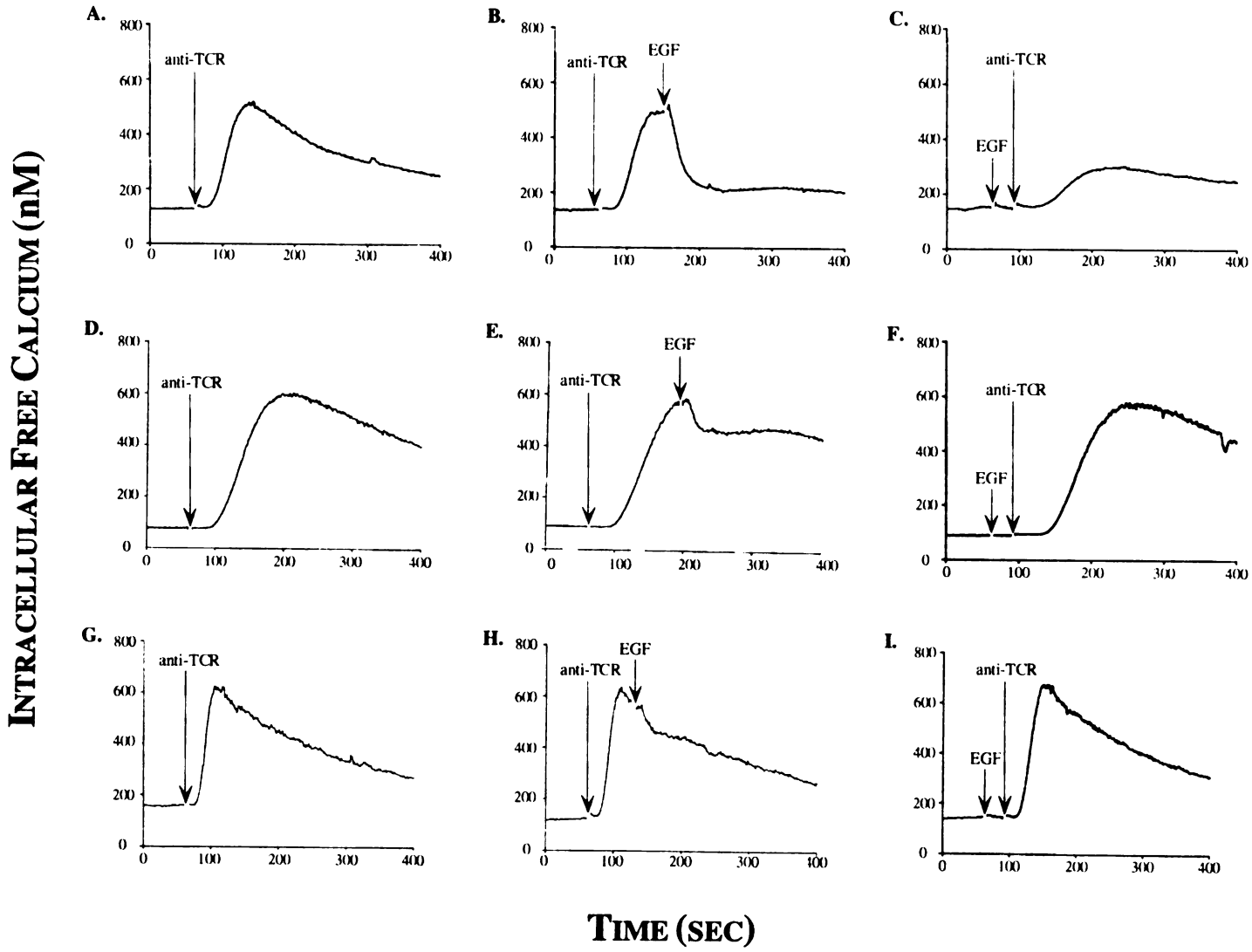
CHIMERA
EGFR-CD45
EGFR-CD45/E624A
EGFR-CD45/E624R
A.
B.
C.
D.
E.
F.
G.
H.
I.
anti-TCR
EGF
INTRACELLULAR FREE CALCIUM (nM)
TIME (SEC)

dimerization, the mutant chimeras have reduced capacity to inhibit Ca^{2+} mobilization in response to TCR stimulation.

Stimulation of the TCR results in recruitment and tyrosine phosphorylation of ZAP-70 as a result of activation of the Lck protein tyrosine kinase (*1,6*). TCR stimulation also results in the phosphorylation of MAPK (*1*). These events do not occur in CD45-deficient T cells (Figure 2C,D). Expression of the wild-type EGFR-CD45 chimera in H45.01 cells restored tyrosine phosphorylation of ZAP-70 upon TCR stimulation (Figure 4A). Concurrent administration of EGF or pretreatment with EGF inhibited the tyrosine phosphorylation of ZAP-70 induced by TCR stimulation (Figure 4A). In H45.01 cells stably expressing the EGFR-CD45/E624R chimera, TCR stimulation also resulted in tyrosine phosphorylation of ZAP-70 (Figure 4A). However, the effect of EGF to inhibit tyrosine phosphorylation of ZAP-70 was reduced in these cells (Figure 4A). MAPK was also phosphorylated in response to TCR stimulation in H45.01 cells expressing the wild-type chimera (Figure 4B). MAPK phosphorylation was inhibited in these cells when treated with EGF (Figure 4B). Little or no inhibition was observed with EGF treatment of H45.01 cells expressing the EGFR-CD45/E624R chimera (Figure 4B). Similar results for both ZAP-70 and MAPK phosphorylation were obtained with cells expressing the EGFR-CD45/E624A mutant chimera (data not shown). Thus, in CD45-deficient T cells stably expressing the E624A or E624R mutant chimeras, the effect of EGF on ZAP-70 or MAPK phosphorylation was reduced or eliminated.

Figure 4: Mutation of E624 eliminates inhibition of ZAP-70 and MAPK phosphorylation caused by dimerization of the EGFR-CD45 chimera

The effects of EGF on TCR-mediated ZAP-70 and MAPK phosphorylation in CD45-deficient T cells expressing EGFR-CD45 wild-type (A and B, lanes 1-5) or EGFR-CD45/E624R (A and B, lanes 6-10). Cells were stimulated as indicated: no stimulation (lanes 1 and 6), 2 min with antibody to the TCR (lanes 2 and 7), 3 min with EGF (lanes 3 and 8), 2 min with both antibody to the TCR and EGF (lanes 4 and 9), 1 min pretreatment with EGF, then 2 min with antibody to the TCR (lanes 5 and 10). **(A)** ZAP-70 tyrosine phosphorylation was assessed by immunoprecipitation followed by immunoblotting with antibody to phosphotyrosine (top panel); the same blot was stripped and reprobed with antibody to ZAP-70 (bottom panel). **(B)** MAPK phosphorylation was assessed by blotting a portion of the whole cell lysate with antibody specific for phosphorylated MAPK (top panel); the same blot was stripped and reprobed with an antibody to MAPK (bottom panel). In the bottom panel, the variable upper band represents ERK1. Similar results were obtained with multiple independently isolated stable clones (data not shown).

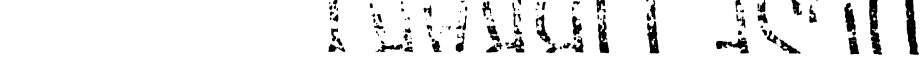

A

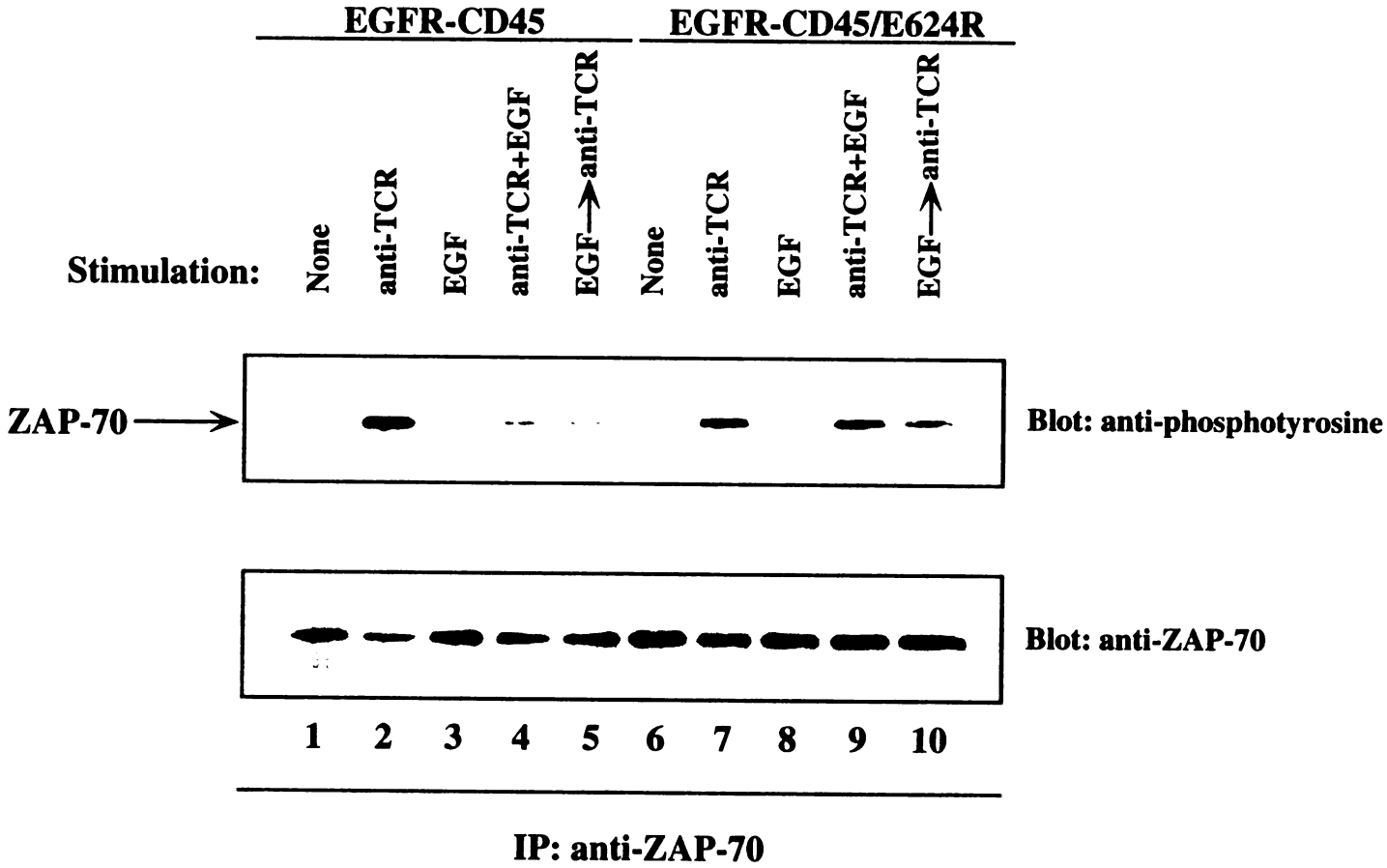
EGFR-CD45
EGFR-CD45/E624R
Stimulation:
None
anti-TCR
EGF
anti-TCR+EGF
EGF→anti-TCR
None
anti-TCR
EGF
anti-TCR+EGF
EGF→anti-TCR
ZAP-70
Blot: anti-phosphotyrosine
Blot: anti-ZAP-70
1 2 3 4 5 6 7 8 9 10
IP: anti-ZAP-70

B

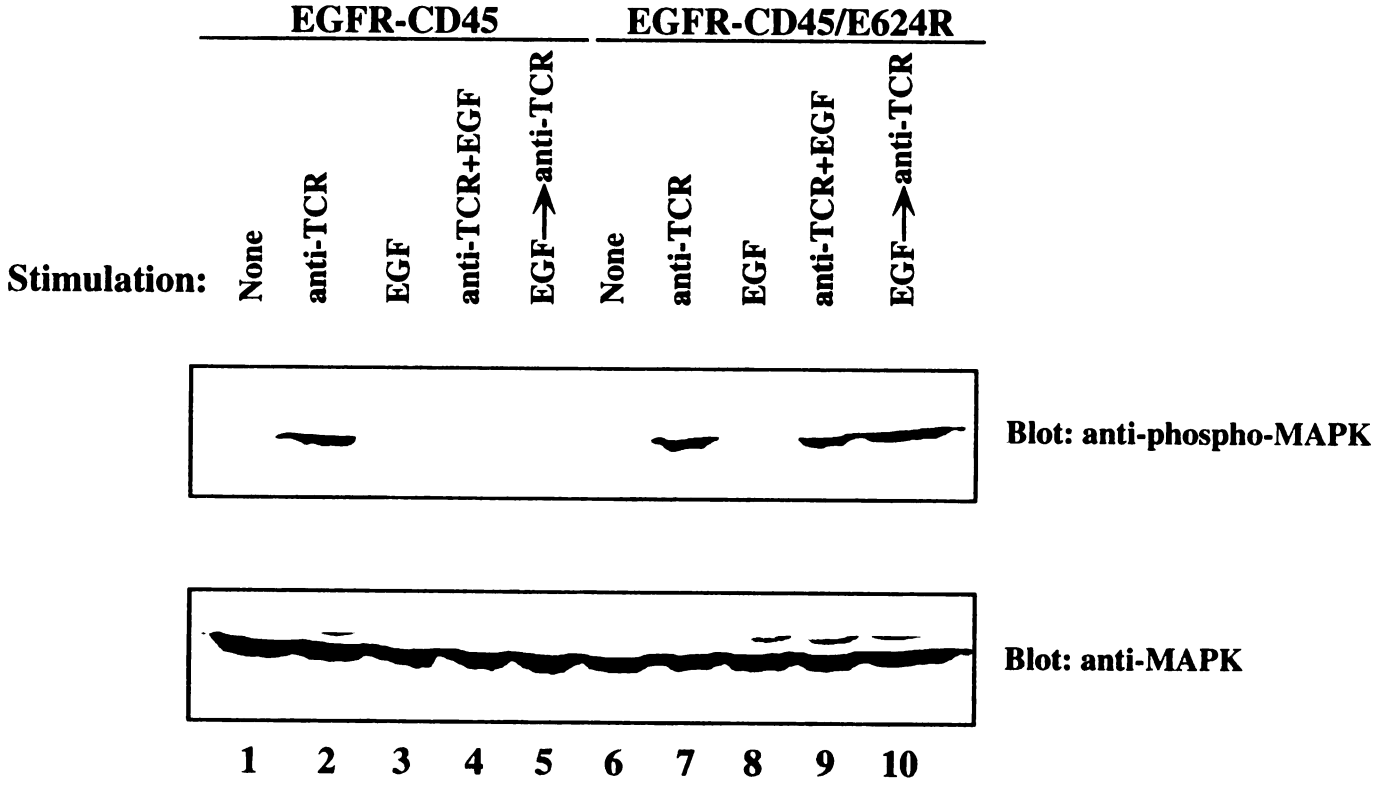
EGFR-CD45
EGFR-CD45/E624R
Stimulation:
None
anti-TCR
EGF
anti-TCR+EGF
EGF→anti-TCR
None
anti-TCR
EGF
anti-TCR+EGF
EGF→anti-TCR
Blot: anti-phospho-MAPK
Blot: anti-MAPK
1 2 3 4 5 6 7 8 9 10

Discussion

The hallmarks of T cell activation following TCR stimulation are production of IL-2 and increased cell proliferation, which require both activation of the Ras pathway (leading to MAPK phosphorylation) and Ca^{2+} mobilization (*1*). Here we have shown that both signaling pathways are less effectively inhibited by ligand-induced dimerization of E624-mutant EGFR-CD45 chimeric molecules. Thus, it appears that T cells expressing E624A or E624R mutant CD45 molecules would continue to be activated in the presence of an inhibitory ligand.

Although ligands for several RPTPs have been determined (*50,60*), the natural ligand for CD45 remains unknown. CD45 can form dimers (*55*) and some antibodies which can dimerize CD45 inhibit its function (*52-54*). The interaction of CD45 with its ligand may induce its dimerization and in turn regulate the activity of Lck. In the absence of ligand, both wild-type and mutant CD45 molecules are catalytically active monomers. In the presence of a CD45 ligand, both wild-type and mutant CD45 may dimerize, with different consequences for Lck activity. In cells expressing wild-type CD45, the catalytic site of each molecule would be blocked by the wedge containing glutamate 624 from the partner molecule, inhibiting CD45 phosphatase activity. Consequently, Lck would remain in the phosphorylated, inactive conformation, and TCR signals would be inhibited. In E624R-mutant CD45 molecules, the wedge is altered so that the catalytic sites are not occluded in the ligand-induced dimer. CD45 phosphatase activity would be retained and maintain Lck in its active conformation.

We chose to mutate glutamate 624 of CD45 because it is analogous to aspartate 228 within the putative inhibitory wedge of RPTPα (*59*). Aspartate 228 of one monomer contacts the mobile loop in the active site of the opposing monomer through a hydrogen bond between the side chain carboxyl moiety of D228 and a backbone amide of the loop. This interaction, along with other contacts, would preclude the necessary movement of the loop upon substrate binding, rendering the phosphatase inactive. Mutation of glutamate 624 of CD45 presumably disrupts the analogous interaction in CD45 dimers, thereby allowing the mobile loop to change conformation upon substrate binding, resulting in an active CD45 phosphatase.

Ligand-induced dimerization plays an essential role in the regulation of receptor tyrosine kinases, leading to autophosphorylation and activation of protein tyrosine kinase activity (*48*). Ligand-induced dimerization may also play an essential role in the regulation of receptor protein tyrosine phosphatases. However, instead of leading to activation, dimerization of RPTPs results in inhibition.

Experimental Procedures

Cloning and Generation of Stable Cell Lines

The EGFR-CD45 chimera (consisting of residues 1 to 646 of the human EGFR and residues 580 to 1281 of human CD45, numbered after the signal sequence from isoform ABC) has been described (*36*). The E624A and E624R mutations were introduced into the wild-type EGFR-CD45 chimera by oligonucleotide-based mutagenesis using the polymerase chain reaction (PCR) and confirmed by nucleotide sequencing. H45.01 (*22*) cells (a CD45-deficient derivative of the HPB.ALL T cell line) were transfected with plasmids encoding the EGFR-CD45 mutant chimeric molecules. Subsequent limiting dilution and selection in geneticin-containing medium (2 mg/ml) yielded H45XLE624A.5 (expressing the EGFR-CD45/E624A mutant chimera) and H45XLE624R.3 (expressing the EGFR-CD45/E624R mutant chimera). H45XL2 (expressing the EGFR-CD45 wild-type chimera) was derived in a similar manner (*36*). Multiple clones expressing each of the chimeric molecules were isolated and analyzed.

Flow Cytometry

Cells were stained with a control mAb (goat antibody to mouse IgG, Caltag Laboratories), LA22 (antibody to EGFR, Upstate Biotechnology Inc.) for the EGFR-CD45 chimera, Hle-1 (Becton-Dickinson) for CD45, and Leu4 (antibody to CD3ε,Becton-Dickinson) for the TCR. Cells were stained at 4°C with saturating concentrations of fluorescein isothiocyanate (FITC)-conjugated primary antibody

(control, Hle-1, and Leu4) or primary antibody (LA22) followed by FITC-conjugated goat antibody to mouse IgG. Cells were analyzed on a FACScan (Becton-Dickinison).

Measurement of Intracellular Free Calcium

Intracellular free calcium concentration was measured with the calcium sensitive dye Indo-1 as described (*62*). Cells (5 x 10^6/ml) were treated with antibody to CD3 (mAb 235 1:3000 dilution of ascites) or EGF (100 µg/ml).

Cell Stimulations, Immunoprecipitation, and Western Blotting

Cells were harvested, washed twice with phosphate-buffered saline (PBS), and resuspended at 2 x 10^8/ml in PBS. Cells were incubated at 37°C for 15 min. For each sample, 2 x 10^7 cells were used and an equal volume of stimulus in PBS warmed to 37°C was added for the indicated time so that final conditions were as follows: cells 1 x 10^8/ml, 235 ascites (anti-CD3 mAb) 1:500 dilution, and EGF 100 ng/ml. Cells were sedimented in a microfuge and lysed in 200 µl lysis buffer: 1% Triton X-100, 150 mM NaCl, 10 mM Tris (pH 8.0) supplemented with protease and phosphatase inhibitors as described (*43*). Lysates were incubated at 4°C for 30 min, followed by centrifugation at 13,000g for 10 min. 90% of the lysate were subjected to immunoprecipitation with polyclonal rabbit antibody to ZAP-70 (1598 (*63*)) and protein A-Sepharose beads for 2 hr at 4°C, after which immune complexes were washed. Immune complexes and 10% of the untreated lysate were resolved separately by SDS-polyacrylamide gel electrophoresis (PAGE) and transferred to polyvinylidene fluoride (PVDF) membranes (Millipore). Immunoblotting was done with monoclonal antibody to phosphotyrosine (4G10, Upstate

Biotechnology Inc.) or anti-phospho-MAPK (New England Biolabs) followed by visualization by enhanced chemiluminescence (ECL) (Amersham). The blots were stripped and reprobed with antibody to ZAP-70 (1598) or antibody to MAPK (Santa Cruz Biotechnology), respectively.

CHAPTER 3

A POINT MUTATION IN THE PUTATIVE INHIBITORY WEDGE OF CD45 ELIMINATES NEGATIVE REGULATION BY DIMERIZATION IN VIVO

Summary

A model has been proposed for the regulation of CD45, and by homology other RPTPs, in which dimerization inhibits phosphatase activity through symmetrical interactions between an inhibitory structural wedge and the catalytic site. I have provided functional evidence for this model by demonstrating that one of these wedge residues, glutamate 624 of human CD45, is required for ligand-induced negative regulation of CD45 function in TCR signal transduction in vitro. One prediction derived from these in vitro studies is that mutation of the inhibitory structural wedge in vivo will lead to inappropriate RPTP activation under normal dimerizing conditions. In the case of CD45, such dysregulated activity would cause inappropriate src-kinase activation, with potentially pathological consequences. Here I report the phenotype of mice with a single point mutation, glutamate 613 (murine homologue of human E624) to arginine, that inactivates the inhibitory wedge of CD45. CD45 E613R mice appear normal during the first few months of life; however, they subsequently develop a lymphoproliferative syndrome with apparent polyclonal T and B lymphocyte activation, and severe autoimmune nephritis with autoantibody production. As a result, these mice die prematurely. Both homozygotes and heterozygotes develop pathology, indicating genetic dominance of CD45 E613R. The dramatic phenotype of CD45 E613R mice demonstrates the in vivo importance of negative regulation of CD45 by dimerization, strongly supporting the model for regulation of CD45, and RPTPs in general.

Introduction

The receptor-like transmembrane protein tyrosine phosphatases (RPTPs) constitute a large family of widely expressed signal transduction molecules (*50,51*). Due to the importance of tyrosine phosphorylation in numerous cellular signal transduction pathways, it is assumed that RPTPs perform important regulatory functions. However, the physiological roles and direct biochemical substrates of most RPTPs are poorly characterized.

CD45 is a RPTP expressed on all nucleated hematopoietic cells, where it is required for signal transduction through antigen receptors (*1,17,18,20*). The requirement for CD45 has been demonstrated by studies of (1) numerous CD45-deficient T and B cell lines (*21-24*), which fail to respond to antigen receptor stimulation, (2) CD45-deficient mice, which show profound blocks in both T and B cell development and function (*25,26*), and (3) CD45-deficient humans, who have a severe combined immunodeficiency (SCID) phenotype similar to that observed in CD45-deficient mice (*27,28*). At least one function of CD45 is to dephosphorylate the C-terminal site of negative regulatory tyrosine phosphorylation within src-family kinases (*29-33,61*), thereby maintaining them in a "primed" state capable of full activation upon antigen receptor stimulation (*64,65*).

Like most members of the RPTP family, CD45 consists of an extracellular domain, a single transmembrane domain, and a cytoplasmic domain containing tandemly duplicated protein tyrosine phosphatase (PTP) domains. The extracellular domain possesses several features consistent with a role in regulating CD45 function. First, CD45 contains multiple fibronectin type III repeats (*66*) and a cysteine rich motif found

within numerous receptors (*19*), which may be involved in protein-protein interactions. Second, CD45 exists as several isoforms due to alternative splicing of exons 4, 5, and 6 within the extracellular domain (*18*). The alternatively spliced exons encode multiple sites of O-linked glycosylation so that the extracellular domain of high molecular weight isoforms ($CD45RA^+$) differs in structure and overall charge from the low molecular weight isoform (CD45R0) that lacks these three exons (*44*). Finally, in T cells the alternative splicing of CD45 is regulated so that naïve T cells predominantly express $CD45RA^+$ isoforms and switch to expression of CD45R0 upon activation (*67,68*). These observations suggest that the extracellular domain regulates CD45 function, perhaps by binding to a ligand or by mediating dimerization.

Dimeric forms of the RPTPs CD45 and RPTPα have been identified. In the case of CD45, homodimers have been detected biochemically through chemical crosslinking and sucrose gradient centrifugation (*55*). Dimers of RPTPα have been detected by biochemical "trapping" using an engineered disulfide linkage (*69*). However, the mechanism by which dimerization of these molecules is regulated is not currently known.

The consequences of dimerization on RPTP function were tested with a chimeric molecule consisting of the extracellular and transmembrane domains of the EGF receptor fused to the cytoplasmic domain of CD45 (EGFR-CD45) (*36*). EGFR-CD45 restored TCR-mediated signal transduction in a CD45-deficient T cell line. Strikingly, EGF-induced dimerization of EGFR-CD45 inhibited TCR-mediated signal transduction. This inhibition depended on dimerization of the CD45 cytoplasmic domain, suggesting that CD45 is negatively regulated by dimerization.

A potential molecular explanation for this negative regulation was provided by the crystal structure of the membrane-proximal region and PTP domain 1 of RPTPα (*59*). This protein fragment forms a symmetrical dimer in which the catalytic site of one molecule is blocked by specific contacts with a structural wedge from the membrane-proximal region of the other. Amino acid residues forming this wedge, including two acidic residues at the tip, are conserved within the membrane-proximal regions of RPTPs, including CD45 (*59*). Moreover, sequences within this region of CD45 are conserved phylogenetically from shark to human, potentially indicating an important conserved structure and function. These observations suggest a general model for the regulation of RPTPs in which dimerization inhibits phosphatase activity, and consequently function, through symmetrical interactions between the catalytic site and the structural wedge containing the acidic residues (*49*).

To test this model, we mutated a glutamic acid residue in the tip of the putative inhibitory wedge of CD45, in the context of EGFR-CD45, and used this mutant chimera to reconstitute TCR-mediated signaling in CD45-deficient T cells (*70*). Treatment of these cells with EGF, however, failed to inhibit TCR-mediated signal transduction, providing evidence of a critical role for the inhibitory wedge in negative regulation of CD45 function by dimerization. Recent studies with RPTPα have also indicated an essential role for the structural wedge in the negative regulation of RPTPα activity by dimerization (*69*). Cells in which dimeric RPTPα was "trapped" with an engineered disulfide linkage exhibited increased phosphorylation of Y527 in src, the substrate for RPTPα, demonstrating dimerization-induced inhibition of RPTPα activity; significantly, mutations in the structural wedge restored activity to RPTPα dimers.

These experiments supporting the model for dimerization-mediated negative regulation of RPTPs by the inhibitory wedge were conducted in vitro using modified RPTPs. One prediction derived from these in vitro studies is that mutation of the inhibitory structural wedge in vivo will lead to inappropriate RPTP activation under normal dimerizing conditions. In the case of CD45, such dysregulated activity would cause inappropriate src-kinase activation, with potentially pathological consequences. Here we report the phenotype of "knock-in" mice in which a single critical glutamate in the inhibitory structural wedge of CD45 has been mutated to arginine (CD45 E613R). CD45 E613R mice appear normal during the first few months of life; however, they subsequently develop a lymphoproliferative syndrome with apparent polyclonal T and B lymphocyte activation, and severe autoimmune nephritis with autoantibody production. As a result, these mice die prematurely. The dramatic phenotype of CD45 E613R mice demonstrates the in vivo importance of negative regulation of CD45 by dimerization, strongly supporting the model for regulation of CD45, and RPTPs in general.

Results

Generation of CD45 E613R "Knock-In" Mice

Previous studies with the EGFR-CD45 chimera indicated that mutation of glutamate 624 to arginine within the inhibitory wedge of human CD45 eliminates negative regulation of CD45 by dimerization (*70*). In order to study the role of dimerization-mediated inhibition in vivo, the homologous residue in the mouse, glutamate 613, was mutated to arginine (E613R) using a gene targeting "knock-in" strategy. A genomic fragment containing glutamate 613 in exon 18 of murine CD45 was selected for the targeting construct. The E613R mutation was introduced into exon 18, and a loxP-flanked neomycin-resistance cassette was inserted into the downstream intron (Figure 1A). Transfection of this construct into 129-derived ES cells targeted the endogenous CD45 locus by homologous recombination at a frequency of 3 out of 1200 clones (Figure 1B). Germline transmission was achieved after microinjection of 2 of these clones. The two mutant mouse lines were subsequently bred to ß-actin Cre transgenic mice in order to eliminate the neomycin-resistance cassette (Figure 1A,B). An additional cross to C57BL/6 eliminated the ß-actin Cre transgene resulting in mice carrying only the E613R mutation and an insertion of approximately 140 nucleotides into the downstream intron. The data presented here are derived from mice on this mixed background; similar results were obtained with both independently-derived "knock-in" lines. The presence of the E613R mutation in CD45 mRNA was verified by sequencing of RT-PCR products (data not shown). These mice will be referred to as CD45 E613R mice.

Figure 1: Generation of CD45 E613R "knock-in" mice

(**A**) Schematics of the genomic, E613R targeted, and E613R recombined alleles of CD45. The E613R mutation was engineered along with a Pvu I site into exon 18. A novel Hind III site was introduced with a loxP-flanked neomycin resistance cassette into the downstream intron at an EcoR I site. Germline targeted mice were bred to β-actin Cre transgenic mice eliminating the neomycin-resistance cassette, while retaining the Hind III site. Fragment sizes generated by digestion with Hind III are indicated, along with the probes used for Southern blot analysis.

(**B**) Southern blot analysis of DNA prepared from ES cell lines (left) and mouse tails (right). DNA was digested with Hind III and the blot was probed with the 3' probe. Expected fragments are indicated to the right. Genotypes are indicated above each lane.

(**C**) Equivalent surface expression of CD45 on thymocytes, lymph node cells, and splenocytes. Cells from wild type (plain), heterozygote (dotted), and homozygote (bold) tissues were stained with a pan-specific anti-CD45 antibody and analyzed by flow cytometry. Unstained cells are indicated with the shaded histogram. The plain, dotted, and bold lines superimpose in each case.

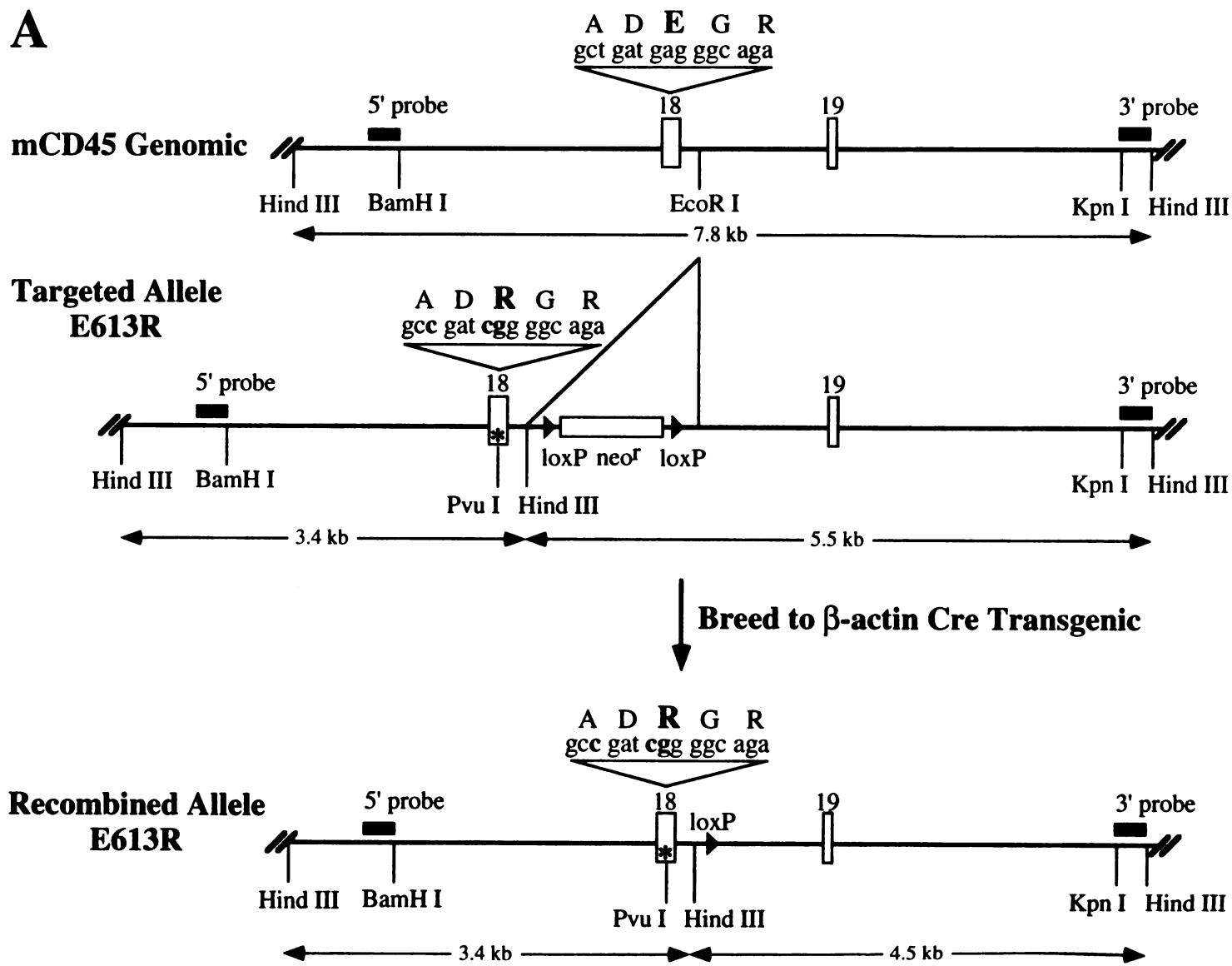
A
A D E G R
gct gat gag ggc aga
mCD45 Genomic
5' probe
18
19
3' probe
Hind III
BamH I
EcoR I
Kpn I
Hind III
7.8 kb
Targeted Allele
E613R
A D R G R
gcc gat cgg ggc aga
5' probe
18
19
3' probe
loxP neo^r loxP
Hind III
BamH I
Pvu I
Hind III
Kpn I
Hind III
3.4 kb
5.5 kb
Breed to β-actin Cre Transgenic
A D R G R
gcc gat cgg ggc aga
Recombined Allele
E613R
5' probe
18
loxP
19
3' probe
Hind III
BamH I
Pvu I
Hind III
Kpn I
Hind III
3.4 kb
4.5 kb

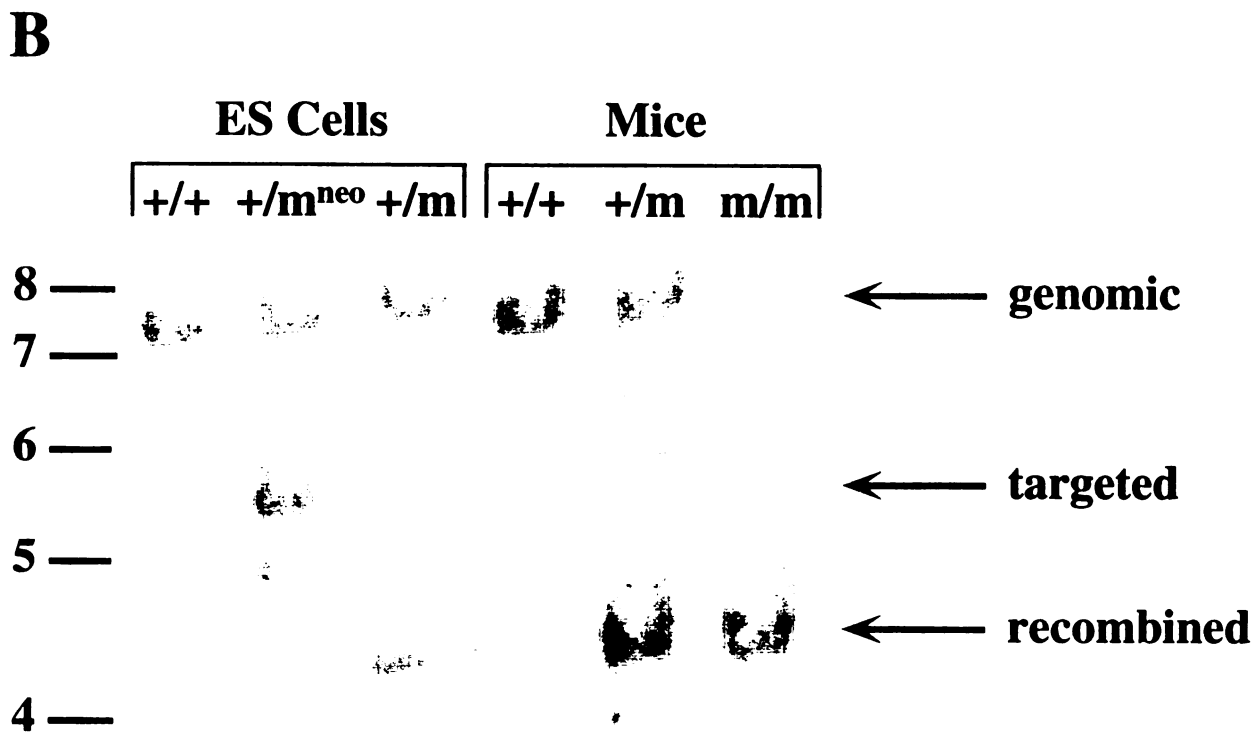
B
ES Cells
Mice
+/+
+/m^neo
+/m
+/+
+/m
m/m
8
7
6
5
4
genomic
targeted
recombined

C

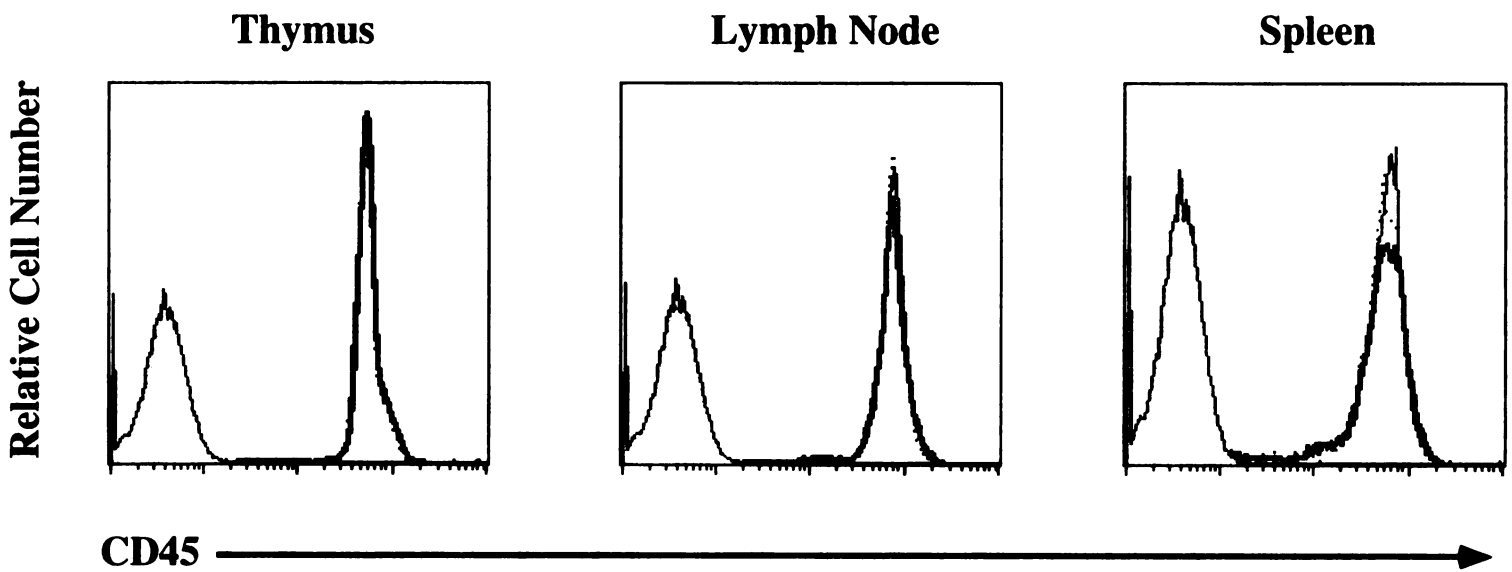

CD45 E613R heterozygous mice were interbred to generate homozygous mice. Both homozygotes and heterozygotes were born at Mendelian frequencies and appeared normal at birth. To assess any disruption of CD45 expression caused by the E613R mutation, the surface level of CD45 was analyzed by flow cytometry using a pan-CD45 antibody. Wild type, heterozygous, and homozygous mutant mice showed indistinguishable levels of CD45 on the surface of thymocytes, lymph node cells, and splenocytes (Figure 1C).

Normal Lymphocyte Development and Activation in 4-Week Old CD45 E613R Mice

CD45 is required for normal lymphocyte development in both mice and humans. T cell development in CD45 E613R mice was assessed by analyzing thymocytes from 4-week old wild type, heterozygous, and homozygous mutant mice. Total thymic cellularity was similar between these mice. Furthermore, no significant differences were observed in the percentages of $CD4^-CD8^-$ double negative, $CD4^+CD8^+$ double positive, or $CD4^+CD8^-/CD4^-CD8^+$ single positive thymocytes (Figure 2A, top). Analysis of thymocytes from CD45 E613R mice carrying a MHC Class I-restricted TCR transgene which recognizes the male-specific HY antigen, indicated no differences compared to wild type HY TCR transgenic mice in thymic cellularity or CD4/CD8 profile for both females and males (data not shown), suggesting no major effect of CD45 E613R on positive and negative selection events in the thymus.

B cell development in CD45 E613R mice was assessed by analyzing surface expression of IgM and IgD on splenocytes from 4-week old mice. B cells migrating from the bone marrow to the spleen start as IgM^{hi}/IgD^{lo}, progress to IgM^{hi}/IgD^{hi}, and mature

Figure 2: Normal lymphocyte development and activation in 4-week old CD45 E613R mice

(**A**) Normal lymphocyte development. Cells from thymus and spleen of 4-week old mice were stained with anti-CD4 and anti-CD8 (thymus) or anti-IgD and anti-IgM (spleen) and analyzed by flow cytometry. The percentages of cells within defined regions are indicated. Genotypes are indicated above the panels. The decreased number of IgM^{lo}/IgD^{hi} splenic B cells in homozygous mutant mice was not consistently observed. Data is representative of 3 separate analyses.

(**B**) Normal lymphocyte activation. Cells from lymph nodes and spleens of 4-week old mice were stained with anti-CD3 and anti-CD69 (lymph node) or anti-CD19 and anti-CD69 (spleen) and analyzed by flow cytometry. The percentage of $CD3^+$ or $CD19^+$ cells staining with CD69 is indicated. Genotypes are indicated above the panels. Data is representative of 3 separate analyses.

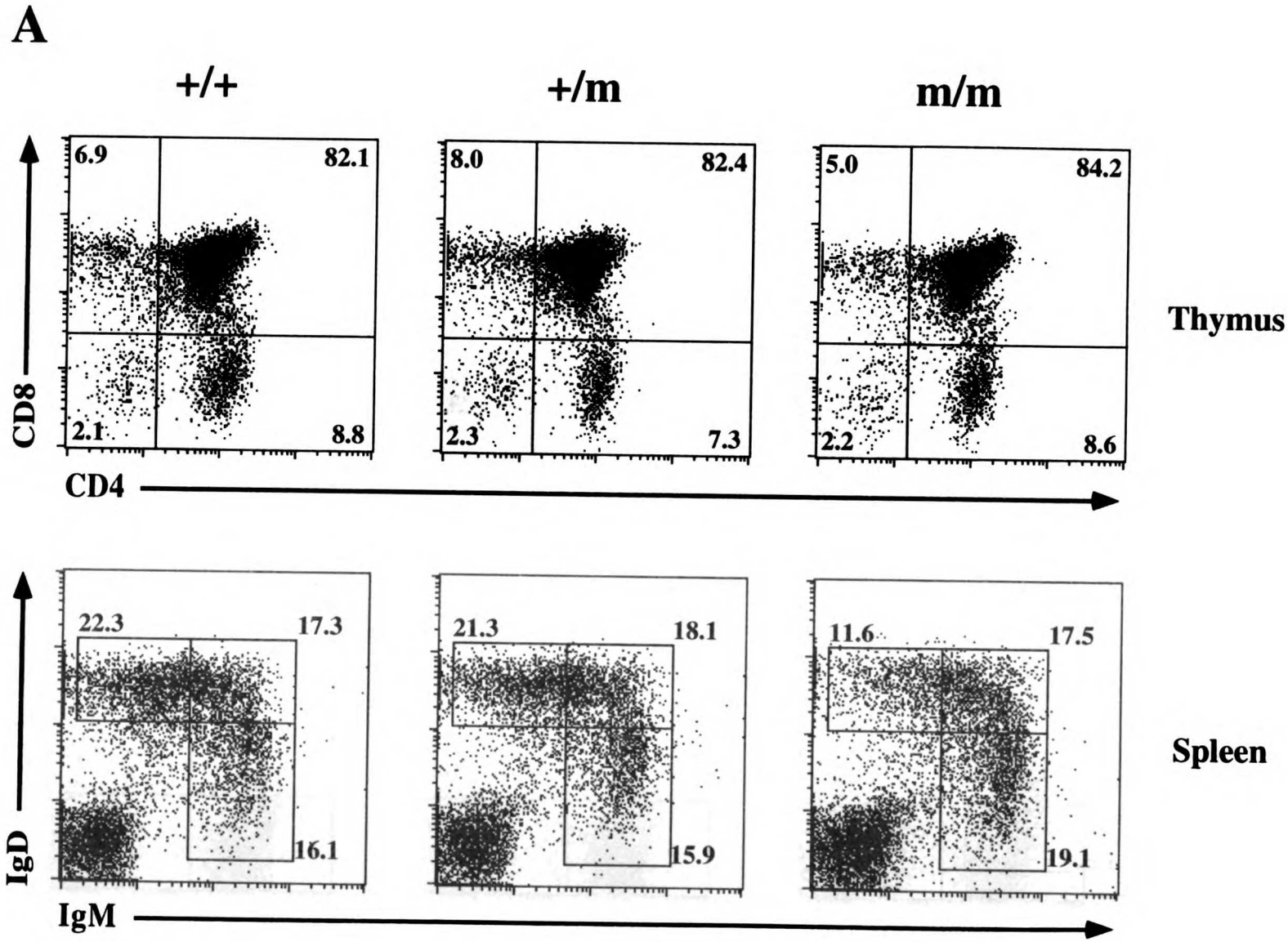

old CD45

4-week old

d anti-IgM

iin defined

sed number

y observed.

4-week old

9 and anti-

CD19⁺ cells

ls. Data is

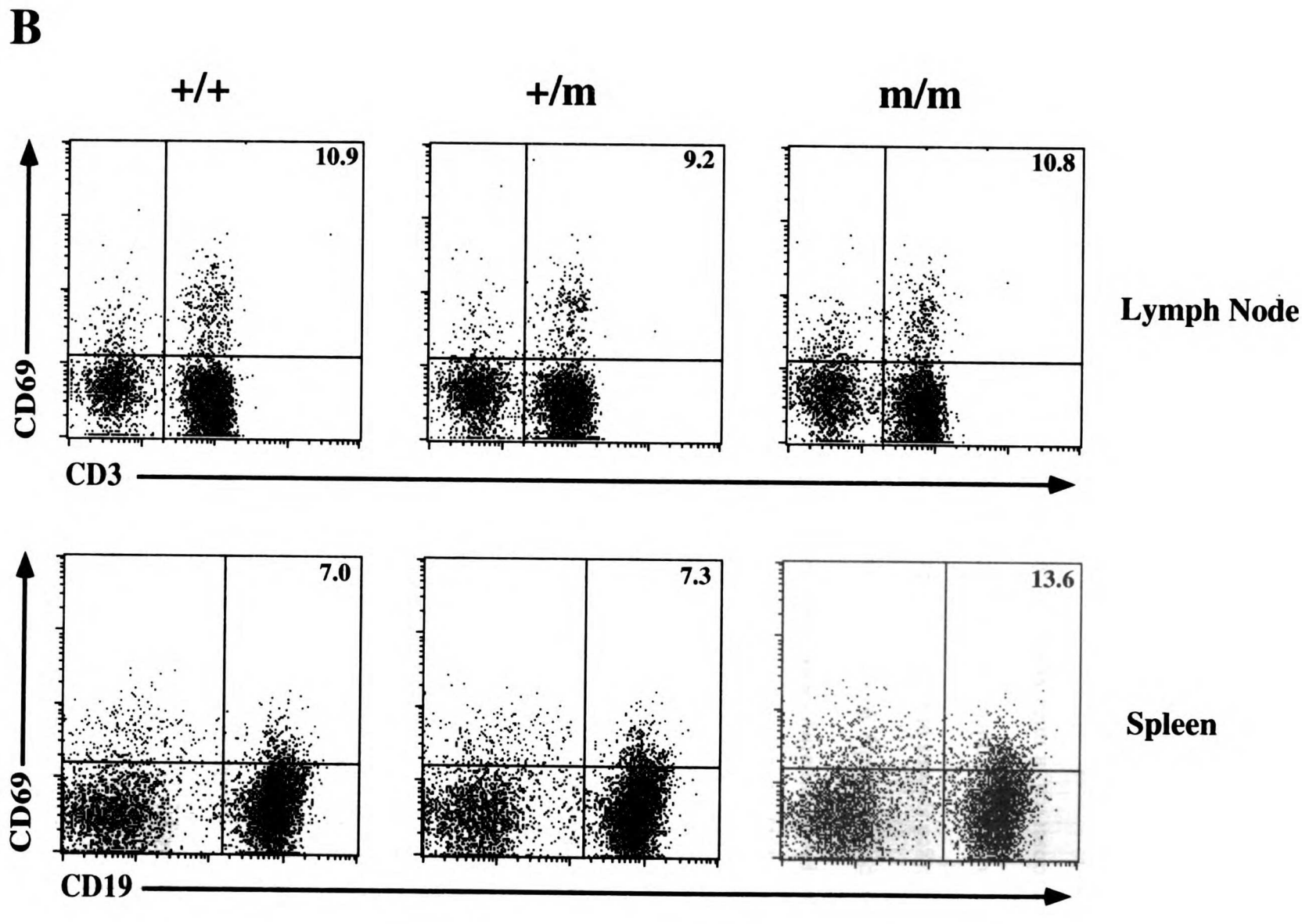
B
+/+
+/m
m/m
10.9
9.2
10.8
CD69
CD3
Lymph Node
7.0
7.3
13.6
CD69
CD19
Spleen

into IgM^{lo}/IgD^{hi} resting B cells. No major differences in these B cell subpopulations were observed in spleens from wild type, heterozygous, and homozygous mutant mice (Figure 2A, bottom). Thus, lymphocyte development in CD45 E613R mice appears to proceed normally.

In order to assess the activation state of lymphocytes in 4-week old CD45 E613R mice, surface expression of the lymphocyte activation marker CD69 was analyzed on $CD3^+$ lymph node T cells and $CD19^+$ splenic B cells. No differences in the percentage of $CD69^+$ T cells or B cells were detected (Figure 2B). These data indicate that there is no increase in the frequency of activated lymphocytes in 4-week old CD45 E613R mice.

Lymphoproliferation With Polyclonal T and B Cell Activation in CD45 E613R Mice

Young CD45 E613R mice appeared normal, but as they aged, mutant mice developed progressive lymphadenopathy and splenomegaly. The degree of tissue enlargement observed varied from mild (not shown) to severe (Figure 3A). Generalized lymphadenopathy was observed in severe cases; however, in mild cases, lymphadenopathy was often confined to the cervical and submandibular lymph nodes. Enlarged spleens of CD45 E613R mice weighed between 3 to 10 times more than spleens from wild type mice. No enlargement of the thymus was noted. Lymphadenopathy was not observed in mice younger than 15 weeks nor in wild type mice of any age (n=13); however, 15% of heterozygotes (n=24) and 70% of homozygotes (n=20) older than 15 weeks developed lymphadenopathy, with approximately half being severe.

Histological analysis of enlarged lymph nodes from CD45 E613R mice demonstrated intact follicular architecture with expansion in all areas including cortical

Figure 3: Lymphadenopathy and splenomegaly in CD45 E613R mice

(**A**) Lymph nodes (left) and spleen (right) from an age-matched wild type mouse and a CD45 E613R homozygous mutant mouse with severe lymphadenopathy and splenomegaly. Scale bars represent 0.5 cm.

(**B**) Lymph node and spleen histology. Panels on the left (a,c,e,g) are derived from age-matched wild type mice while those on the right (b,d,f,h) are from CD45 E613R homozygous mutant mice with severe lymphadenopathy and splenomegaly. (a-d) are from lymph nodes. (e-h) are from spleens. (a,b) Intact follicular architecture in enlarged CD45 E613R lymph nodes. Expansion is observed in all areas: cortical follicles, interfollicular T cell zones, and medullary sinuses. (c,d) Normal mixed cellular composition in the interfollicular and medullary areas of wild type mice (c) and increased plasmacytoid cells with extensive dark gray cytoplasm (arrows) in a background of normal mixed cells in mutant mice (d). A single enlarged plasmacytoid cell is shown in the inset (d). (e,f) Expansion of red pulp and white pulp in enlarged CD45 E613R spleens. Note the increased cellularity of the red pulp in mutant mice (f). Fissures in (e) are an artifact of tissue processing. (g,h) Extensive extra-medullary hematopoiesis in enlarged CD45 E613R spleens. An occasional megakaryocyte (M) is observed in wild type spleens (g); however, numerous megakaryocytes (M) and islands of erythropoiesis and granulopoiesis (arrows) are observed in mutant spleens (h). All panels were stained with hematoxylin and eosin (H&E). (a,b,e,f) Scale bars represent 100μM. (c,d,g,h) Scale bars represent 5μM.

A

wild type CD45 E613R

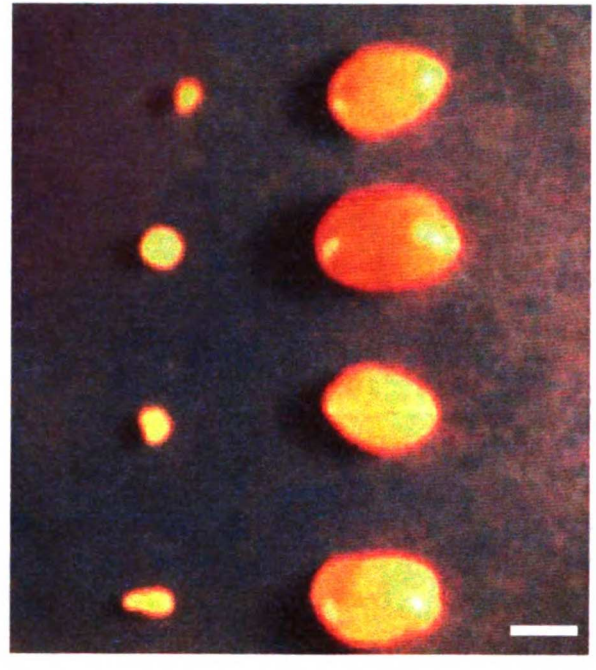

wild type CD45 E613R

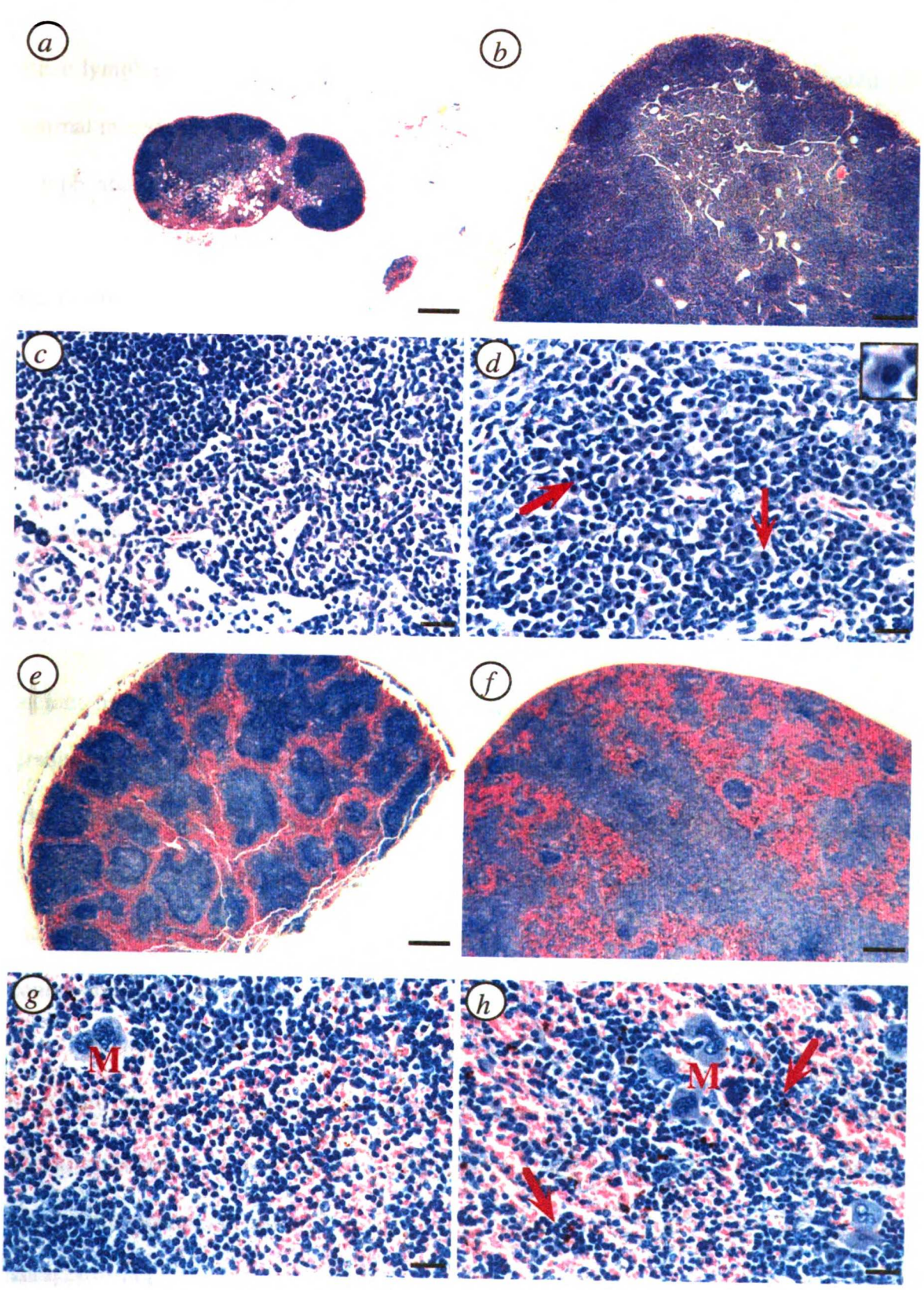
B
wild type
CD45 E613R
a
b
c
d
e
f
g
h
M
M

primary follicles, interfollicular T cell zones, and medullary sinuses (Figure 3B, panel b). Prominent germinal centers, which are readily seen in wild type mice, are not observed in these lymph nodes (Figure 3B, panels a,b). Higher power examination demonstrated the normal mixed cellular composition of the interfollicular and medullary areas in wild type lymph nodes (Figure 3B, panel c); however, a marked increase in plasmacytoid cells within the background of normal mixed cells was observed in enlarged lymph nodes from CD45 E613R mice (Figure 3B, panel d).

Histological analysis of enlarged spleens from CD45 E613R mice demonstrated expansion of both the red pulp and white pulp (Figure 3B, panels e,f). Expansion of the splenic red pulp was accompanied by a marked increase in extra-medullary hematopoiesis (EMH) in the spleen. Some degree of EMH is normal in the mouse, as indicated by the occasional megakaryocyte detected in wild type spleens (Figure 3B, panel g). However, this contrasts with the extensive EMH in the enlarged spleens from mutant mice. Along with numerous megakaryocytes, islands of erythropoiesis and granulopoiesis were observed throughout the enlarged spleens (Figure 3B, panel h); additionally, a significant increase in TER-119$^+$ erythroid progenitor cells was observed by flow cytometry (data not shown). Analysis of the bone marrow indicated abnormally increased granulopoiesis and a paucity of erythropoiesis; however, the complete blood counts of these mice were normal (data not shown).

Examination of the lymphoid tissue of the splenic white pulp revealed an absence of clearly demarcated germinal centers (Figure 3B, panels e,f). Similar to the lymph nodes, an increase in plasmacytoid cells was observed along with the normal mixed cellular composition of the white pulp (data not shown). Thus, the general architecture

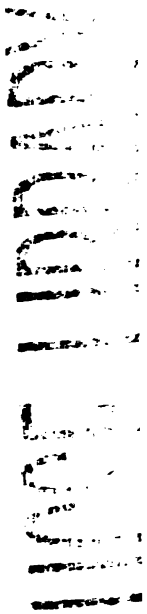

and cellular composition of the lymphoid tissue is preserved in CD45 E613R mice with lymphadenopathy and splenomegaly, but with an increase in plasmacytoid cells and splenic EMH. Such a histological picture is consistent with a lymphoproliferative syndrome.

Single-cell suspensions were prepared from lymph nodes of CD45 E613R mice with mild and severe lymphadenopathy; data representative of 5 separate analyses is presented (Figure 4). The total number of cells in these lymph nodes was found to be increased 2-8 fold over wild type; additionally, an increase in large cells was noted based on the forward scatter profile (data not shown). Both control and lymphoproliferative nodes contained similar percentages of $CD3^+$ T cells and $CD19^+$ B cells, with approximately 50-75% T cells (Figure 4A). Analysis of expression of a panel of Vβ TCR gene segments on T cells failed to reveal any differences between control and lymphoproliferative nodes; similarly, no difference in the proportion of λ light chain-expressing B cells was noted (data not shown). These data suggest that polyclonal T and B cell expansion is responsible for the lymphadenopathy.

Both T and B cells in lymphoproliferative nodes were found to be activated as determined by surface expression of CD69. On T cells, CD69 expression was increased from 21% in wild type to 34% in mild lymphadenopathy, and 57% in severe lymphadenopathy; CD69 expression was increased on B cells from 26% in wild type to 62% and 70%, in mild and severe lymphadenopathy, respectively (Figure 4B,C).

T cells were further examined for expression of CD25, CD44, CD62L, CD45RB, CD40L, CTLA-4, Fas, and FasL. No increase in CD25 expression was noted in either mild or severe cases of lymphadenopathy (data not shown). High CD44 expression was

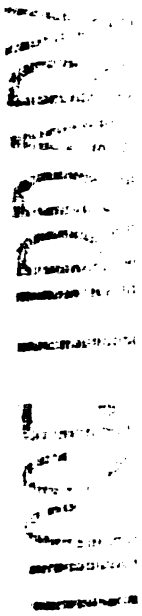

Figure 4: Lymphocyte activation in CD45 E613R mice

Lymph node cells from a wild type mouse (left), a CD45 E613R homozygote with mild lymphadenopathy (center), and a CD45 E613R heterozygote with severe lymphadenopathy (right) were stained with antibodies specific for the indicated cell surface markers and analyzed by flow cytometry. (**A**) The percentages of cells within defined regions are indicated. (**B,D,E,F**) The percentage of $CD3^+$ cells staining with the indicated marker is noted. (**C**) The percentage of $CD19^+$ cells staining with CD69 is indicated. Data is representative of 5 separate analyses.

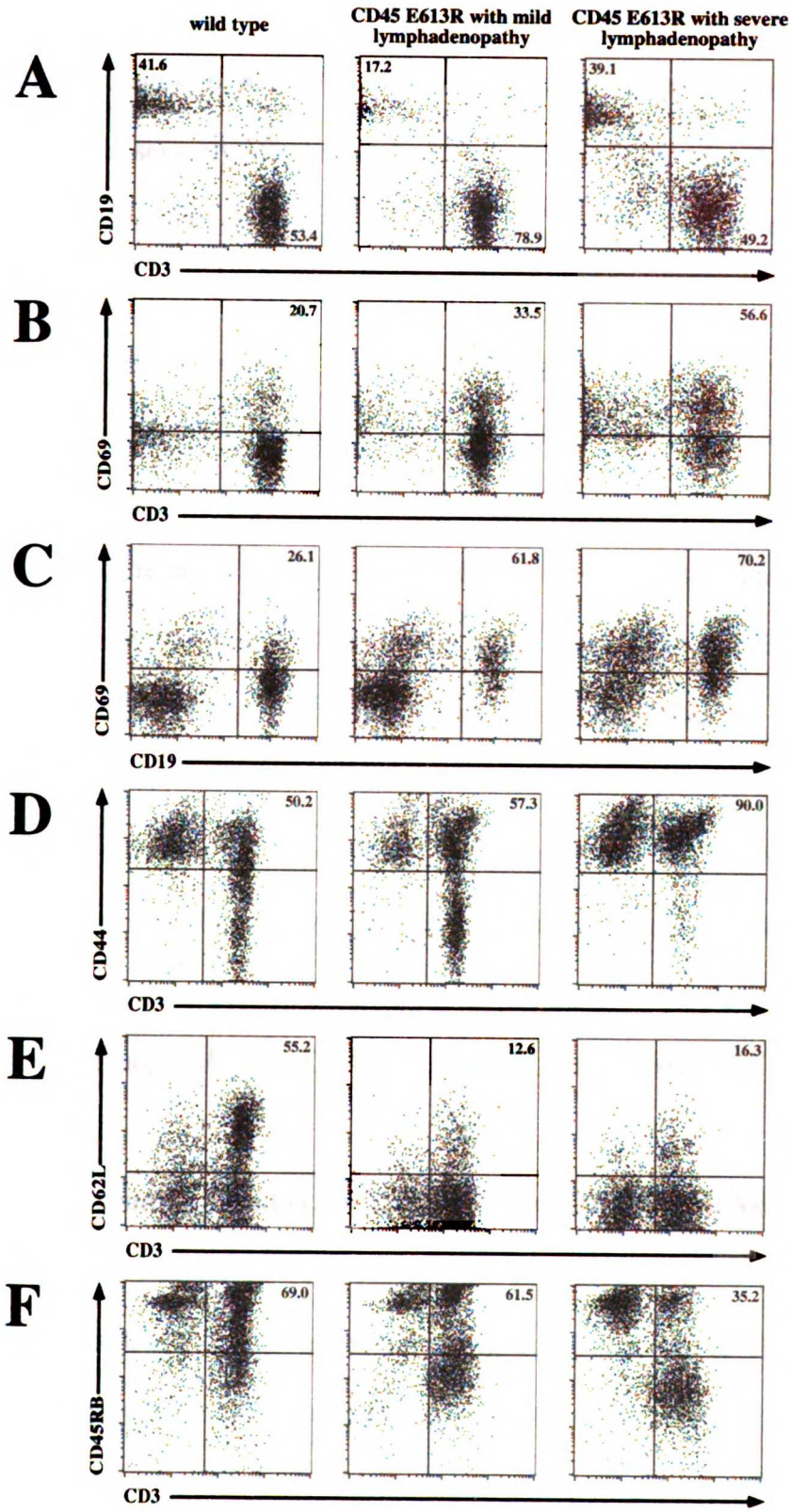

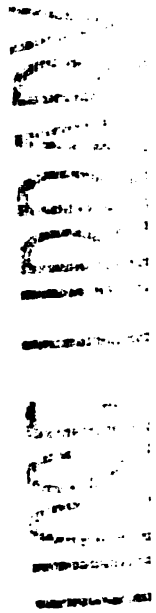

detected on 50% of wild type T cells and was increased only in mice with severe lymphadenopathy to 90% (Figure 4D). Decreased expression of CD62L and CD45RB was noted in severely affected mice, 55% versus 16% for CD62L and 69% compared to 35% for CD45RB (Figure 4E,F). CD45 E613R mice with mild lymphadenopathy exhibited a decrease only in CD62L from 55% in wild type to 13% in CD45 E613R. These surface expression patterns identify activated T cells in CD45 E613R lymphoproliferative nodes, with indications of more extensive activation in mice with severe lymphadenopathy.

No differences in surface expression of CD40L, Fas, or FasL were noted between T cells from wild type and CD45 E613R mice; furthermore, no difference in the number of $CD4^+CD25^+CTLA\text{-}4^+$ regulatory T cells was detected (data not shown). Expression of the costimulatory molecules B7-1 and B7-2 was similar on both B cells and $Mac1^+$ cells; additionally, there was no increase in the percentage of $CD5^+IgM^+$ B cells in either the spleen or peritoneal cavity of CD45 E613R lymphoproliferative mice (data not shown). Single-cell suspensions of splenocytes had a similar surface phenotype as lymph node cells in lymphoproliferative CD45 E613R mice (data not shown).

Elevated Serum IgA and IL-10 Transcripts in CD45 E613R Mice

Serum immunoglobulin levels were measured to assess global immune system activation in CD45 E613R mice. Serum IgM and total IgG levels were similar in wild type, heterozygous, and homozygous mutant mice (Figure 5A). Analysis of individual IgG isotypes revealed a 12-fold increase in serum IgG2a levels in heterozygous and homozygous CD45 E613R mice; all other IgG isotypes were statistically equivalent

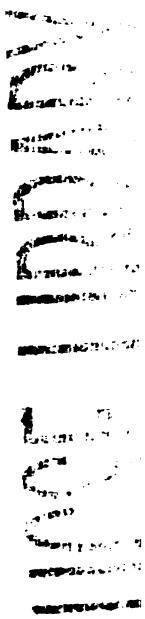

Figure 5: Evaluation of serum immunoglobulin levels and cytokine expression in CD45 E613R mice

(**A**) Elevated serum IgG2a and IgGA in CD45 E613R mice. Serum IgG2a is increased 12-fold in both CD45 E613R heterozygous and homozygous mice. Serum IgA is increased in heterozygotes (7-fold) and markedly in homozygotes (35-fold) compared to wild type mice. Serum levels of IgM, total IgG, and other individual IgG isotypes showed no significant differences. All levels were measured by enzyme-linked immunosorbent assay (ELISA). Average age of mice (in weeks) was as follows: +/+ 16.9 (n=4), +/m 16.1 (n=6), and m/m 13.5 (n=10).

(**B**) Increased IL-10 and IFN-γ transcripts in lymphoproliferative CD45 E613R mice. Expression of a panel of cytokines, including IL-4, 5, 10, 13, 15, 9, 2, 6, and IFN-γ was determined using RNA from lymph nodes and spleens of lymphoproliferative CD45 E613R mice. Quantitative RNA protection indicated an increase in the level of IL-10 and IFN-γ transcripts, but not of the other cytokines. Protected fragments corresponding to IL-10, IFN-γ, and the controls L32 and GAPDH are indicated. Data is representative of 4 control-matched mice.

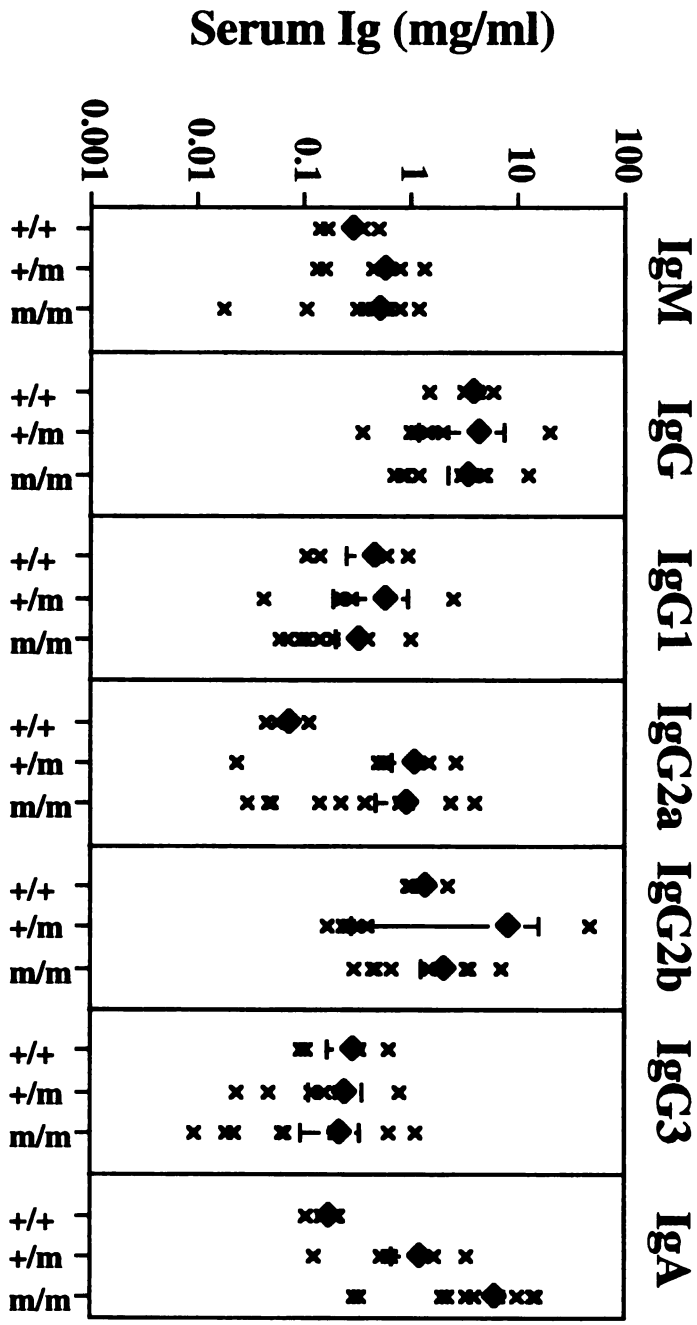
A
Serum Ig (mg/ml)
0.001
0.01
0.1
1
10
100
IgM
IgG
IgG1
IgG2a
IgG2b
IgG3
IgA
+/+
+/m
m/m

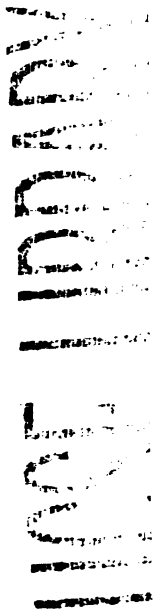

B

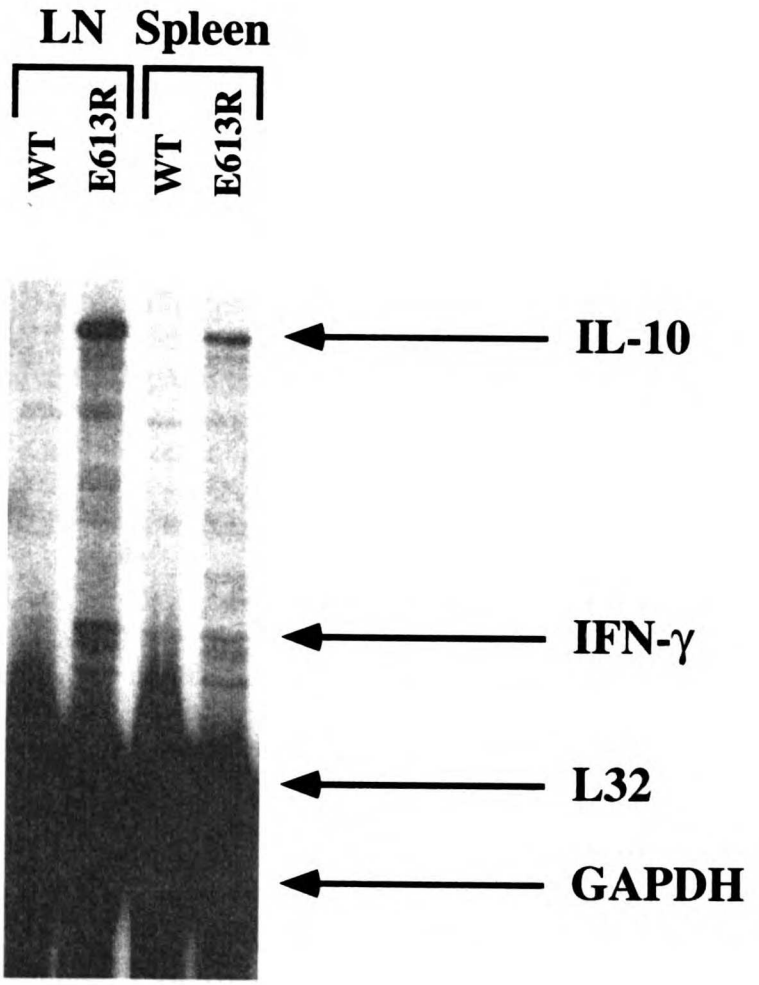

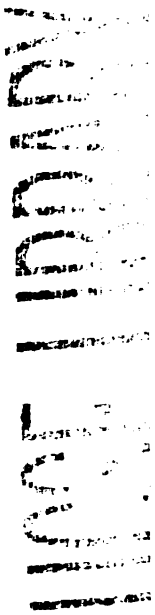

(Figure 5A). The most striking finding was a 35-fold elevated serum IgA in homozygous mutant mice, with a 7-fold increase in heterozygotes (Figure 5A).

IgA class switching and production is commonly stimulated by TGFβ; however, no increase in total TGFβ was detected in serum from these mice (data not shown). Expression of a panel of cytokines, including IL-4, 5, 10, 13, 15, 9, 2, 6, and IFN-γ was assayed using RNA from lymph node and spleen of lymphoproliferative CD45 E613R mice. Quantitative RNA protection indicated an increase in the levels of IL-10 and IFN-γ transcripts, but not of the other cytokines (Figure 5B). Increased IFN-γ probably reflects increased immune system activation in these mice and likely contributes to the elevated serum IgG2a. Accumulating evidence suggests that IL-10 has immunosuppressive functions; its elevation in CD45 E613R mice may be part of a negative feedback loop stimulated by the global immune activation found in these mice.

Autoimmune Lupus Nephritis With Autoantibody Production in CD45 E613R Mice

In the course of analyzing mice presenting with lymphadenopathy, it was observed that their kidneys appeared grossly pale and shrunken. Histological analysis of kidney sections derived from these mice demonstrated interstitial nephritis characterized by the presence of numerous mononuclear cells, tubular epithelial cell injury, interstitial fibrosis, and edema (Figure 6, panel b). Some dilated tubules contained proteinaceous casts (Figure 6, panel b). The glomeruli exhibited increased cellularity, thickened capillary loops, and an increase in mesangial matrix; in addition, karyorrhexis was noted in a segmental pattern (Figure 6, panel d). Positive silver staining in mesangial areas indicated the presence of increased matrix (Figure 6, panel f). Silver staining of the

Figure 6: Lupus nephritis in CD45 E613R mice

Panels on the left (a,c,e,g,i) are derived from age-matched wild type mice while those on the right (b,d,f,h,j) are from CD45 E613R homozygous mice.

(a,b) Normal renal architecture in wild type mice (a) and patchy interstitial nephritis (arrow) characterized by chronic inflammation, tubular injury and interstitial nephritis in mutant mice (b). (H&E)

(c,d) Normocellular glomeruli in wild type mice (c) and hypercellular glomerulus with karyorrhexis and mesangial matrix expansion in mutant mice (d). Note also the interstitial inflammation and tubular injury. (H&E)

(e,f) Slight matrix increase in glomeruli of wild type mice (e); mutant mice show a greater degree of matrix increase and double contours (arrow) in capillary loops (f). Note also pink-staining deposits within the capillary loops. (PAS-Jones silver)

(g,h) Electron micrographs showing a single capillary loop. The wild type mice had normal glomerular basement membrane without subendothelial deposits (g); foot processes are generally preserved although some coarsening is present. In contrast, mutant mice showed numerous subendothelial deposits (D) and widespread foot process effacement; additionally, note reduplication of glomerular basement membrane (arrow), which represents the double contour seen on silver stain (h). (Uranyl acetate+lead citrate)

(i,j) Immunofluorescence of kidney sections stained with FITC-labeled anti-mouse IgG. No staining is noted in wild type mice (i) while granular loop staining is noted in mutant mice (j). Scale bars (a,b,i,j) 10μM (c,d,e,f) 2μM (g,h) 1μM.

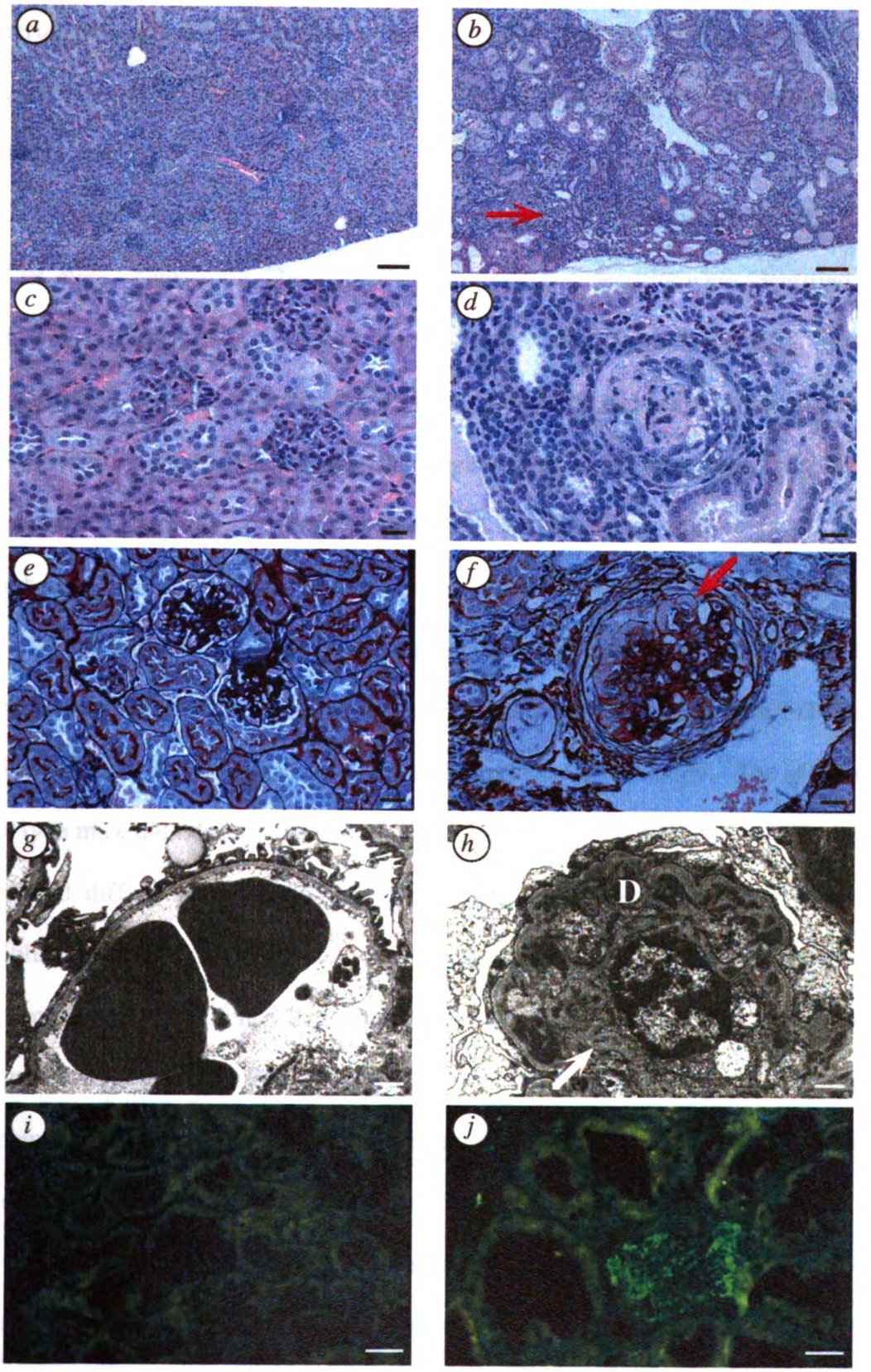
wild type
CD45 E613R
a
b
c
d
e
f
g
h
D
i
j

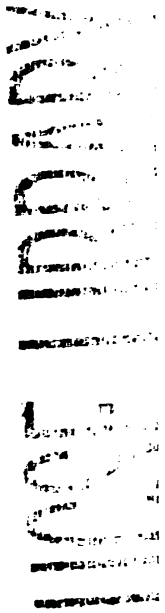

glomerular basement membrane (GBM) showed "double contours" with pink staining material between the two contours consistent with the presence of protein deposits (Figure 6, panel f). These findings were not observed in control mice (Figure 6, panels a,c,e).

Electron microscopy was performed to further analyze the glomeruli of CD45 E613R mice. Numerous subendothelial and mesangial deposits were identified, along with widespread epithelial cell foot process effacement (Figure 6, panel h). Wild type mice showed some patchy regions of foot process coarsening and small mesangial deposits, but no subendothelial deposits (Figure 6, panel g). Together, these light and electron microscopy findings support a pathological diagnosis of diffuse membranoproliferative glomerulonephritis in CD45 E613R mice.

In an attempt to identify the protein deposits within the glomeruli of CD45 E613R mice, kidney sections from wild type and mutant mice were stained with FITC-labeled anti-mouse IgG and analyzed by immunofluorescence microscopy. The glomeruli of wild type mice did not stain for IgG (Figure 6, panel i). In contrast, the mutant glomeruli exhibited diffuse granular staining of capillary loops for IgG (Figure 6, panel j), establishing that the deposits seen on both light and electron microscopy represented immune complexes. Since the serum IgA levels in the mutant mice were elevated (Figure 5A), possible IgA deposition in the glomeruli was evaluated by immunofluorescence microscopy; however, no IgA deposits were found in either the wild type or mutant mice (data not shown).

In summary, CD45 E613R mice develop immune complex-mediated glomerulonephritis identified by the presence of a diffuse membranoproliferative pattern

of glomerular injury in conjunction with both subendothelial and mesangial deposits containing IgG. This pathology is also observed in human systemic lupus erythematosus (SLE), where it is frequently accompanied by interstitial nephritis as seen here. The lesions observed in the mutant mice would be considered class IV-diffuse proliferative lupus nephritis. Thus, CD45 E613R mice develop nephritis pathologically identical to that found in humans with SLE.

The identification of immune complex deposits within the glomeruli of CD45 E613R mice strongly suggests an autoimmune etiology. In SLE, numerous autoantibodies are produced, many of which are directed against nuclear antigens. While no single type of autoantibody is diagnostic for SLE, antibodies directed against double stranded DNA (anti-dsDNA) are specific for SLE, and are detectable in serum from 60% of patients. To assess the development of autoimmunity in CD45 E613R mice, serum was collected and screened for the presence of anti-dsDNA antibodies. No wild type mice had positive titers for anti-dsDNA antibodies; however, 25% of heterozygous and 63% of homozygous mutant mice were positive with similar average titers (Figure 7A). Positive titers were detected in homozygotes as early as 9 weeks of age and in heterozygotes at 18 weeks. Thus, CD45 E613R mice spontaneously develop autoimmunity characterized by the production of anti-dsDNA autoantibodies and resulting in autoimmune glomerulonephritis.

Proteinuria, Renal Failure, and Reduced Survival in CD45 E613R Mice

The pathological identification of diffuse membranoproliferative autoimmune glomerulonephritis in CD45 E613R mice suggested that compromised renal function may

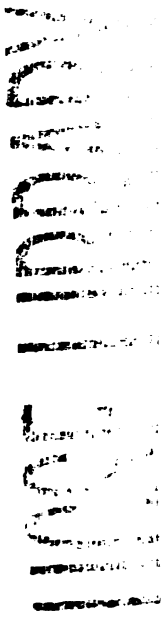

Figure 7: Autoantibodies, renal disease, and reduced survival in CD45 E613R mice

(A) Autoantibody production in CD45 E613R mice: anti-dsDNA antibody titers. Serum was prepared from mice of various ages at the time of sacrificing and anti-dsDNA antibody titers were determined by ELISA. The titer was considered positive if greater than 1/128. NA: not applicable.

(B) Kinetics of proteinuria in CD45 E613R mice. Cumulative incidence of proteinuria was measured weekly with urine dipsticks and considered to be positive if greater than 30 mg/dL (+ on a scale from 0 to ++++). Percent of mice that had positive proteinuria, defined as 2 or more positive tests, by the indicated time is shown. Cohort included: +/+ (n=11), +/m (n=12), and m/m (n=13).

(C) Reduced survival of CD45 E613R mice. The multiple pathologies of CD45 E613R mice lead to premature death so that by 30 weeks of age 89% of heterozygous and only 67% of homozygous CD45 E613R mice are alive. Cohort included: +/+ (n=11), +/m (n=12), and m/m (n=14).

A

Genotype	Positive Titers		Ave Positive Titer	Age Range	Ave Age (Weeks)
+/+	0%	(n=10)	NA	8.9 - 31.4	21.2
+/m	25%	(n=28)	1/1024	8.6 - 65.6	23.7
m/m	63%	(n=19)	1/1664	8.6 - 30.9	18.1

B

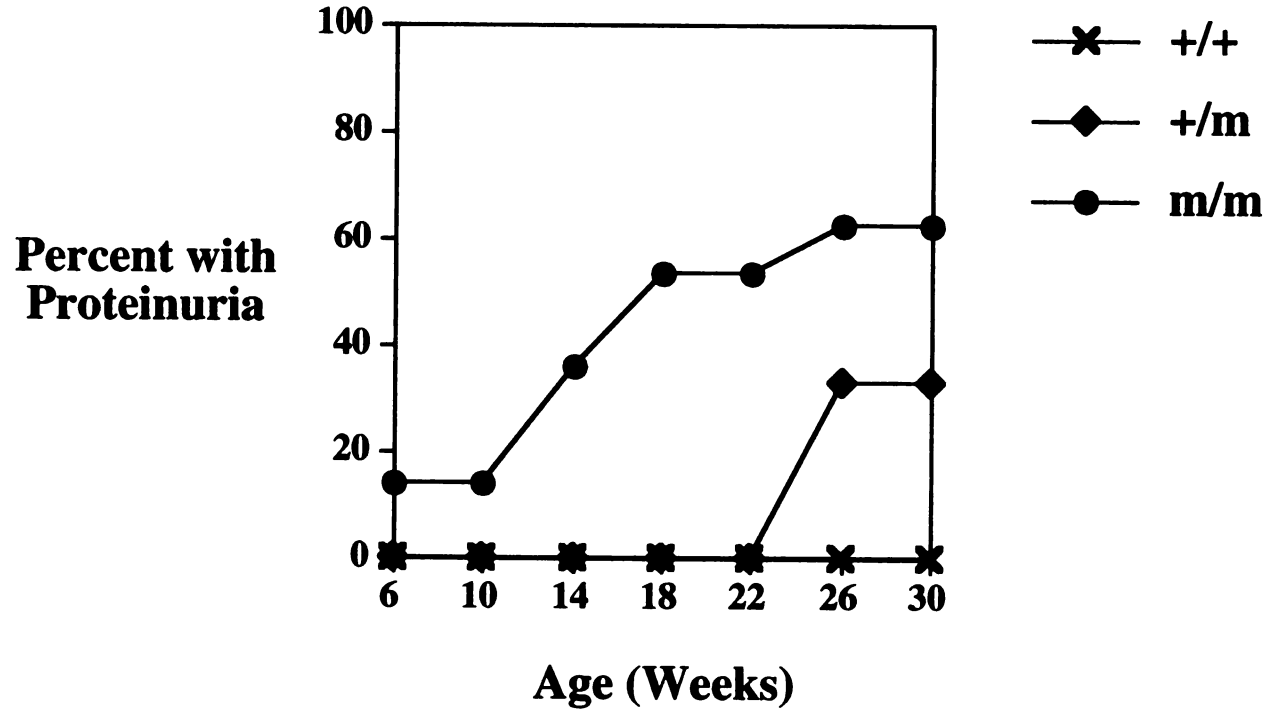
Percent with Proteinuria
100
80
60
40
20
0
6
10
14
18
22
26
30
Age (Weeks)
+/+
+/m
m/m

C

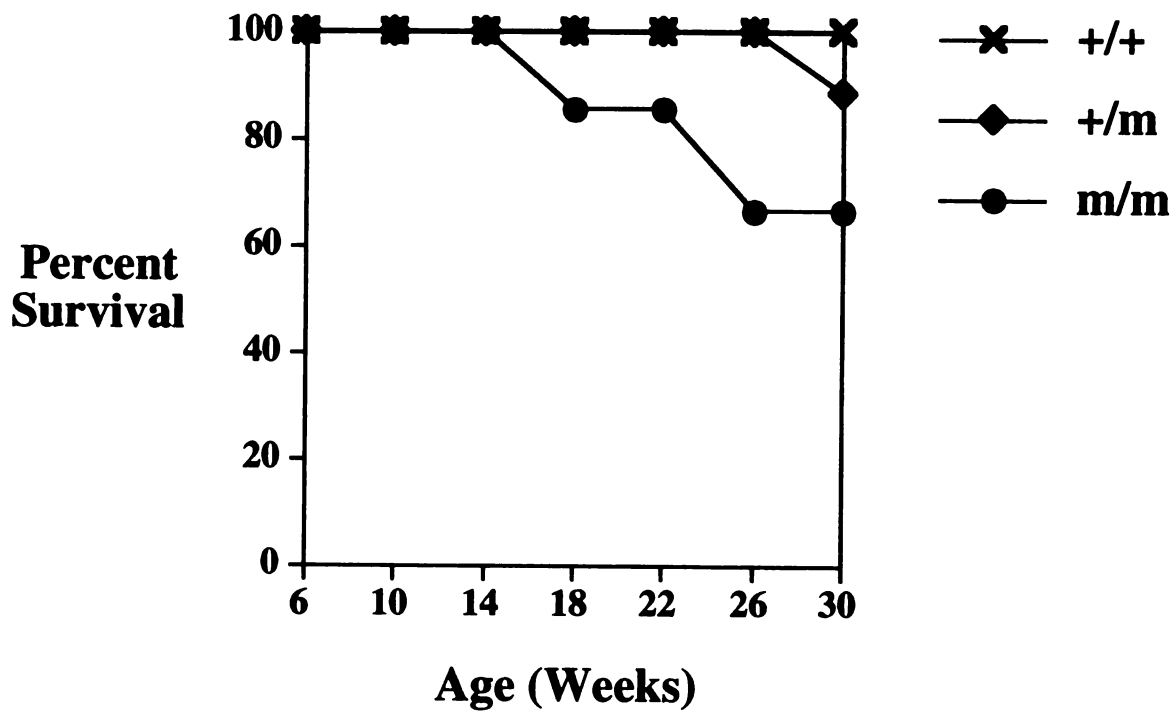
100
80
60
40
20
0
Percent Survival
6
10
14
18
22
26
30
Age (Weeks)
+/+
+/m
m/m

develop in these mice. Renal damage was confirmed by the discovery of significant proteinuria in several older mutant mice. In order to characterize the kinetics and severity of renal disease, proteinuria in a cohort of young mice was progressively followed (Figure 7B). Proteinuria, greater than 30 mg/dL, was observed in homozygous mutant mice as early as 6 weeks of age, and by 14 weeks was detected in 36% of these mice. At 22 weeks, 54% of homozygotes had exhibited abnormal proteinuria, while none was detected in heterozygous or wild type mice. However, by 26 weeks of age 33% of heterozygotes, but 0% of wild type mice, had developed proteinuria. Proteinuria was observed in both female and male mutant mice at a similar frequency. Finally, some CD45 E613R mice developed oliguria and subsequently died, suggesting renal failure leading to death.

During necropsy analysis of some CD45 E613R mice observed to be extremely thin and profoundly lethargic, massively enlarged stomachs full of undigested food were noted. No subcutaneous fat was detected in these mice, suggesting malnutrition, secondary to gastric retention of food, which may have contributed to their death. Histological analysis of the stomach and gastrointestinal tract demonstrated normal tissue architecture, including normal gut-associated lymphoid tissue (data not shown). Additionally, the stomachs were acidified, indicating normal parietal cell function. To date, no examination of gastric structure or function has been found to be abnormal in these mice; however, this phenotype is still being investigated. Strikingly, this gastric retention was observed only in female CD45 E613R mice, all of which had significant renal disease. As many human SLE patients develop peripheral neuropathies and/or peripheral vasculitis, it is possible that the gastric retention observed here is a

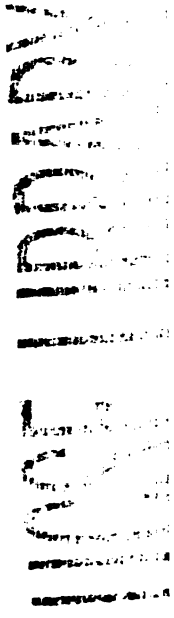

manifestation of autoimmune peripheral neuropathy and/or vasculitis. Finally, no abnormalities were noted in heart, lung, pancreas, liver, skin, or peripheral joints in any mutant mice (data not shown).

CD45 E613R mice develop multiple pathologies including lymphoproliferation, autoimmune nephritis leading to renal failure, and gastric retention leading to malnutrition. As a consequence, these mice die prematurely (Figure 7C). At 30 weeks of age, 100% of wild type mice are alive, while 89% of heterozygotes, and only 67% of homozygotes have survived. Shortened survival has also been observed in older heterozygous mice (data not shown).

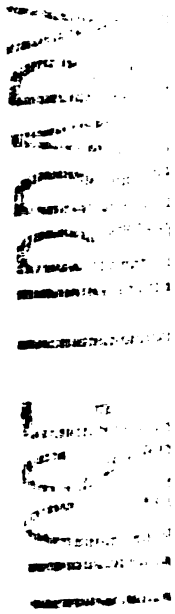

Discussion

We have proposed a model for the regulation of the RPTP CD45 in which dimerization inhibits CD45 through the symmetrical interactions of the structural wedge of one molecule with the catalytic site of the other (Figure 8A) (*49*). One prediction of this model is that mutation of the structural wedge in vivo will result in inappropriate CD45 activation under normally inhibitory dimerizing conditions, resulting in inappropriate lymphocyte activation with pathological consequences (Figure 8B).

Here we report the phenotype of mice with a single point mutation, glutamate 613 to arginine, engineered into the putative inhibitory wedge of CD45. Glutamate 613 was selected for mutagenesis based on in vitro experiments indicating that this residue is critical for negative regulation of CD45 by dimerization. The CD45 E613R mutation has no overt effect on lymphocyte development, but causes a lymphoproliferative syndrome with apparent polyclonal T and B lymphocyte activation, gastric retention, and severe autoimmune nephritis with autoantibody production. As a result, these mice die prematurely. The dramatic phenotype of CD45 E613R "knock-in" mice strongly supports our model for negative regulation of CD45 by dimerization.

Mechanistic consideration of the model predicts that dimerization of CD45 will result in inappropriate CD45 activation not only in mice homozygous for CD45 E613R, but also in mice heterozygous for this mutation. CD45 dimers in heterozygotes are expected to possess half the CD45 activity found in homozygotes, potentially leading to delayed kinetics or a less severe phenotype. This is indeed the case, as we have observed delayed onset of identical pathology in heterozygotes as seen in homozygotes.

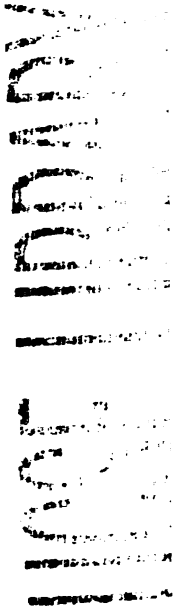

Figure 8: Model for regulation of wild type CD45 and CD45 E613R by dimerization

Both monomeric wild type CD45 and CD45 E613R dephosphorylate Lck at its negative regulatory site of tyrosine phosphorylation (Y505) allowing Lck to adopt its "primed" conformation. (A) Dimerization inhibits wild type CD45 activity through the symmetrical interaction of the inhibitory wedge and the catalytic site of phosphatase domain 1, resulting in inactive Lck and inhibition of immune responses. (B) Dimerization does not inhibit CD45 E613R activity facilitating inappropriate Lck activation leading to lymphoproliferation and autoimmunity. This models depicts the src-family kinase Lck which is highly expressed in T cells, but can apply to any src-family kinase in hematopoietic cells.

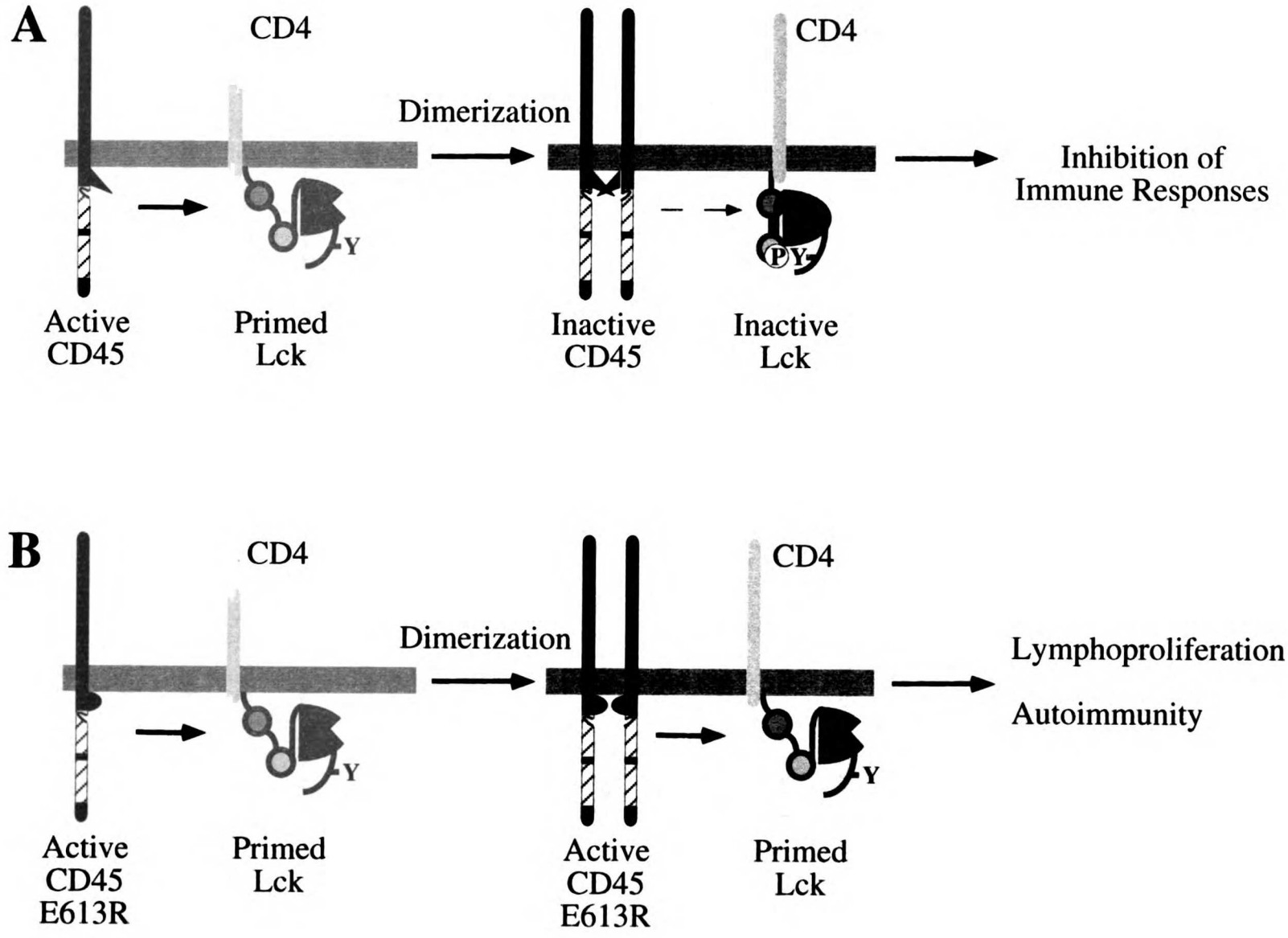

rization
negative
primed"
ugh the
phatase
s. (B)
ute Lck
the src-
family

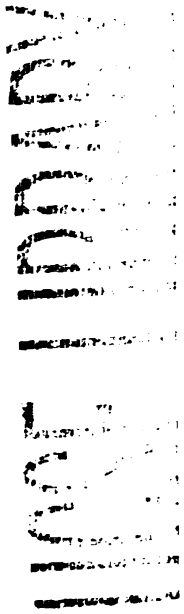

Heterozygotes develop lymphadenopathy and splenomegaly with upregulation of lymphocyte activation markers, increased IL-10 transcripts, and elevated serum IgA (Figures 4, 5 and data not shown). Heterozygotes also develop autoimmune nephritis with anti-dsDNA antibodies and proteinuria (Figure 7). However, in each case, the pathology takes longer to manifest than in homozygotes; for example, abnormal proteinuria is detected as early as 6 weeks in homozygous mutant mice, but not until 26 weeks in heterozygotes (Figure 7). The observation of a similar phenotype with delayed kinetics in heterozygous mice is consistent with our model for negative regulation of CD45 by dimerization and further indicate that E613R functions as a genetically dominant mutation.

In Which Cells Does Regulation of CD45 by Dimerization Occur?

T and B lymphocyte activation are observed in CD45 E613R mice (Figure 4), indicating that both cell types are affected by the mutation. However, the regulation of CD45 by dimerization, and thus the primary effect of the E613R mutation, may be restricted to one of these cell types, with activation of the other a secondary event. In vitro proliferative responses of purified lymph node T cells and splenic B cells from CD45 E613R mice were indistinguishable from those of wild type mice (data not shown), and so failed to identify the affected cell type. Furthermore, we have found no evidence for activation of any src-kinase, including Lck, from CD45 E613R mice, using an antiserum that specifically detects activated src-kinases (data not shown). We are currently investigating the independent contributions of T and B cells to pathology in these mice using genetic approaches.

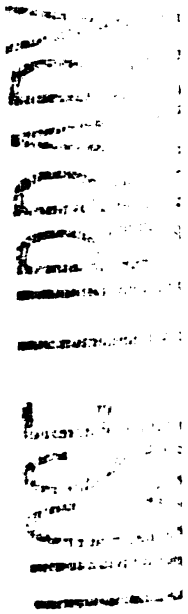

While the observation of T and B cell activation in CD45 E613R mice suggests that these cells are responsible for the pathology observed in these mice, it is possible that the primary defect occurs in non-lymphocytes as CD45 is expressed on all nucleated hematopoietic cells. For example, dysregulation of CD45 in dendritic cells could inappropriately activate these cells, in turn leading to polyclonal T and B cell activation. Such possibilities are currently being explored using CD45 E613R/ $Rag1^{-/-}$ double mutant mice, which are deficient in both T and B cells.

Regulation of CD45 Dimerization

Dimeric forms of CD45 have been observed by covalent chemical crosslinking in T cell lines, indicating that it is possible for CD45 to form dimers (*55*). One potential means of regulating CD45 dimerization is through interaction with a ligand, or perhaps differential interaction of a ligand with the various isoforms of CD45. To date, numerous attempts by many investigators have failed to definitively identify any ligand for CD45, though they do not rule out its existence. Another possible mechanism for regulating CD45 dimerization is differential spontaneous homodimerization of CD45 isoforms. The alternatively spliced exons of CD45 encode multiple sites of O-linked glycosylation so that the extracellular domain of $CD45RA^{+}$ isoforms carries a strong negative charge, which could form an electrostatic repulsive barrier to homodimerization. On the other hand, CD45R0 does not contain these glycosylation sites, and thus may homodimerize more efficiently.

Whatever the mechanism that regulates CD45 dimerization, we hypothesize that only CD45R0 dimerizes substantially and, consequently, is subject to negative regulation

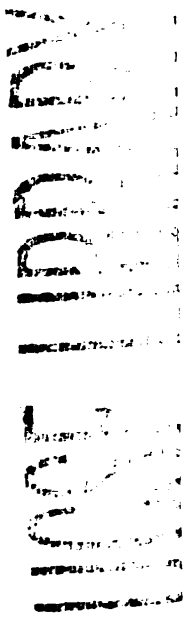

by the inhibitory wedge. We propose a model in which activated T cells, over the course of several days following stimulation, switch from expression of CD45RA$^+$ isoforms to CD45R0, which forms inactivated dimers contributing to the cessation of the primary T cell response. In CD45 E613R mice, CD45R0 dimers form normally, but fail to be inactivated due to the wedge mutation, resulting in inappropriate sustained T cell activation with pathological consequences. Thus, the T cell activation-induced alternative splicing to CD45R0 may be part of a regulatory feedback loop involved in terminating the primary T cell response to antigen through CD45 dimerization.

Regulation of Receptor Protein Tyrosine Phosphatases

The structural wedge was first identified in the dimeric crystal structure of the membrane proximal region and phosphatase domain 1 (D1) of RPTPα. Sequence alignment of the analogous region from a subset of RPTPs identified a consensus sequence for the wedge; furthermore, database screening with this consensus sequence retrieved all available D1 primary sequences, but no RPTP domain 2 or non-receptor PTP sequences (*59*). In the other RPTP crystal structures available, RPTPμ D1 (*71*) and the cytoplasmic domain of LAR (*72*), the structural wedge is also observed. These results suggest that the wedge is structurally conserved within the family of RPTPs and may also have a conserved function.

Does the structural wedge have an inhibitory function in all RPTPs? The symmetrical inhibitory interaction between the wedge and the catalytic site detected in the dimeric crystal structure of RPTPα D1 was not observed in the structures of RPTPμ D1 or LAR. In fact, only monomers were detected in both of these structures, the small

region of contact observed with RPTPμ D1 was suggested to be an artifact of crystal packing. On this basis, these authors have suggested that inhibitory dimers of RPTPμ and LAR may not form. However, as crystal structures represent only selected conformations of a molecule, these results do not rule out dimerization as a regulatory mechanism for RPTPμ and LAR. In the context of the full length molecules, dimerization mediated by the extracellular domain could alter the conformation of the cytoplasmic domain favoring interactions between the structural wedge and catalytic sites. Functional studies will be necessary to determine if these molecules dimerize and if they are negatively regulated by dimerization.

While it is possible that negative regulation of dimerization is restricted to a subset of RPTPs including CD45 and RPTPα, the primary sequence conservation and structural conservation of the wedge within the RPTP family along with the functional studies of CD45 and RPTPα support a general model for the negative regulation of RPTPs by dimerization, in which inhibition is mediated by the structural wedge.

Autoimmunity in CD45 E613R Mice

Autoimmune lupus nephritis with autoantibody production is observed in CD45 E613R mice. T cell responses required for the initiation of this autoimmune response are most likely directed against endogenous antigens. This possibility is being explored by fixing the TCR repertoire with MHC Class I or Class II-restricted TCR transgenes, which are predicted to prevent autoimmune disease; subsequent immunization with the TCR-specific peptide may then initiate disease. What antigen(s) are responsible for initiating autoimmunity? The mice used in this study were housed in a specific-pathogen free

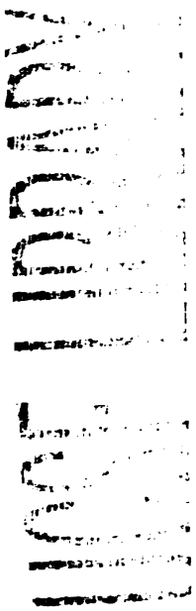

barrier facility; however, it is possible that these mice fail to control normally innocuous immune responses against food antigens or antigens from normal gut flora. These possibilities could be investigated by providing non-antigenic food, administering antibiotics to eliminate normal gut flora, or rearing the mice under notobiotic conditions. Spontaneous autoimmunity in CD45 E613R mice has been limited to anti-dsDNA antibody production and lupus nephritis. However, these mice may have a generally increased susceptibility to autoimmunity which could be revealed by immunization with autoantigens. For example, we are exploring the possibility that immunization with collagen may cause rheumatoid arthritis-like disease in CD45 E613R mice.

Our findings have significant implications regarding the genetics of human SLE. Several autoimmune mouse models of SLE exist, including complex polygenic disorders (NZB/NZW) as well as single gene disorders (ex. MRL/lpr, gld), which result in lupus-like disease when present in the background of an autoimmune prone strain (*73-75*). However, to our knowledge, CD45 E613R is the first single genetic lesion that functions dominantly in causing lupus. Although human SLE has been widely speculated to result from complex multigene factors, it is possible that this disease is a collection of rare simple Mendelian disorders as well as polygenic disorders. The ability of CD45 E613R to function as a dominant allele causing an SLE-like syndrome in mice suggests that some cases of human SLE could result from alleles that disrupt the dimer-induced inhibition of CD45 function. Studies of human SLE patients are in progress to address this; however, it is noteworthy that 3 genome analyses have identified a polymorphic allele adjacent to the CD45 locus that is weakly associated with SLE (*76-79*).

Conclusion

We have shown here that a single point mutation in the inhibitory structural wedge of CD45 is sufficient to cause lymphocyte activation leading to lymphoproliferation and spontaneous autoimmunity in mice. The dramatic phenotype of CD45 E613R mice demonstrates the in vivo importance of negative regulation of CD45 by dimerization. These results strongly support a model for the regulation of CD45, and by homology other RPTPs, in which dimerization inhibits phosphatase activity, and consequently function, through symmetrical interactions between the inhibitory structural wedge and the catalytic site.

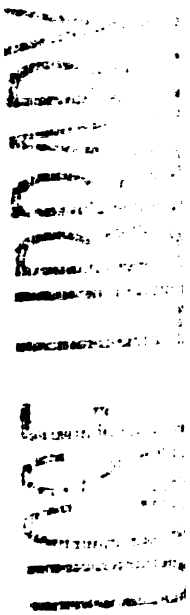

Experimental Procedures

Preparation of Targeting Construct

A P1 clone containing exon 18 of murine genomic CD45 was obtained by PCR screening (Genome Systems). Restriction mapping identified a 6.5 kb BamH I to Kpn I fragment suitable for the targeting construct which was cloned into pBluescript KS (Stratagene). Oligonucleotide-directed mutagenesis of glutamate 613 to arginine was accomplished by PCR using the following oligos: (1) gCD45mut5: tggtcagggacctttatc (2) gCD45mut3: tcactttgggtaaatgggg (3) gCD45E613R: attgccgatcggggcagactg (4) complement of gCD45E613R , and was confirmed by nucleotide sequencing. This mutagenesis scheme introduced a novel Pvu I site into exon 18, along with the E613R mutation. A lox P-flanked neomycin-resistance cassette from pL2-neo-2 (*80*) was inserted into the EcoR I site in the downstream intron. An HSV-thymidine kinase cassette from pBS/MC1-TK (*81*) was cloned into the non-homologous region of the targeting construct at a Not I site. The whole construct was linearized with Sac II, prior to transfection into 129-derived ES cells (*82*).

Generation of CD45 E613R "Knock-In" Mice

Transfected ES cells were processed and screened by standard techniques (*82*). Homologous recombination was detected in 3 out of 1200 clones by Southern blot genotyping. Two of these clones were used to generate chimeric male mice by blastocyst injection (*83*) which were bred to C57BL/6 females (The Jackson Laboratory) to identify germline transmitters. Heterozygous progeny from both lines were subsequently bred to

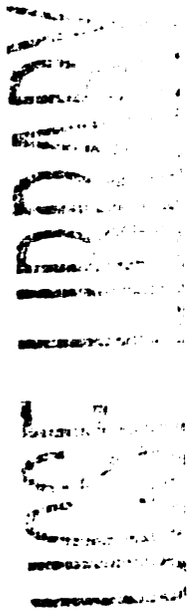

β-actin Cre transgenic mice (*84*). To identify offspring with germline excision of the lox P-flanked neomycin-resistance cassette, these mice were bred to C57BL/6 and progeny were screened for both elimination of the β-actin Cre transgene and the recombined CD45 E613R allele. Such mice represent true heterozygotes and were interbred to generate homozygous CD45 E613R mice. All mice were housed in the specific-pathogen free barrier facility at UCSF and were provided food and water ad libitum.

Southern Blot Analysis and Genotyping

Tail DNA was prepared by standard methods (*83*), digested with Hind III, and separated on a 0.8% analytical agarose gel. DNA fragments were transferred to Hybond N membrane (Amersham), and hybridized with ^{32}-P labeled probe (Rediprime II from Amersham) for at least 1 hour at 68°C, followed by low stringency washes at room temperature and a high stringency wash at 60°C. Hybridization with the 3' probe (Kpn I to Hind III 300 bp fragment) to the wild type CD45 allele produces a 7.8 kb fragment and to the E613R allele produces a 4.5 kb fragment. Genotyping was also performed by PCR using the gCD45mut5 and gCD45mut3 primers. The wild type allele generates an 800 bp band with these primers while the E613R allele produces a 950 bp band.

Flow Cytometry

Single cell suspensions were prepared from thymus, lymph node, and spleen. 10^6 cells were stained for each sample and analyzed on a FACSCalibur (Becton Dickinson). Antibodies were used at 1/100 or 1/200 and were directed against: pan-CD45-FITC, IgD-FITC, IgM-PE, CD3-biotin, CD19-PE, CD69-FITC, CD44-FITC (all from Pharmingen),

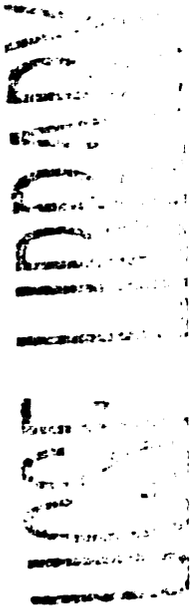

and CD62L-PE, CD45RB-biotin, CD4-PE, CD8-TC, streptavidin-tricolor (all from Caltag).

Tissue Processing and Histology

For hematoxylin and eosin or PAS-Jones staining, tissue fragments were fixed in 10% formalin for a minimum of 24 hours and were subsequently embedded in paraffin, sectioned, and stained using standard techniques. For immunofluorescence, tissue fragments were embedded in OCT, flash-frozen in liquid nitrogen, and sectioned with a cryostat. Sections were stained with sheep anti-mouse IgG-FITC (The Binding Site) at 1/50 dilution. For electron microscopy, tissue fragments were fixed in glutaraldehyde for a minimum of 24 hours; electron micrographs were prepared using standard procedures.

Serum Processing and Ig/anti-dsDNA ELISA

Serum was prepared from blood harvested by cardiac puncture at the time of sacrificing. Serum immunoglobulin levels were determined by enzyme-linked immunosorbent assay (ELISA) using an immunoglobulin isotyping kit (Southern Biotech) and standards (Southern Biotech) as per the manufacturer's protocol. IgG antibodies to dsDNA in sera from individual mice were measured by ELISA as described (*85*).

RNA Protection Assay

Single cell suspensions of lymph node cells and splenocytes were solubilized in RNAzol B (Tel-Test) and RNA was prepared following the manufacturer's protocol.

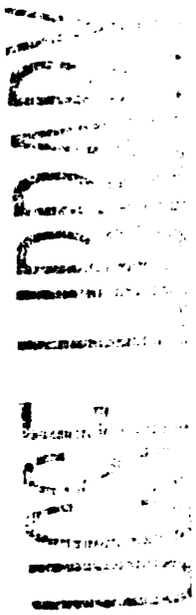

Cytokine transcript levels were determined by RNA protection assay using the Riboquant kit (Pharmingen) with the mCK-1 primer set as per the manufacturer's protocol.

Proteinuria Analysis

A cohort of mice was selected for weekly analysis of proteinuria. Urine was obtained from each mouse by manually applying pressure on the bladder. The urine was applied to a colorimetric dipstick (Bayer) and read on a scale from 0 to ++++.

CHAPTER 4

REGULATION OF CD45 AND OTHER RECEPTOR PROTEIN TYROSINE PHOSPHATASES AND FUTURE EXPERIMENTS

Summary

A model has been proposed for the regulation of CD45, and by homology other RPTPs, in which dimerization inhibits phosphatase activity, and consequently function, through symmetrical interactions between the catalytic site and the structural wedge. I have provided functional and physiological evidence supporting this model through mutagenesis of a critical glutamic acid within the wedge. The dramatic phenotype of CD45 E613R mice demonstrates the in vivo importance of negative regulation of CD45 by dimerization. However, I have been unable to demonstrate that CD45 phosphatase activity is inhibited by dimerization, a basic component of this model. In this concluding chapter, I discuss these results with a particular emphasis on a model for the regulation of CD45 dimerization during T cell activation. I also discuss the regulation of other RPTPs with an emphasis on recent experiments analyzing the regulatory role of the wedge. Finally, I conclude with a discussion of future experiments based on this work.

A model for the negative regulation of CD45 by dimerization

An original observation was made with the EGFR-CD45 chimeric molecule that ligand-induced dimerization of the CD45 cytoplasmic domain inhibited CD45 function in TCR signal transduction. The dimeric crystal structure of the membrane-proximal region and phosphatase domain 1 of RPTPα suggested a possible molecular mechanism for functional inhibition of CD45 by dimerization. A model was proposed that dimerization inhibits phosphatase activity, and consequently function, through symmetrical interactions between the catalytic site and the structural wedge. The experiments presented in this thesis were designed both to test this model and to examine the physiological role of negative regulation of CD45 by dimerization.

The first experimental approach used to test this model involved mutating residues in the putative inhibitory wedge of CD45 in the context of the EGFR-CD45 chimera and assessing the ability of EGF to inhibit CD45 function in T cell signal transduction. Two conserved acidic residues at the tip of the wedge, aspartic acid 623 and glutamic acid 624, were selected for mutagenesis. All mutations of aspartic acid 623 failed to reconstitute TCR signal transduction in CD45-deficient cells, suggesting global disruption of CD45 structure or activity. However, single point mutants in glutamate 624 were able to reconstitute these cells; furthermore, dimerization of glutamate 624-mutant EGFR-CD45 had no inhibitory effect on TCR signal transduction. This result suggested that the structural wedge was critical for negative regulation of CD45 by dimerization as dictated by the model.

The identification of a mutation capable of eliminating negative regulation of CD45 presented the opportunity to test this model in vivo and to simultaneously examine

the physiological role of negative regulation of CD45 by dimerization. The experimental approach utilized involved the generation of mice with a germline targeted mutation inactivating the inhibitory wedge of CD45 (E613R). The model predicts that this mutation will lead to inappropriate CD45 activation under normal dimerizing inhibitory conditions; such dysregulated activity would cause inappropriate src-kinase activation, with potentially pathological consequences. CD45 E613R mice were generated by standard homologous recombination techniques. These mice appear normal during the first few months of life; however, they subsequently develop a lymphoproliferative syndrome with apparent polyclonal T and B lymphocyte activation, and severe autoimmune nephritis with autoantibody production. As a result, these mice die prematurely. The dramatic phenotype of CD45 E613R mice demonstrates the in vivo importance of negative regulation of CD45 by dimerization in regulating lymphocyte activation, and, furthermore, supports the model for regulation of CD45 by the structural wedge.

These functional and physiological experiments tested and supported the proposed model, yet a major component of this model, that dimerization of CD45 directly inhibits its activity, remained to be demonstrated. Many experimental approaches were utilized to test this aspect of the model. Early experiments analyzing the in vitro phosphatase activity of immunoprecipitated EGFR-CD45 in the presence and absence of EGF failed to detect any inhibition with multiple different substrates. Further in vitro experiments with recombinant CD45 cytoplasmic domain proteins also failed to detect any difference in activity between dimers and monomers. Additional experiments were performed in cultured cells to analyze CD45 activity in the context of a full length

transmembrane molecule by assessing phosphorylation of substrate. First, analysis of tyrosine phosphorylation of total cellular Lck Y505 revealed no differences in EGFR-CD45 expressing T cells with and without EGF treatment. Second, no difference in CD45 activity was detected with a model membrane targeted substrate, CD4-LckY394F, when co-transfected with EGFR-CD45 and assayed in the presence and absence of EGF, both in 293T cells and CD45-deficient T cells. Finally, while no difference in total cellular Lck Y505 phosphorylation was detected in EGFR-CD45 expressing T cells, decreased phosphorylation of CD3-zeta and ZAP-70 was observed with addition of EGF. These molecules are substrates of Lck implying that Lck activity is inhibited upon CD45 dimerization. These observations are suggestive of increased Lck Y505 phosphorylation due to inhibition of CD45 activity as dictated by the model, but not conclusive.

Why is it that no inhibition of CD45 activity has been observed in these experiments? One possibility is that the correct assay of CD45 activity has not been utilized. Immunoprecipitation of CD45 may disrupt the inhibitory dimeric interaction; additionally, molecular constraints imposed by the plasma membrane may be essential for inhibition to occur. However, experiments in cultured cells were still unable to detect any inhibition of CD45 activity. Perhaps these experiments did not assay the correct substrate. Clearly, phospho-LckY505 is a major substrate of CD45 in cells; yet, not all the phospho-LckY505 in the cell may be a substrate for CD45. It may be necessary to assay a subset of Lck in order to detect any differences in CD45 activity. At this point one can only speculate that this subset of Lck resides in GEMs. Experiments designed to assay this pool of Lck will be critical in testing this idea (Appendix B).

Another possibility for the failure to detect inhibition of CD45 activity by dimerization is that the model is incorrect and such inhibition does not occur. While the functional and physiological experiments indicate the critical role of the structural wedge in negative regulation of CD45 by dimerization, it is possible that the wedge inhibits CD45 function through some means other than inhibition of activity. Some possibilities include: (1) interaction of the wedge with other molecules sequesters CD45 away from phospho-LckY505, (2) interaction of the wedge with other molecules directs CD45 into GEMs where it can inhibit T cell signal transduction by dephosphorylating multiple tyrosine phosphorylated substrates, and (3) intermolecular interactions of the wedge within dimers may shift CD45 substrate specificity towards phospho-LckY394, leading to downregulation of Lck activity. The structure of the CD45 cytoplasmic domain, and in particular the membrane proximal region and phosphatase domain 1, will be critical in distinguishing these possibilities.

In summary, the experiments presented in this thesis provide functional and physiological evidence in support of the model that dimerization inhibits CD45 activity and function through the interactions of the catalytic site and the structural wedge. Furthermore, these results clearly establish the in vivo importance of negative regulation of CD45 by dimerization in regulating lymphocyte activation. Unfortunately, additional experiments failed to demonstrate inhibition of CD45 activity by dimerization; this aspect of the model awaits further experimentation.

Regulation of CD45 dimerization

The experiments presented in this thesis have focused on the proposed model for the negative regulation of CD45 by dimerization. However, they do not address the significant issue of how dimerization of CD45 is regulated. Dimeric forms of CD45 have been observed by covalent chemical crosslinking in T cell lines, indicating that it is possible for CD45 to form dimers (*55*). One potential means of regulating CD45 dimerization is through interaction with a ligand, or perhaps differential interaction of a ligand with the various isoforms of CD45. CD45 is a member of the receptor-like protein tyrosine phosphatase family, so named because thus far, few ligands have been identified for proteins of this family; however, the extracellular domains of these proteins often contain motifs found in other receptors and implicated in protein-protein interactions (*50,51*). To date, numerous attempts by many investigators have failed to definitively identify any ligand for CD45, though they do not rule out its existence. CD45 does appear to make an adhesive interaction with CD22 through carbohydrate recognition, although this interaction does not regulate CD45 function (*18*). Another possible mechanism for regulating CD45 dimerization is differential spontaneous homodimerization of CD45 isoforms. The alternatively spliced exons of CD45 encode multiple sites of O-linked glycosylation so that the extracellular domain of CD45RA$^+$ isoforms carries a strong negative charge, which could form an electrostatic repulsive barrier to homodimerization. On the other hand, CD45R0 does not contain these glycosylation sites, and thus may homodimerize more efficiently.

Whatever the mechanism that regulates CD45 dimerization, I hypothesize that only CD45R0 dimerizes substantially and, consequently, is subject to negative regulation by the inhibitory wedge. I propose a model in which activated T cells, over the course of

several days following stimulation, switch from expression of CD45RA$^+$ isoforms to CD45R0, which forms inactivated dimers contributing to the cessation of the primary T cell response (Figure 1). In CD45 E613R mice, CD45R0 dimers form normally, but fail to be inactivated due to the wedge mutation, resulting in inappropriate sustained T cell activation with pathological consequences. Thus, the T cell activation-induced alternative splicing to CD45R0 may be part of a regulatory feedback loop involved in terminating the primary T cell response to antigen through CD45 dimerization.

This model implies that the pathology observed in CD45 E613R mice is derived from dysregulated CD45R0 on T cells; B cell activation and autoantibody production is presumed to be secondary to T cell activation. This implication will be tested through the generation of bone marrow chimeras in which CD45 E613R T cell precursors will be mixed with wild type B cell precursors to reconstitute irradiated Rag-deficient mice with the prediction that these mice will still develop pathology. Another experiment to test this model is to generate mice which lack expression of CD45R0. This can be accomplished by engineering a mutation into exon 4 which disrupts splicing of CD45 RNA to form CD45R0 (*86,87*), with the prediction that these mice will develop pathology similar to CD45 E613R mice. Hopefully, these experiments will clarify the role this model plays in negative regulation of CD45.

Regulation of other receptor protein tyrosine phosphatases

Additional experiments with RPTPα have indicated an essential role for the structural wedge in the negative regulation of RPTPα activity by dimerization. RPTPα is a widely expressed RPTP, with high expression in the brain (*88*). RPTPα consists of a

Figure 1: Model for regulation of CD45 dimerization during T cell activation

Naive T cells primarily express CD45RA$^+$ isoforms which exist as catalytically active monomers; consequently, Lck is in its primed conformation. Stimulation with the appropriate MHC/peptide ligand on an antigen presenting cell (APC) leads to Lck activation, and over the course of several days, a swtich to expression of CD45R0 due to alternative splicing of CD45. CD45R0 forms catalytically inactivated dimers, resulting in phosphorylation of LckY505 and Lck inactivation. This mechanism serves as a negative feedback loop to terminate the primary T cell response.

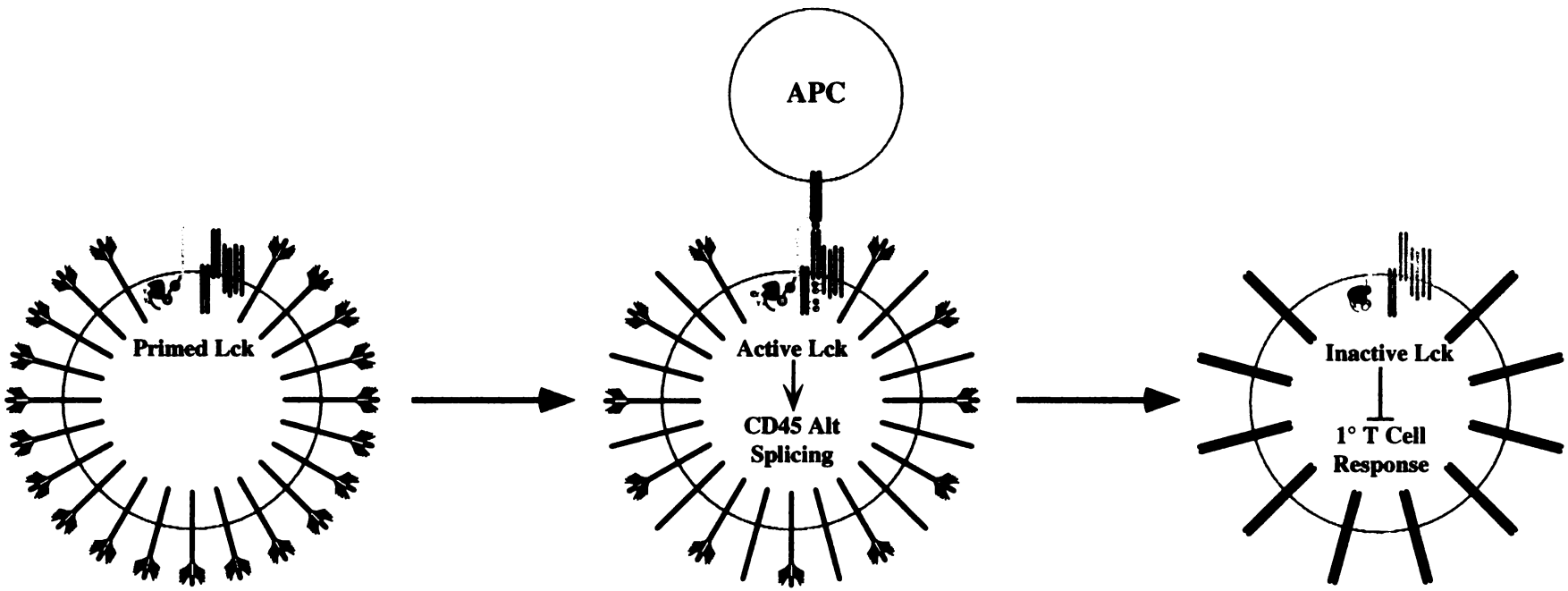
APC
Primed Lck
Active Lck
CD45 Alt
Splicing
Inactive Lck
1° T Cell
Response
Naive T Cell
CD45RA+
Stimulated T Cell
CD45RA+/CD45R0
Post-Activation T Cell
CD45R0

heavily glycosylated short extracellular domain, a single transmembrane domain, and a cytoplasmic domain containing two PTP domains. Evidence is accumulating that RPTPα functions to dephosphorylate the C-terminal site of negative regulatory tyrosine phosphorylation in the Src protein tyrosine kinase, Y529. Dimeric forms of RPTPα were "trapped" through disulfide linkages created by introduction of a cysteine residue immediately N-terminal to the transmembrane domain (*69*). Different rotational dimeric interfaces were generated by placing cysteine every 2 residues over a single turn of an alpha helix. RPTPα$^{-/-}$ cells were transduced with retroviruses encoding the various forms of RPTPα. Expression of one of four dimeric forms of RPTPα resulted in reduced Src kinase activity and hyperphosphorylation of Y529, indicating inhibition of RPTPα phosphatase activity. The fact that inhibition was observed with only one of four dimers, indicates that the manner in which the two molecules are brought together is critical for inhibition. Finally, mutations in the structural wedge of this dimeric RPTPα restored phosphatase activity, supporting the model for negative regulation of RPTPα by dimerization.

RPTPs are expressed in non-mammalian organisms including *Drosophila* where 5 RPTPs have been identified (*51*). Genetic analysis has indicated an essential role for several of these RPTPs in motor axon guidance and retinal axon target selection (*89-91*); furthermore, mutants of a specific RPTP, PTP69D, are not viable due to unknown developmental defects (*89*). PTP69D consists of an extracellular region containing two immunoglobulin-like domains and three fibronectin type III domains, a single transmembrane domain, and a cytoplasmic region with two PTP domains. Structure-function analysis of PTP69D in retinal axon targeting was accomplished through the

transgenic introduction of PTP69D mutants into the null background, which indicated that the fibronectin type III repeats and phosphatase activity are required for proper axonal targeting (*92*). The requirement for the fibronectin type III repeats indicates that the extracellular domain of PTP69D regulates its function, possibly through interaction with a regulatory ligand or by mediating adhesive interactions. These authors tested the model described above for regulation of RPTPs through the introduction of a PTP69D wedge mutant. This mutant was able to normally reconstitute the axon targeting defect in PTP69D nulls, suggesting that negative regulation by dimerization does not occur in retinal axon targeting. However, it showed poor rescue of lethality raising the possibility that PTP69D is normally inhibited by dimerization in other developmental contexts.

The functional and physiological experiments described above strongly support the model for negative regulation of CD45 and RPTPα by dimerization. However, it is not clear if the structural wedge has an inhibitory function in all RPTPs. The structural wedge was first identified in the dimeric crystal structure of the membrane proximal region and phosphatase domain 1 (D1) of RPTPα. Alignment of the analogous region from other RPTPs indicates sequence conservation suggesting a conserved structure. Consistent with this, the structural wedge (helix-turn-helix) is also observed in the two other RPTP crystal structures available, RPTPμ D1 (*71*), and the cytoplasmic domain of LAR (*72*). Thus, it is likely that the wedge is structurally conserved within the family of RPTPs and may also have a conserved function.

It is tempting to speculate that the conserved function of the wedge is to mediate symmetrical inhibition of RPTP dimers. However, the inhibitory interaction between the wedge and the catalytic site detected in the dimeric crystal structure of RPTPα D1 was

not observed in the structures of RPTPμ D1 or LAR. In fact, only monomers were detected in both of these structures; the small region of contact observed with RPTPμ D1 was suggested to be an artifact of crystal packing. On this basis, these authors have suggested that inhibitory dimers of RPTPμ D1 and LAR may not form. However, as crystal structures represent only selected conformations of a molecule, these results do not rule out dimerization as a regulatory mechanism for RPTPμ and LAR. In the context of the full length molecules, dimerization mediated by the extracellular domain could alter the conformation of the cytoplasmic domain favoring interactions between the structural wedge and catalytic sites. Functional studies will be necessary to determine if these molecules dimerize and if they are negatively regulated by dimerization.

While it is possible that negative regulation by dimerization is restricted to a subset of RPTPs including CD45 and RPTPα, the primary sequence conservation and structural conservation of the wedge within the RPTP family along with the functional studies of CD45 and RPTPα support a more general model for the negative regulation of RPTPs by dimerization, in which inhibition is mediated by the structural wedge.

The discovery that RPTPs can be negatively regulated by dimerization raises the important question of how dimerization of RPTPs is regulated. The extracellular regions of RPTPs often possess a wide array of protein motifs implicated in protein-protein interactions, including immunoglobulin-like domains, fibronectin type III domains, carbonic anhydrase-like domains, cysteine-rich regions, and others, suggesting that these molecules may be regulated by ligands or homotypic aggregation (*51,60*). In the case of RPTPα, inactivated homodimers were "trapped" through a disulfide linkage created by introduction of a cysteine residue near the transmembrane domain, suggesting that this

RPTP is able to spontaneously dimerize (*69*); however, the manner in which the monomer-dimer transition is regulated is not clear. The ectodomains of RPTPμ and RPTPκ were found to mediate homophilic binding interactions (*93-95*), but no effect of these interactions on phosphatase activity was detected. Thus, while some protein-protein interactions have been defined for specific RPTPs, in most cases regulatory mechanisms have not been identified.

Multiple ligand interactions have been defined for RPTPß/ζ, a RPTP expressed in the developing nervous system primarily on glial cells in a pattern suggestive of a function in neuronal migration and axon pathfinding (*96*). The extracellular domain of RPTPß/ζ has been demonstrated to interact with several molecules including, contactin, tenascin, multiple cell adhesion molecules (CAMs), pleiotrophin, and others. Interaction of RPTPß/ζ with these molecules, particularly contactin, affects cell adhesion and neurite outgrowth (*97*). Thus, RPTPß/ζ seems to function as a regulatory ligand for these other molecules. It is also possible that these molecules serve as regulatory ligands for RPTPß/ζ. Recently, binding of pleiotrophin, a soluble heparin-binding cytokine, to RPTPß/ζ was found to inhibit the phosphatase activity of RPTPß/ζ (*98*). This is the first demonstration of a soluble, regulatory ligand for any RPTP. Although pleiotrophin-induced RPTPß/ζ dimerization was not demonstrated, this result is consistent with the model outlined above for regulation of RPTPs by dimerization. Furthermore, this finding increases the likelihood that additional soluble regulatory ligands will be identified for other RPTPs.

Future experiments to analyze regulation of CD45

The experiments presented in this thesis support a model for the negative regulation of CD45 by dimerization through symmetrical interactions between the catalytic site and the structural wedge. However, all aspects of this model have not been thoroughly established. In particular, inhibition of CD45 phosphatase activity by dimerization has not been observed. As discussed above, the most pressing experiment to address this issue is the comparison of Lck Y505 phosphorylation in GEM-associated Lck, using the phospho-Src-specific antisera, between CD45 monomers and dimers. The mutagenesis experiments presented here indicate an essential role for the structural wedge in negative regulation of CD45 function. As discussed above, there are other possibilities for the function of the wedge besides inhibition of CD45 catalytic activity. These other possibilities can best be evaluated with a crystal structure of the CD45 cytoplasmic domain, in particular, the membrane proximal-region and phosphatase domain 1, potentially using the rD1 recombinant protein (*42*). Additionally, a yeast-two hybrid screen with the structural wedge of CD45 as the bait might identify proteins that interact with this structural motif, and, thus, may be involved in regulating CD45.

The proposed model for the regulation of CD45 is dependent on the formation of CD45 dimers. While there is chemical crosslinking evidence from the literature that CD45 can form dimers (*55*), there is no evidence that CD45 forms dimers in living cells. Several experimental approaches can be employed to address this issue. First, fluorescence resonance energy transfer (FRET) can be used to assess CD45 dimer formation in living cells. Second, engineered disulfide linkages can be used to trap CD45 dimers, as disulfide bonds will only form between molecules within dimers (*69*). Third, the β-galactosidase complementation assay can be used to measure in vivo dimerization

of CD45 (*99*). These experiments will be essential for understanding CD45 dimerization in whole cells.

Even if CD45 dimers are detected, it is still unclear how CD45 dimerization is regulated. As described above, no ligand has been identified for CD45 despite major investigative efforts. Besides ligand-induced dimerization, it is also possible that CD45 may spontaneously dimerize. It is tempting to speculate that the different isoforms of CD45 are able to differentially homodimerize, or differentially interact with a ligand. By comparing the different isoforms in the dimerization assays described above, such a regulatory mechanism may be revealed. An understanding of the mechanism by which CD45 dimerization is regulated is the major unresolved issue in the biology of CD45 and should attract the most attention in future experimentation.

Autoimmunity in CD45 E613R Mice

Autoimmune lupus nephritis with autoantibody production is observed in CD45 E613R mice. T cell responses required for the initiation of this autoimmune response are most likely directed against endogenous antigens. This possibility can be explored by fixing the TCR repertoire with MHC Class I or Class II-restricted TCR transgenes, on the TCRα-/- background, so that only the transgenic TCR is present. I predict that restricting T cell specificities in this manner will prevent autoimmune disease; subsequent immunization with the TCR-specific peptide may then initiate disease.

What antigen(s) are responsible for initiating autoimmunity? All CD45 E613R mice were housed in a specific-pathogen free barrier facility, which is not a completely sterile environment. It is possible that these mice fail to control normally innocuous

immune responses against food antigens or antigens from normal gut flora. These possibilities could be investigated by providing non-antigenic food, administering antibiotics to eliminate normal gut flora, or rearing the mice under notobiotic conditions.

These findings have significant implications regarding the genetics of human SLE. Several autoimmune mouse models of SLE exist, including complex polygenic disorders (NZB/NZW) as well as single gene disorders (ex. MRL/lpr, gld), which result in lupus-like disease when present in the background of an autoimmune prone strain (*73-75*). However, to my knowledge, CD45 E613R is the first single genetic lesion that functions dominantly in causing lupus. Although human SLE has been widely speculated to result from complex multigene factors, it is possible that this disease is a collection of rare simple Mendelian disorders as well as polygenic disorders. The ability of CD45 E613R to function as a dominant allele causing an SLE-like syndrome in mice suggests that some cases of human SLE could result from alleles that disrupt the dimer-induced inhibition of CD45 function. Studies of human SLE patients are in progress to address this; however, it is noteworthy that 3 genome analyses have identified a polymorphic allele adjacent to the CD45 locus that is weakly associated with SLE (*76-79*).

Future experiments with CD45 E613R mice

The phenotype of CD45 E613R mice clearly establishes the in vivo importance of negative regulation of CD45 by dimerization in regulating lymphocyte activation. However, little is understood about the specifics of this regulation. The major question to be explored is in which cell type does regulation of CD45 by dimerization occur? T and B cell polyclonal activation is observed in CD45 E613R mice indicating that both cell

types are affected by the mutation. However, the regulation of CD45 by dimerization, and thus the primary effect of the E613R mutation, may be restricted to one of these cell types, with activation of the other a secondary event. Analysis of the independent contributions of T and B cells to the pathology of CD45 E613R mice can be investigated using genetic approaches. The CD45 E613R mutation can be bred onto the $TCR\alpha^{-/-}$ and $Ig\mu^{-/-}$ backgrounds. These mice are deficient in T cells and B cells respectively, due to developmental arrest caused by the lack of these receptors. Analysis of these mice should indicate if T cells or B cells are either required or sufficient for development of disease, which can be easily monitored by following proteinuria. It seems almost certain that B cell-deficient CD45 E613R mice will not develop immune complex-mediated kidney disease; however, the phenotype of T cell-deficient CD45 E613R mice will be informative regarding the requirement for T cells in this disease. I speculate that both T and B cells are required for disease development.

This analysis still leaves open the possibility that while both cell types are required for disease, mutant CD45 needs to be present only in one. As described above, I favor a model in which CD45 E613R is required in T cells, but not B cells; however, B cells are required for the disease as factors produced by the dysregulated T cells will act on B cells to produce autoantibodies leading to pathology. This possibility can be tested through the generation of mixed bone marrow chimeras in irradiated Rag-deficient mice, utilizing the T and B cell-deficient CD45 E613R mice. Bone marrow from these mice as well as CD45 wild type T and B cell-deficient mice can used to generate bone marrow chimeras with combinations of T and B cells. I predict that mice reconstituted with a mixture of mutant T marrow (CD45 E613R/$Ig\mu^{-/-}$) with wild type B marrow (CD45

WT/TCR$\alpha^{-/-}$) will still develop pathology, consistent with the model proposed above for the regulation of CD45R0 on activated T cells described above.

While the observation of T and B cell activation in CD45 E613R mice suggests that these cells are responsible for the pathology observed in these mice, it is possible that the primary defect occurs in non-lymphocytes as CD45 is expressed on all nucleated hematopoietic cells. For example, dysregulation of CD45 in dendritic cells could inappropriately activate these cells, in turn leading to polyclonal T and B cell activation. This possibility can be tested by generating CD45 E613R/ Rag1$^{-/-}$ double mutant mice, which are deficient in both T and B cells. These animals can be reconstituted with CD45 wild type bone marrow and assessed for the development of disease, which would be present if the primary defect resides in a non-lymphoid cell. However, I predict that this will not be the case. These animals will also be useful to determine if the increase in extramedullary hematopoiesis observed in CD45 E613R mice is due to a primary defect in granulopoiesis or if the increase is secondary to lymphoid activation.

The experiments described here so far have focused on spontaneously developing pathology observed in CD45 E613R mice. These mice are on a mixed genetic background which may predispose them to lupus-like nephritis. Breeding these mice onto other genetic backgrounds may exacerbate or alleviate this disease, or result in the development of new disease altogether. Beyond spontaneous disease, it is possible that these mice possess an increased predisposition to autoimmunity which may be revealed by immunization with autoantigens. Such an immunization in wild type mice will have no affect, but in CD45 E613R mice it may cause autoimmune disease. Immunization with collagen may lead to a rheumatoid arthritis-like disease in these mice; or perhaps

immunization with myelin basic protein will lead to experimental autoimmune encephalitis. These experiments may not only indicate an increased predisposition towards autoimmunity, but may facilitate development of tissue-specific autoimmune animals models.

The experiments described above are focused on pathological issues related to CD45 E613R mice; however, the function of the immune system of CD45 E613R mice in response to antigenic stimulation is another important uncharacterized area. It is possible that these mice will be hyperresponsive to primary antigenic stimulation or potentially have altered development of immunological memory; additionally, they may be hyperresponsive to secondary stimulation once memory has been established. Measurement of the primary and secondary immune response against a well-characterized antigen should indicate the general function of the immune system in these mice. More complete analysis could include assays of specific immunologic functions such as T helper cell development, cytotoxic T cell killing, delayed type hypersensitivity reactions, T-dependent and T-independent B cell responses, and pathogen challenge. T cell proliferation in response to stimulation with anti-TCR antibodies revealed no differences between wild type and E613R mice. A more sensitive analysis of T cell responses can be performed with a MHC class II-restricted TCR transgene and its specific peptide.

CD45 E613R mice were generated to test the proposed model for the negative regulation of CD45 by dimerization, and the phenotype of these mice supports this model. However, there is no direct evidence from these mice that CD45 activity is increased or that the activity of src-kinases, Lck in particular, is increased. Analysis of

Lck Y394 phosphorylation in lysates derived from enlarged lymph nodes showed no difference from wild type lymph node lysates. It is possible that analysis of total cellular Lck will not be informative, as described in Appendix B. However, two additional experiments may indicate differences in Lck activation between wild type and mutant cells. First, Lck activation may be more sustained in mutant than in wild type T cells. This can be assessed by measuring Lck Y394 phosphorylation in in vitro stimulated T cells over a time course of several days. Second, Lck activation may be affected only in CD45R0 expressing T cells. Primary T cells can be stimulated in vitro and then restimulated once they have switched to CD45R0 expression. Restimulated cells can be assayed for proliferation and for Lck Y394 phosphorylation. One final genetic experiment may implicate Lck in the pathology observed in CD45 E613R mice. These mice can be bred to $Lck^{-/-}$ mice to generate CD45 E613R/$Lck^{+/-}$ mice, which should have half the normal level of cellular Lck. If the pathology is dependent on Lck activity, it may be alleviated with less Lck present. Hopefully, these experiments will help clarify the molecular basis for the pathology observed in CD45 E613R mice.

Conclusion

The results presented in this thesis support a proposed model for the negative regulation of CD45 by dimerization in which phosphatase activity and function are inhibited by symmetrical interactions between the catalytic site and a structural wedge. Many aspects of this model remain to be thoroughly established, and should be an area of future experimentation. In particular, the major unresolved issue in the biology of CD45 is an understanding of the mechanism by which dimerization of CD45 is regulated.

Nonetheless, CD45 E613R mice are a valuable reagent for exploring the role of negative regulation of CD45 by dimerization in lymphocyte activation in vivo.

APPENDIX A

EXPRESSION AND PURIFICATION OF RECOMBINANT CD45 PROTEINS WITH ANALYSIS OF IN VITRO PHOSPHATASE ACTIVITY

Summary

A model has been proposed for the regulation of CD45, and by homology other RPTPs, in which dimerization inhibits phosphatase activity, and consequently function, through symmetrical interactions between the catalytic site and the structural wedge containing the acidic residues. I have provided evidence supporting this model including functional and physiological assays. However, it remains to be demonstrated that CD45 phosphatase activity is inhibited by dimerization, an essential component of this model. Recently, recombinant CD45 phosphatase domain 1 has been expressed and purified in *E. Coli* and found to consist primarily of dimers. Here I describe the expression and purification of recombinant CD45 proteins and assays of phosphatase activity upon dimerization. Recombinant domain 1 dimers with an E613R mutation were found to have the same activity as wild type domain 1 dimers. Furthermore, using an inducible dimerization system, no difference in phosphatase activity was detected between monomeric and dimeric full length CD45, although the existence of dimers was not formally demonstrated. Thus, these experiments failed to demonstrate wedge-dependent inhibition of CD45 phosphatase activity upon dimerization.

Introduction

The cytoplasmic domain of CD45 can be subdivided into 5 domains: a membrane-proximal region (containing the wedge), phosphatase domain 1, a spacer region, phosphatase domain 2, and a C-terminal tail (Figure 1). Recombinant proteins comprising the whole cytoplasmic domain have been expressed and purified in *E. Coli* and found to be active against a large number of phosphotyrosine containing substrates in vitro (*40,41*).

Early experiments focused on the independent contributions of PTP domain 1 and PTP domain 2 to total CD45 phosphatase activity. Mutation of the essential catalytic cysteine of domain 1 completely eliminated activity of the recombinant protein, while mutation of the catalytic cysteine of domain 2 had no effect on total phosphatase activity, suggesting that only domain 1 is catalytically active (*40,41*). More recent experiments have determined the chemical mechanism of protein tyrosine phosphatase catalysis (*39*). In addition to the cysteine nucleophile, a consensus sequence has been identified with invariant residues essential for catalysis. These residues are present in the primary sequence of CD45 PTP domain 1, but not CD45 PTP domain 2. Thus, PTP domain 2 cannot contribute directly to the catalytic activity of CD45.

Early experiments with recombinant proteins failed to demonstrate any phosphatase activity from CD45 PTP domain 1 alone, leading to the suggestion that PTP domain 2 is required for domain 1 to be active (*40*). However, recently a recombinant protein consisting of the membrane-proximal region and phosphatase domain 1 (rD1) has been carefully purified and found to be catalytically active (Figure 1) (*42*). Intriguingly,

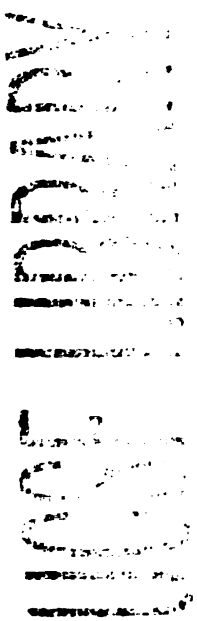

Figure 1: Schematic representation of the CD45 cytoplasmic domain and recombinant rD1 protein

The cytoplasmic domain of CD45 can be subdivided into 5 domains (top): a membrane-proximal region (MP), phosphatase domain 1 (PTP D1), a spacer region (SP), phosphatase domain 2 (PTP D2), and a C-terminal tail (CT). The recombinant rD1 protein found to have phosphatase activity consists of the membrane-proximal region, phosphatase domain 1, and the spacer region (bottom).

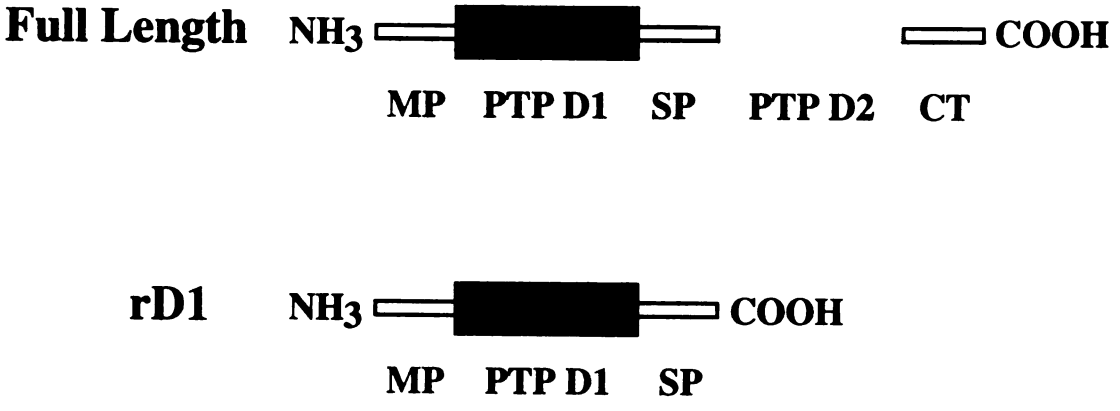
Full Length
NH3
COOH
MP
PTP D1
SP
PTP D2
CT
rD1
NH3
COOH
MP
PTP D1
SP

rD1 was found to be less active than the full-length cytoplasmic domain. Gel filtration analysis indicated that while the full-length cytoplasmic domain is a monomer, rD1 is a dimer. One explanation for these observations is that phosphatase domain 1 activity is inhibited in dimers due to the interaction of the wedge with the opposing catalytic site; in the full length protein, this interaction is prevented by the presence of domain 2, which could form an intramolecular interaction with the membrane-proximal region or domain 1. In fact, these authors detected such an interaction using GST-pull downs and tryptic protein fragments. Here I describe an experiment to test this model by generating rD1 protein with an E613R mutation in the wedge; the model predicts that the E613R rD1 protein will have increased activity compared to the wild type rD1 protein. However, I detected no difference in the activities of these proteins.

Another approach to assess the consequences of dimerization of CD45 on phosphatase activity is to employ a system for inducible dimerization. Inducible dimerization of the CD45 cytoplasmic domain in vitro can be accomplished by fusing it to *E. Coli* DNA gyrase B. A subunit of DNA gyrase B (GyrB) is the target for the antibiotics novobiocin and coumermycin (*100*). While novobiocin binds a single molecule of GyrB, coumermycin contains two binding sites which bind two molecules of GyrB in a dimer. Thus, fusion of GyrB to a protein should enable dimerization through the addition of coumermycin, with novobiocin serving as a monomeric control (*101*). Here I describe the expression and purification of a CD45-GyrB fusion protein and phosphatase activity assays in the presence of coumermycin and novobiocin. No difference in the activity of the CD45-GyrB fusion protein was detected in the presence or absence of coumermycin, although the existence of dimers was not formally

demonstrated. Collectively, these experiments failed to demonstrate wedge-dependent inhibition of CD45 phosphatase activity upon dimerization.

Results and Discussion

Analysis of recombinant CD45 E613R domain 1 protein

A recombinant protein consisting of the membrane-proximal region and phosphatase domain 1 of CD45 (rD1) was found to form dimers with reduced activity compared to the full length cytoplasmic domain (*42*). To test the possibility that the wedge is responsible for inhibition of catalytic activity in these dimers, I collaborated with these authors to generate an identical recombinant protein containing the E613R mutation in the wedge. Mutagenesis and preparation of the expression constructs was performed by me, while expression, purification, and phosphatase activity assays were preformed by the collaborators. The results indicated that the activity of the E613R rD1 protein is not different than the wild type rD1 protein.

The wild type rD1 protein was originally found to have 3-fold less activity than the full length cytoplasmic domain protein (*42*). This fact along with the observation that rD1 forms dimers suggested that the dimers may be inhibitory. However, the rD1 protein is expressed very poorly and in small quantities. In fact, these investigators are the only ones to successfully prepare catalytically active D1 protein; presumably, the protein is unstable and unfolds easily. Thus, the reduced activity of the wild type rD1 dimers may arise from the presence of misfolded protein in the sample. Why is there no effect of the E613R mutation on rD1 activity? It is possible that the rD1 protein does not dimerize with a wedge/catalytic site interaction. Such a conformation may require the context of the full length protein anchored to the membrane. In the absence of such an interaction, one would expect no effect of the E613R mutation on rD1 activity. The best way to

resolve these possibilities is by determining the stucture of the rD1 protein using X-ray crystallography.

Analysis of recombinant CD45-GyrB fusion protein

In order to inducibly dimerize the CD45 cytoplasmic domain, GyrB was fused to the C-terminus of CD45 and subcloned into a 6xHis-tagged expression vector for *E. Coli*. This expression construct was transformed into BL21-codon plus *E. Coli* which were subsequently used for protein expression. Since recombinant CD45 is unstable, the protocol for purification is modified from standard protocols so that induction of protein expression is carried out at 25°C. The protein purificiation procedure consists of three main steps: (1) preparation of bacterial lysate, (2) purification on a nickel resin, and (3) FPLC anion exchange chromatography (see detailed protocol in experimental procedures). FPLC fractions were analyzed for tyrosine phosphatase activity and for protein by Coomassie staining and western blotting (Figure 2 A,B,C). Fractions containing the recombinant protein were pooled, desalted, concentrated, and stored in 50% glycerol at -70°C.

The phosphatase activity of the CD45-GyrB fusion protein was assayed using a Lck phospho-Y505 peptide as the substrate and measuring the release of free phosphate. Coumermycin was added over a range of 0.05 nM to 50 μM final concentration. No difference in the release of free phosphate was detected over this entire range, indicating no modulation of the activity of CD45-GyrB by coumermycin.

Several possibilities exist for the failure to detect inhibition of CD45-GyrB fusion proteins by the addition of coumermycin. (1) Coumermycin may not actually dimerize

Figure 2: Purification of recombinant CD45 and CD45-GyrB fusion proteins

(**A**) Fast pressure liquid chromatography (FPLC) traces of anion exchange chromatography of 6xHis:CD45 (left) and 6xHis:CD45-GyrB (right). The blue trace indicates the UV reading (OD_{280}) of each fraction. The red trace indicates salt concentration (not working on left trace). Fraction numbers are indicated on the UV trace. Note that most of the protein does not stick to the column and runs out in the flow through. There is a large peak from fractions 5-9 and a second peak around fractions 11-14. Phosphatase activity of fractions 5-14 is indicated as OD_{405} from pNPP hydrolysis at the bottom. Most activity is found in fractions 5-9, but a second peak of activity is detected in fractions 11-14.

(**B**) Coomassie stain of proteins in FPLC fractions. Proteins in the indicated FPLC fractions were separated by SDS-PAGE and stained with Coomassie. 6xHis:CD45 (~85 kDa) is present primarily in fractions 5-8. 6xHis:CD45-GyrB (~113 kDa) is present primarily in fractions 7-9. Molecular mass markers are indicated on the left. Note that fractions 11-14 (the second peak of phosphatase activity) contain a protein of approximately 50-55 kDa.

(**C**) Western blot of proteins in FPLC fractions. Proteins in the indicated FPLC fractions were separated by SDS-PAGE and blotted with antibody directed against the Xpress epitope in the N-terminus of the 6xHis expression vector. Proteins of the expected sizes are detected for both 6xHis:CD45 (~85 kDa) and 6xHis:CD45-GyrB (~113 kDa). Molecular mass markers are indicated on the left. Note that the 50-55 kDa protein detected in fractions 11-14 is detected with the anti-Xpress antibody suggesting that it is a proteolytic or partial fragment of 6xHis:CD45.

A

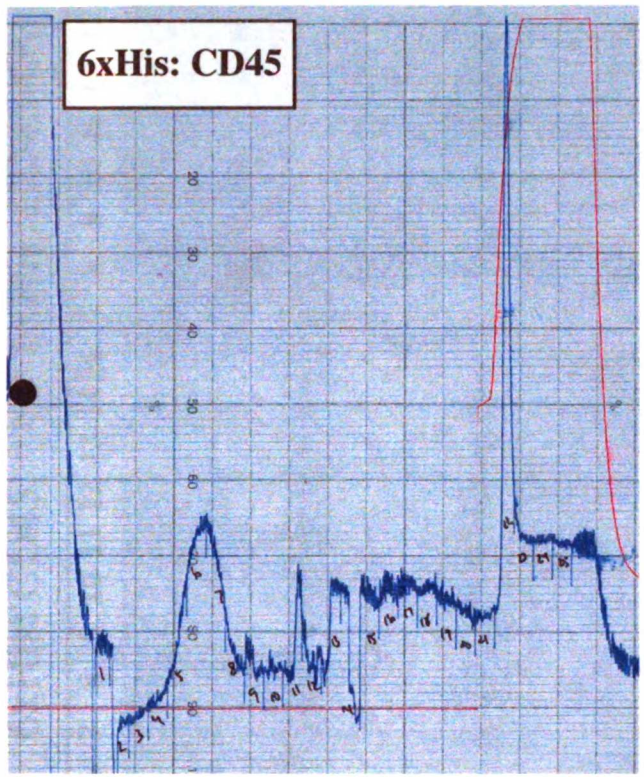

5	6	7	8	9	10	11	12	13	14
0.45	1.07	1.08	0.63	0.31	0.22	0.54	0.66	0.33	0.17

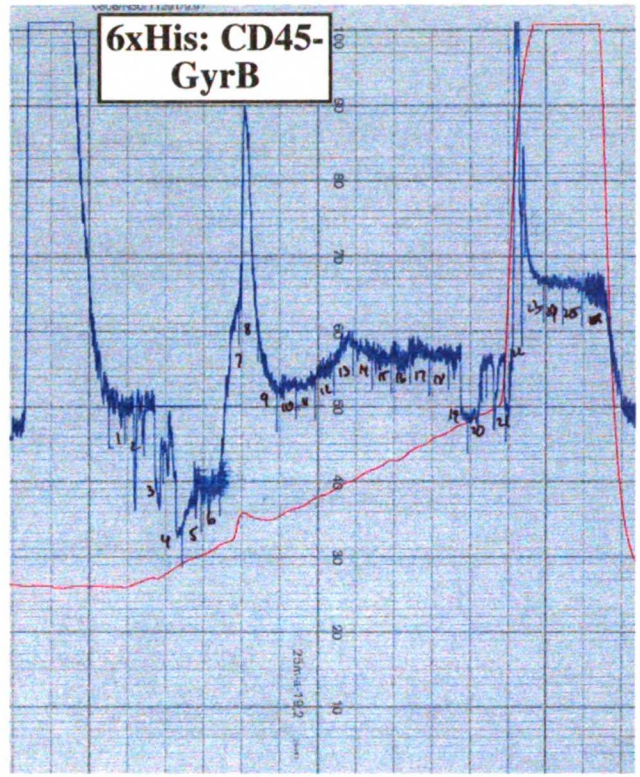

5	6	7	8	9	10	11	12	13	14
0.10	0.24	0.58	1.16	0.42	0.18	0.18	0.28	0.46	0.38

B

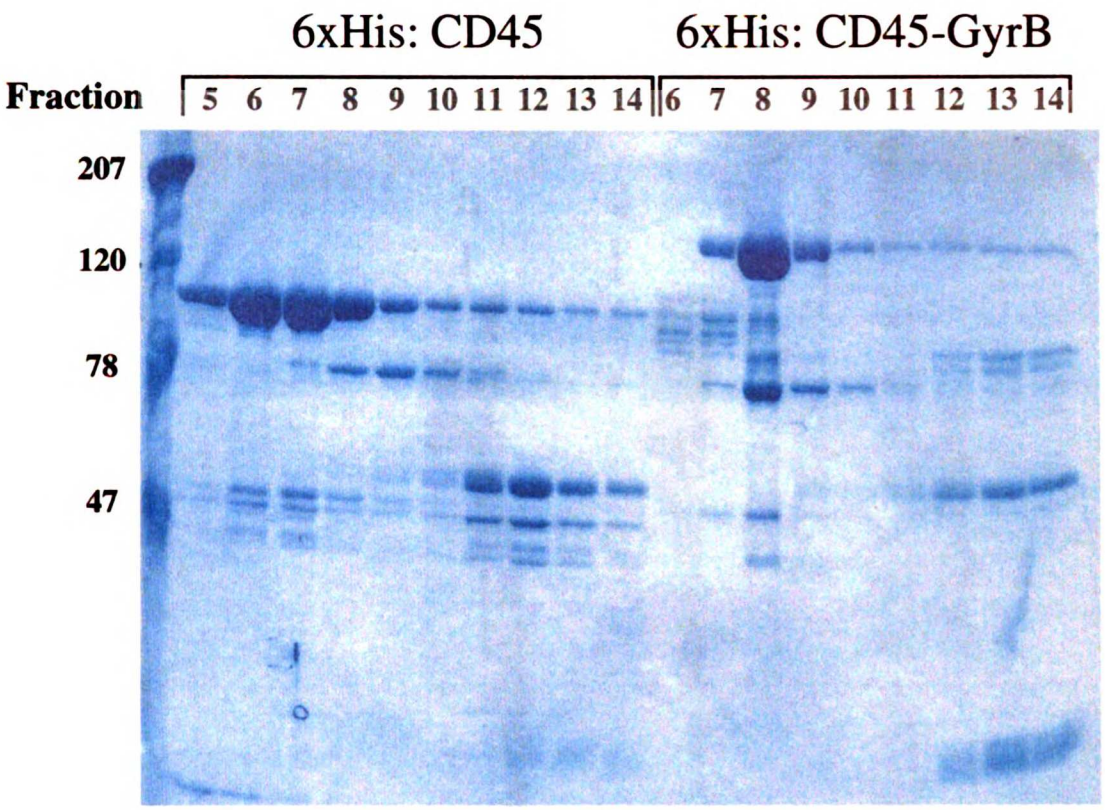
6xHis: CD45
6xHis: CD45-GyrB
Fraction
5 6 7 8 9 10 11 12 13 14
6 7 8 9 10 11 12 13 14
207
120
78
47

C

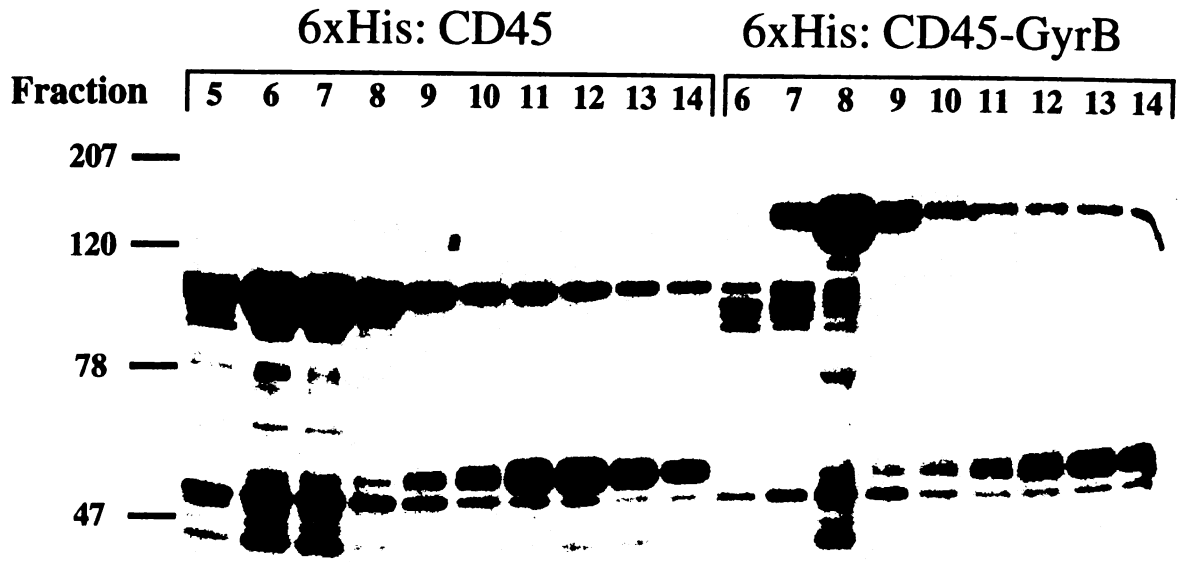
6xHis: CD45
6xHis: CD45-GyrB
Fraction
5 6 7 8 9 10 11 12 13 14
6 7 8 9 10 11 12 13 14
207
120
78
47

CD45-GyrB under the conditions utilized here. It remains to be formally demonstrated that dimers do form; this can be best accomplished through the use of equilibrium sedimentation analysis but requires higher protein purity than accomplished here. The use of a gel filtration step to separate impurities would make such analysis possible. One advantage of this analysis is that it requires little protein which is salvagable after the experiment. (2) Dimerization does occur, but it does not result in the interaction of the wedge with the opposing catalytic site. Such an interaction may require the molecular constraints imposed by the transmembrane domain of CD45. Additionally, it is possible that the GyrB-mediated dimerization brings the wrong face of CD45 together in the dimer. The C-terminal fusion was chosen to allow the cytoplasmic domain of CD45 more rotational freedom in forming dimers; perhaps spacers of different sizes need to be added at the fusion point to change the face of the dimeric interaction. (3) The correct substrate may be the entire Lck protein rather than a peptide. Inhibition of activity towards the whole protein may be more strict than that against a peptide as the presence of the whole protein adds additional steric constraints. Furthermore, the substrate may have to be present in lower concentrations to detect any inhibition; unfortunately, detection of free phosphate release requires a higher concentration of substrate. Radioactively labeled substrate would be more sensitive and permit lower substrate concentrations. The CD45-GyrB fusion approach may still prove to be successful with the modifications described here.

Partial fragment of 6xHis:CD45 has phosphatase activity

In the course of purifying 6xHis:CD45, it was observed that a second peak of phosphatase activity was eluting at a slightly higher salt concentration than the main peak from FPLC anion-exchange chromatography. This second peak corresponded to a small peak in the UV trace in fractions 11-14 (Figure 2A). Coomassie and western blot analysis indicated that the phosphatase activity co-purified with a 50-55 kDa protein that contained the N-terminal epitope of the 6xHis expression construct, suggesting that it is a partial fragment or proteolytic product of 6xHis:CD45 (Figure 2B,C). Based on the size, this protein would consist primarily of phosphatase domain 1. It would be interesting to find out the identity of this protein fragment, and in particular its C-terminal sequence, as it probably represents a stable domain 1 protein. This can be accomplished by C-terminal peptide sequencing which does not require large quantities of protein.

Experimental Procedures

Generation of Expression Constructs

(1) Preparation of E613R rD1 expression construct

The E613R mutation was introduced into pShuttle:RABC (*42*) by overlapping PCR using the following oligos: mCD45.5b: ttgaggtggaaagcttgaaac, mCD45.3: gccagtattctgcgcacttg, and gCD45E613R and its complement (Chapter 3) to generate pShuttle:RABC E613R. pShuttle:RABC E613R and was digested with EcoR V and Xma I and a 1.6 kb insert was cloned into a 5.2 kb vector fragment from pShuttle:RABC D1 (*42*) digested with EcoR V and Xma I to generate pShuttle:RABC E613R D1. Plasmids were verfied by nucleotide sequencing. These vectors were sent back to the collaborators for cloning into the pET3D-6His IEGR expression plasmid.

(2) Preparation of 6xHis:CD45 and 6xHis:CD45-GyrB expression constructs

pBS:KS (Stratagene) was digested with Xba I, filled-in, and ligated to itself to kill the Xba I site generating pBS:KS-Xba. The CD45 cytoplasmic domain was cut out of pBS:CD45CY and cloned into pBS:KS-Xba by digestion with Sal I and Hind III. The stop codon in this vector was mutated to Xba I by overlapping PCR using the following oligos: Y1193F: caacttatacccttcgtgtc, standard T7, GyrB1: aatcaaggttcatctagaaagacataaatg, and its complement GyrB2. The resulting vector was digested with Xba I and Hind III and the Xba I-Hind III fragment of pKS:GyrB (*101*) was subcloned in to generate pBS-Xba:CD45-GyrB. Finally, pBS:CD45CY and pBS-Xba:CD45-GyrB were digested with Xho I and Hind III and the protein encoding

fragments were subcloned into the pTrcHisA expression vector (Invitrogen) digested with Xho I and Hind III. Plasmids were verified by nucleotide seuquencing. pTrcHisA is a prokaryotic expression plasmid designed for inducible expression of 6xHis fusion proteins in *E. Coli.* Immediately C-terminal to the his-tag and upstream of the multiple cloning site is a sequence encoding an Xpress epitope detectable with anti-Xpress antibody (Invitrogen).

Expression and purification of 6xHis:CD45 recombinant proteins

The following is a detailed protocol:

1. Grow 5 ml overnight saturated cultures of expression plasmids in BL21 codon plus (Stratagene)

2. Inoculate 1L TB-Amp (100 μg/ml) with 5 ml culture

3. Grow at 37°C until OD_{600}~0.8-1.0

4. Cool at 4°C for 10 min

5. Induce with 1ml 100 mM IPTG (final 0.1 mM IPTG) and switch to 25°C shaker in cold room

6. Shake for 24 hours

7. Pellet cells 30 min at 3000 rpm in 1L bottles at 4°C

8. Wash 1x with cold saline (**NO PBS**) and transfer to GSA, pellet 4000 rpm 10 min at 4°C

9. Using spatula, transfer pellet to mortar and pestle containing liquid nitrogen

10. Mash bacteria into a fine powder and transfer to a 50 ml conical tube pre-cooled in dry ice

11. Attach cap loosely and use parafilm to secure cap - store in -70°C freezer (long term OK)

12. Resuspend pellet in 10 ml ice cold lysis buffer

13. Sonicate 3 cycles, 30 seconds each cycle (settings 4 and 40)

14. Incubate on ice 15-20 min

15. Transfer to disposable SS34 tubes and spin 20 min, 12000 rpm

16. Transfer supernatant to a fresh 15 ml conical tube on ice

17. Prepare ProBond (Invitrogen) columns (BioRad):

- pack resin to ~ 2 ml packed volume: pipette in resin, place the column in a Falcon tube, and spin at 1000 rpm for 2 min, aspirate and repeat as needed
- wash 2x with distilled water
- wash 3x with lysis buffer (7 ml each wash)

18. Take 5 ml of lysate and add to ProBond column, mix 10 min in cold room

19. Spin 1000 rpm 2 min, take off lysate, and repeat with remaining 5 ml of lysate

20. Wash 2x with lysis buffer

21. Wash 3x with wash buffer (preferably until OD_{280} <0.01)

22. Wash 3x with wash buffer + 100 mM imidazole

23. Add 2.5 ml of elution buffer and mix 10 min in cold room

24. Spin 1000 rpm 2 min, take off sup to a fresh 15 ml conical tube

25. Desalt with PD-10 desalting column (Amersham/Pharmacia) in cold room

- remove top and bottom caps and cut off tip at bottom of column
- equilibrate column by gravity flow with 25 ml of PD-10 buffer
- apply sample in 2.5 ml volume
- elute with 3.5 ml PD-10 buffer

27. Concentrate eluate to a volume less than 2 ml with Centricon 30/50 (Amicon)

- rinse Centricon 1x with cold ddw
- load 2 ml into Centricon 50 and spin 10 min at 6500 rpm in SS34
- add remaining sample and repeat
- collect sample and add PD-10 buffer to ~ 1.75 ml

28. For anion-exhange chromatography, load sample onto HiTrap Q column (Amersham/Pharmacia) and elute using a 25 ml gradient from 150 to 400 mM NaCl, collecting 1 ml fractions (see FPLC instruction manual chapter 5.2)

29. Assay 5 µl of each fraction with pNPP for PTP activity and pool fractions with most activity

30. Concentrate using Centricon 30/50 by repeatedly adding 2 ml to Centricon

31. Add 1.5 ml final buffer and concentrate - repeat 4 times

Final Buffer: 150 mM NaCl
50 mM Tris (pH 8)
1 mM EDTA (pH 8)
1 mM DTT

32. Concentrate maximally and collect protein sample

33. Add glycerol to 50%

34. Quantitate by Bradford and store at -70°C

The following are the various buffers:

Lysis buffer:
1% Triton X-100
20 mM Tris (pH 7.5)
150 mM NaCl
5 mM 2-ME
20 mM imidazole (pH 7.2)
protease inhibitor tablet added fresh (Roche Biochemicals)

Wash Buffer:
1% Triton X-100
20 mM Tris (pH 7.5)
500 mM NaCl
5 mM 2-ME
20 mM imidizole (pH 7.2)
protease inhibitor tablet added fresh
pH to 6.0

Wash Buffer + :
100 mM imidazole
1% Triton X-100
20 mM Tris (pH 7.5)
500 mM NaCl
5 mM 2-ME
100 mM imidizole (pH 7.2)
protease inhibitor tablet added fresh
pH to 6.0

Elution Buffer: 1% Triton X-100
20 mM Tris (pH 7.5)
150 mM NaCl
5 mM 2-ME
1 M imidizole (pH 7.2)
protease inhibitor tablet added fresh
pH to 6.0

PD-10 Buffer: 0.1% Triton
20 mM Tris (pH 8)
150 mM NaCl
1 mM EDTA (pH 8)
5 mM 2-ME
1 mM PMSF
10 µg/ml aprotinin
10 µg/ml leupeptin

FPLC Buffers: 0.1% Triton
20 mM Tris (pH 8)
A: 0 M NaCl
B: 1 M NaCl
1 mM EDTA (pH 8)
5 mM 2-ME
1 mM PMSF
10 µg/ml aprotinin
10 µg/ml leupeptin

Phosphatase assay using Lck phospho-Y505 peptide

Phosphatase activity was determined in an in vitro reaction consisting of: (1) Lck phospho-Y505 peptide: T E G Q Y* Q P Q P at a final concentration of 125 nM (20x 2.5 mM stock prepared in DMSO), (2) 250 ng of purified recombinant protein per sample, (3) coumermycin at a final concentration ranging from 0.05 nM to 50 µM (20x stock prepared in DMSO), and (4) assay buffer consisting of: 150 mM NaCl, 50 mM Tris-Cl (pH 6.8), 1 mM EDTA, and 10 mM DTT. Reactions were performed in a final volume of 20 µl in microtiter plates at room temperature for 1 minute. The reaction was stopped by adding 80 µl of malachite green reagent: 1 part 0.135% malachite green oxalate salt in

ddw, 1 part 4.2% ammonium molybdate in 4N HCl, 2 parts ddw, and Tween-20 to a final of 0.01%. The OD_{650} was read using an ELISA plate reader, and free phosphate released was calculated using a standard curve prepared by 2-fold serial dilutions of 10 nmol K_2HPO_4 in 20 µl. Note that all solutions should be prepared in disposable plasticware as the detergents used in cleaning the glassware contain phosphate; use carbuoy water only for the same reason.

APPENDIX B

A NOVEL CD45 PHOSPHATASE ACTIVITY ASSAY UTILIZING A MODEL MEMBRANE-TARGETED SUBSTRATE IN CULTURED CELLS

Summary

A model has been proposed for the regulation of CD45, and by homology other RPTPs, in which dimerization inhibits phosphatase activity, and consequently function, through symmetrical interactions between the catalytic site and the structural wedge containing the acidic residues. I have provided evidence supporting this model including functional and physiological assays. However, it remains to be demonstrated that CD45 phosphatase activity is inhibited by dimerization, an essential component of this model. Here I describe a novel assay for CD45 phosphatase activity in cultured cells using a membrane-targeted model substrate. While, CD45 efficiently dephosphorylates this substrate, no increase in phosphorylation is observed upon dimerization of CD45. Thus, these experiments failed to demonstrate inhibition of CD45 phosphatase activity upon dimerization. Also, in this appendix, I present experiments suggesting that localization of substrate to glycolipid-enriched membrane subdomains (GEMs) may be critical for the regulation of the enzyme-substrate interaction of CD45 and Lck. Finally, I demonstrate the specificity of new phosphorylation site-specific antisera for Lck, and describe future experiments utilizing these reagents, focusing on GEMs.

Introduction

In T cells the primary substrate for CD45 is the negative regulatory site of tyrosine phosphorylation, Y505, in Lck. The most direct assay of CD45 phosphatase activity in vivo is measurement of Lck Y505 phosphorylation. This can be accomplished by metabolically labeling cells with [^{32}P]-orthophosphate, immunoprecipitating Lck, cleaving it into peptides with CnBr, and analyzing the peptides by SDS-PAGE followed by autoradiography (*43*). This assay has been applied to EGFR-CD45 expressing cells to determine if dimerization inhibits CD45 phosphatase activity; however, no change in the phosphorylation of the Y505 peptide was observed with EGF treatment (D. Desai, unpublished results).

One possible explanation for the failure of this approach to detect inhibition of CD45 activity by dimerization is that only a portion of cellular Lck is subject to regulation by CD45. Immunohistochemistry indicates that Lck is not only localized to the plasma membrane region, but also to unidentified pericentrosomal vesicles (*102*). As CD45 is localized primarily to the plasma membrane (with some intracellular staining in the golgi), this intracellular Lck presumably is not regulated by CD45 (*103*). Additionally, cellular fractionation studies indicate that about 25% of total Lck is soluble in the cytoplasm and exhibits reduced activity compared to the membrane-associated Lck, consistent with its inaccessibility to CD45 (*104*). Furthermore, it has been estimated that CD45 may only directly regulate 5-10% of total cellular Lck (*33*). It is possible that the phosphorylated signal from Y505 of these non-plasma membrane pools of Lck may mask modulation of Y505 phosphorylation by EGF treatment. Thus, assays in which

total cellular Lck is analyzed may not be able to detect subtle changes in CD45 phosphatase activity. Here I describe a novel assay for CD45 phosphatase activity using a model substrate targeted to the plasma membrane. However, while CD45 efficiently dephosphorylates this substrate, no decrease in activity is observed upon dimerization of CD45.

Since the initiation of experiments designed to develop this assay system, it has become clear that the plasma membrane is not a homogeneous lipid bilayer, but instead contains membrane subdomains (*105*). In particular, glycolipid-enriched membrane subdomains (GEMs) have been implicated in numerous signal transduction pathways, including T cell receptor signaling (*106*). These subdomains consist of a different lipid composition than the rest of the plasma membrane possessing a high content of cholesterol, sphingolipids, and glycolipids; as such these subdomains are often referred to as lipid rafts. GEMs are experimentally identified by their resistance to solubilization in 1% Triton and can also be referred to as detergent-insoluble membrane microdomains (DIMMs). Proteins in the plasma membrane are differentially segregated into GEMs and non-GEMs. Targeting to the GEMs appears to occur as the consequence of lipid modification of proteins, in particular palmitoylation, but also isoprenylation. Myristoylation does not appear to be sufficient to target proteins into GEMs.

Evidence is accumulating to suggest that signal transduction through the T cell receptor occurs within GEMs as receptor stimulation leads to the translocation of numerous molecules into GEMs, including the TCR itself; furthermore, chemical disruption of GEMs disrupts signal transduction (*106*). Among T cell signaling molecules, Lck and LAT reside in GEMs in their basal state. The importance of this

localization for Lck and LAT is indicated by genetic experiments in which their palmitoylation sites have been mutated to prevent GEM association, but not membrane localization (*107,108*). In both cases, the mutant molecules are no longer able to reconstitute signaling in deficient cells.

While it is clear that some portion of cellular Lck resides in GEMs, it has also been established that CD45 does not (*109*). Analysis of Lck in GEMs of unstimulated Jurkat T cells demonstrated that it is hyperphosphorylated at Y505 and inactive (*109*). For Lck in the GEMs to become active, it must be dephosphorylated by CD45. Thus, the membrane subdomain localization of Lck and/or CD45 must be dynamic. Recent microscopy analysis indicates that CD45 and Lck move within the membrane upon T cell stimulation; however, the functional consequences of this movement are not clear. Currently, this is an area of active research. Here, I present experiments suggesting that localization of substrate to glycolipid-enriched membrane subdomains (GEMs) may be critical for the regulation of the enzyme-substrate interaction of CD45 and Lck. Finally, I demonstrate the specificity of new phosphorylation site-specific antisera for Lck, and describe future experiments utilizing these reagents, focusing on GEMs.

Results and Discussion

A CD45 phosphatase activity assay utilizing a membrane-targeted CD4-LckY394F chimeric molecule as the substrate in cultured cells

In order to bypass the difficulties in analyzing endogenous Lck in T cells, a CD4-Lck chimeric molecule was selected as a substrate for CD45. The CD4-Lck chimera consists of the extracellular and transmembrane domains of murine CD4 fused to the entire coding sequence for murine Lck except for the first two amino acids (*110*). Transient transfection of a CD4-Lck expression construct into 293 cells resulted in surface expression detected by flow cytometry (data not shown). Thus, co-transfection with CD45 should result in co-localization to the plasma membrane and no intracellular pool of substrate.

Several Lck tyrosine mutants have been generated in the context of this CD4-Lck chimera including Y394F, Y505F, and Y394F/Y505F (double mutant) (*110*). This panel of molecules was transfected into 293 cells, immunoprecipitated, and blotted with anti-phosphotyrosine. The wild type and both single mutants generated a signal while the double mutant exhibited none (Figure 1), indicating that Y394 and Y505 are the only sites of tyrosine phosphorylation within CD4-Lck detectable by this assay. Thus, a phosphotyrosine signal from CD4-LckY394F indicates tyrosine phosphorylation at Y505, and this molecule can serve as a membrane-targeted substrate for CD45.

Cotransfection of CD45 with CD4-LckY394F in 293 cells resulted in a markedly reduced phosphotyrosine signal indicating dephosphorylation of Y505 (Figure 2).

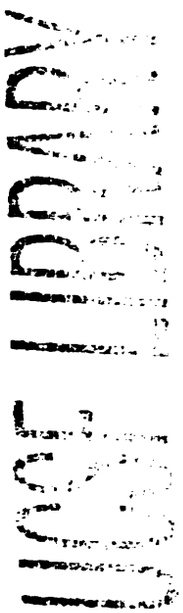

Figure 1: The CD4-Lck chimera is tyrosine phosphorylated on only two residues, Y394 and Y505

Lck tyrosine mutants of the CD4-Lck chimeric molecule including wild type (WT), Y505F, Y394F, and Y394F/Y505F (dF), were transiently transfected into 293 cells. Lysates were immunoprecipitated with anti-CD4, resolved by SDS-PAGE, and western blotted with anti-phosphotyrosine (top). The Y394F/Y505F double mutant exhibited no detectable tyrosine phosphorylation, indicating that Y394 and Y505 are the only sites of tyrosine phosphorylation within CD4-Lck detectable by this assay. The blot was stripped and re-probed with anti-Lck (bottom) to indicate equal levels of immunoprecipitated protein.

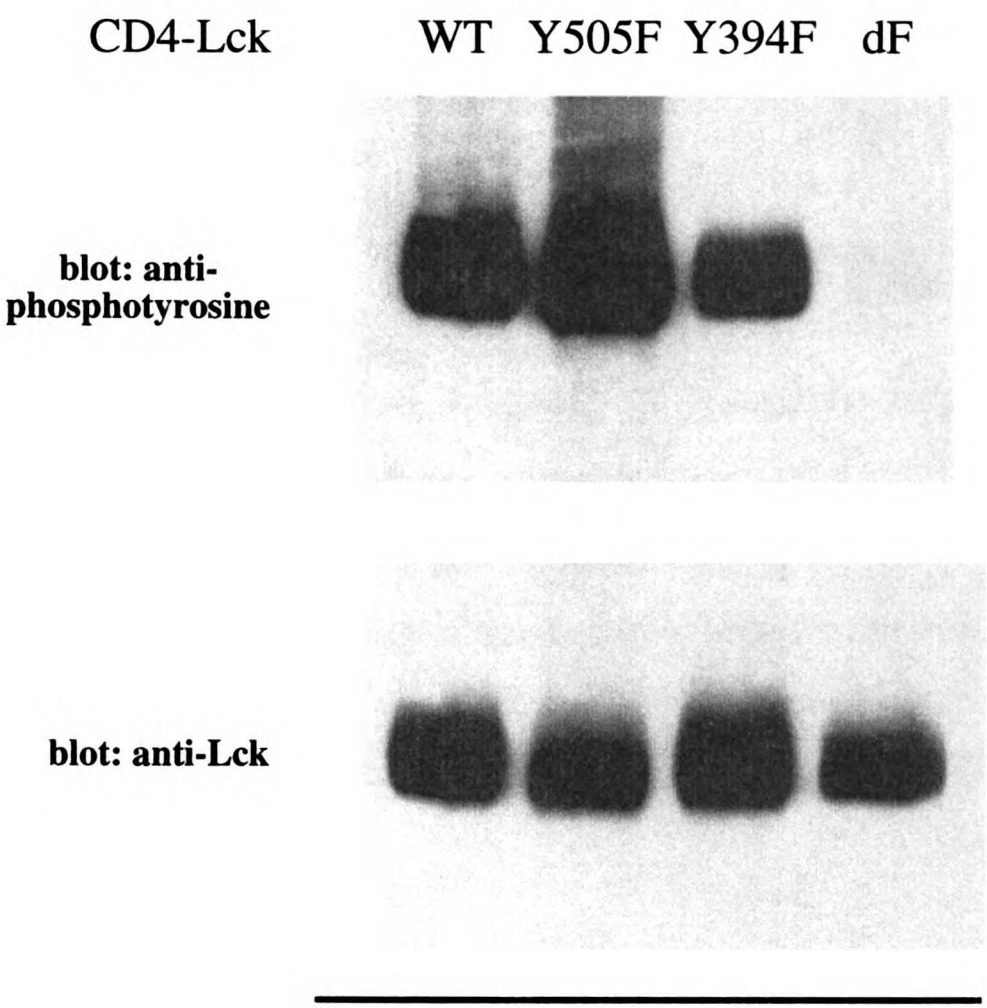
CD4-Lck
WT
Y505F
Y394F
dF
blot: anti-phosphotyrosine
blot: anti-Lck
IP: anti-CD4

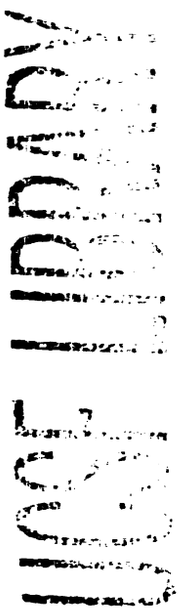

Figure 2: CD45 dephosphorylates Y505 of CD4-Lck in 293 cells

0, 10, or 20 μg of CD45 expression plasmid was transiently co-transfected with CD4-LckY394F into 293 cells. Lysates were immunoprecipiated with anti-CD4, resolved by SDS-PAGE, and western blotted with anti-phosphotyrosine (top). In the absence of CD45, CD4-LckY394F is tyrosine phosphorylated at Y505. With co-expression of CD45, no tyrosine phosphorylation is detected, indicating dephosphorylation of Y505 by CD45. The blot was stripped and re-probed with anti-Lck (bottom) to indicate equal levels of immunoprecipitated protein.

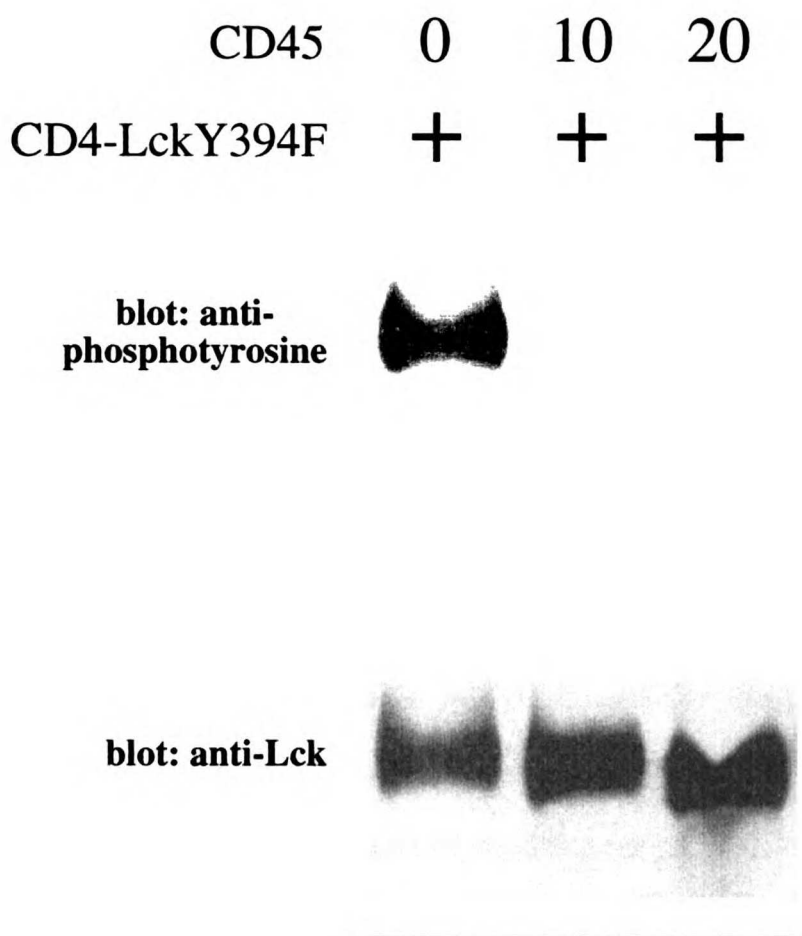
CD45
0
10
20
CD4-LckY394F
+
+
+
blot: anti-phosphotyrosine
blot: anti-Lck
IP: anti-CD4

Catalytically inactive CD45 had no effect (data not shown). Thus, this is a robust assay for measuring CD45 phosphatase activity.

In order to determine if dimerization of CD45 inhibits its activity in this assay, EGFR-CD45 was cotransfected with CD4-LckY394F into 293 cells. Each transfection was split in two; one half was untreated, the other was treated with EGF for 3 minutes followed by lysis and immunoprecipitation of CD4-LckY394F. Anti-phosphotyrosine blotting revealed no differences between the mock-treated and EGF-treated samples (Figure 3). No differences were detected with numerous manipulations including: immunoprecipitation of cell surface CD4-LckY394F only, titration of EGFR-CD45, co-transfection of Csk, co-transfection of LPAP, and analysis in CHO cells, which lack endogenous EGFR (data not shown). Thus, these experiments failed to demonstrate inhibition of CD45 phosphatase activity upon dimerization.

It is possible that there are lymphocyte specific factors essential for the appropriate regulation of CD45 that are not present in heterologous cells, such as 293 and CHO. Additionally, experiments in these heterologous cells lack a positive control for the action of EGF. To account for these possibilities, CD4-LckY394F was stably introduced into CD45-deficient T cells already stably expressing EGFR-CD45. These "double stables" were either unstimulated, TCR-stimulated, or TCR-stimulated in the presence of EGF. CD4-LckY394F was immunoprecipitated and found to be equivalently tyrosine phosphorylated under all conditions (Figure 4A). Moreover, anti-phosphotyrosine blotting of whole cell lysates demonstrated inhibition of TCR signals by EGF (Figure 4B). Thus, EGF inhibited CD45 function in T cell signaling, but not its activity towards CD4-LckY394F.

Figure 3: Dimerization of EGFR-CD45 fails to inhibit CD45 activity against CD4-LckY394F in 293 cells

0, 5, 10, or 20 μg of EGFR-CD45 expression plasmid was cotransfected with CD4-LckY394F into 293 cells. Each transfection was split in two; one half was treated with PBS, the other with EGF for 3 minutes followed by rapid lysis. The lysates were immunoprecipiated with anti-CD4, resolved by SDS-PAGE, and western blotted with anti-phosphotyrosine (top). EGFR-CD45 was able to dephosphorylate Lck Y505; however, no differences were observed between the mock-treated and EGF-treated samples. The blot was stripped and re-probed with anti-Lck (bottom) to indicate equal levels of immunoprecipitated protein.

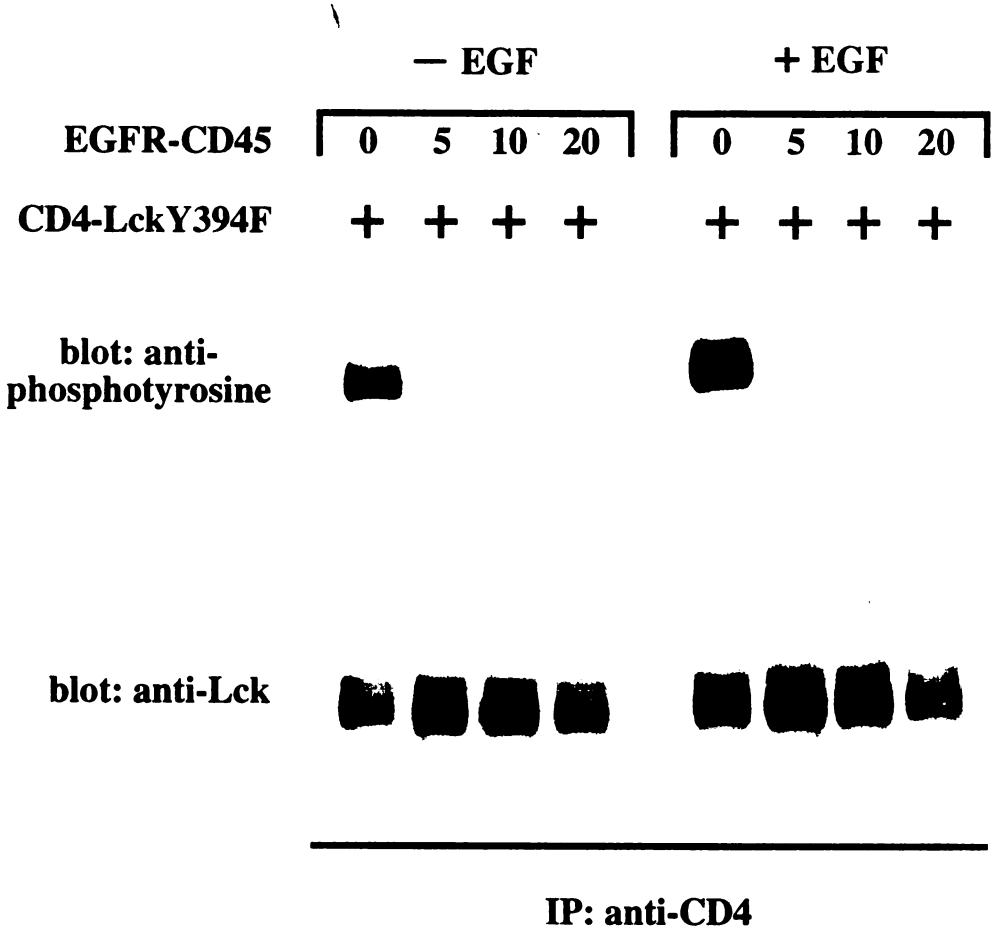
— EGF
+ EGF
EGFR-CD45
0 5 10 20
0 5 10 20
CD4-LckY394F
+ + + +
+ + + +
blot: anti-phosphotyrosine
blot: anti-Lck
IP: anti-CD4

Figure 4: Dimerization of EGFR-CD45 fails to inhibit CD45 activity against CD4-LckY394F in stably transfected T cells

A CD45-deficient T cell line stably reconstituted with EGFR-CD45, was stably transfected with CD4-LckY394F to generate "double stables". Two independently isolated clones were either unstimulated, stimulated with anti-TCR for 2 minutes, or stimulated with anti-TCR in the presence of EGF for 2 minutes.

(**A**) Lysates were immunoprecipiated with anti-CD4, resolved by SDS-PAGE, and western blotted with anti-phosphotyrosine (top). CD4-LckY394F was found to be equivalently tyrosine phosphorylated under all conditions tested. The blot was stripped and re-probed with anti-Lck (bottom) to indicate roughly equal levels of immunoprecipitated protein.

(**B**) Lysates were directly resolved by SDS-PAGE, and western blotted with anti-phosphotyrosine. Treatment with EGF resulted in inhibition of inducible tyrosine phosphorylation in both clones, indicating inhibition of CD45 function by EGF. Molecular mass markers are indicated on the left.

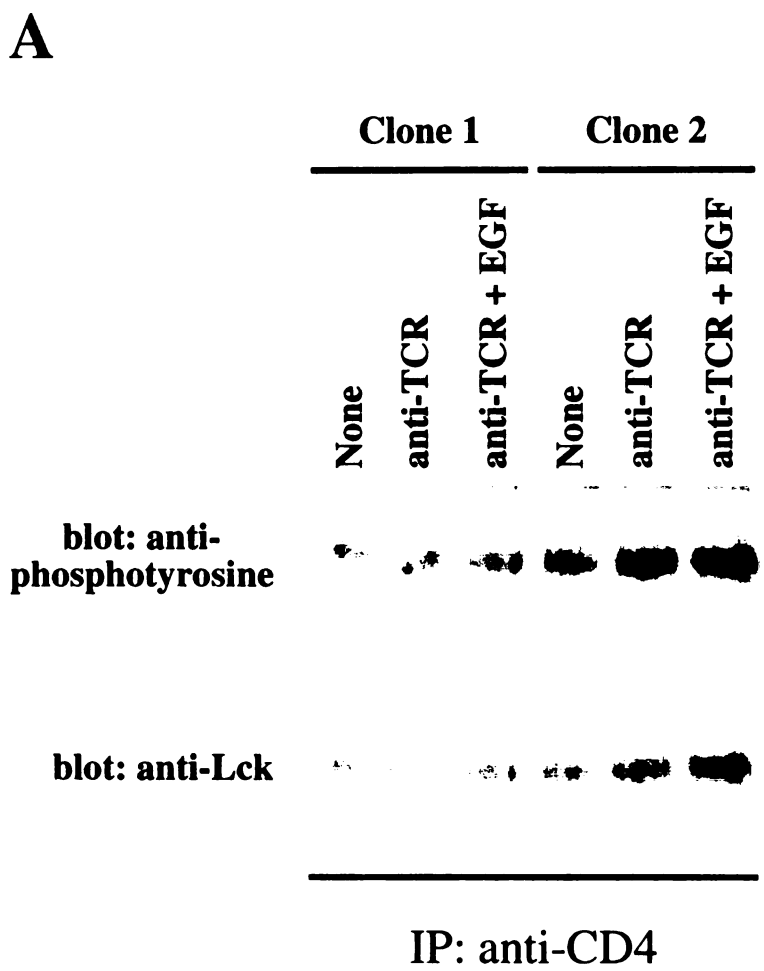
A
Clone 1
Clone 2
None
anti-TCR
anti-TCR + EGF
None
anti-TCR
anti-TCR + EGF
blot: anti-phosphotyrosine
blot: anti-Lck
IP: anti-CD4

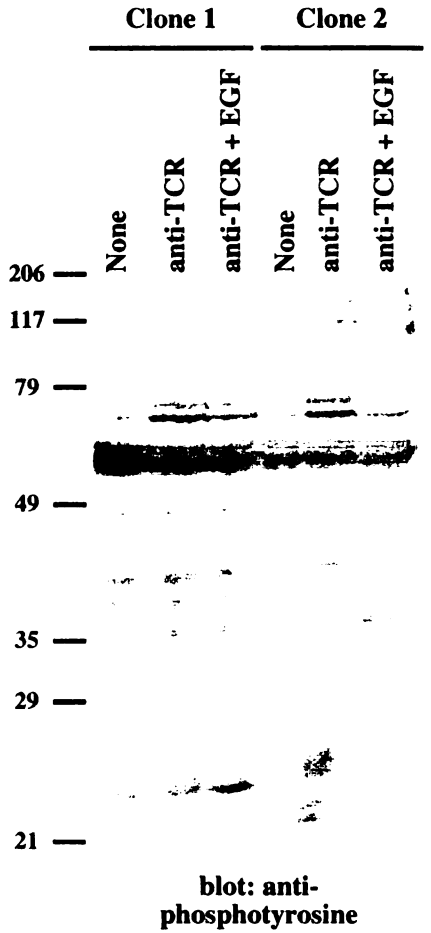
B
Clone 1
Clone 2
None
anti-TCR
anti-TCR + EGF
None
anti-TCR
anti-TCR + EGF
206
117
79
49
35
29
21
blot: anti-phosphotyrosine

Lck, but not CD4-LckY394F, is in GEMs

One possible explanation for this apparent discrepancy is that CD4-LckY394F does not mimic endogenous Lck as an appropriate substrate for CD45. Normally, both CD4 and Lck are palmitoylated and found in GEMs; however, the CD4-Lck fusion protein may not get modified properly and thus may be excluded from GEMs. GEMs were prepared from EGFR-CD45/CD4-LckY394F double stables and blotted with an anti-Lck antiserum which can recognize endogenous Lck and transfected CD4-LckY394F. Approximately 50% of total Lck was readily detected in GEMs; however, no CD4-LckY394F was detected in the GEMs (Figure 5). It is tempting to speculate that Lck must be in the GEMs for it to be properly regulated by CD45 dimerization, and that a better assay would be to assess the phosphorylation state of endogenous Lck Y505 in the GEMs.

How might this be accomplished? Lck could be immunoprecipitated from GEMs prepared from cells radiolabelled with [^{32}P]-orthophosphate and subject to CnBr cleavage and peptide mapping. However, a large amount of material is needed for this extremely hazardous experiment. An alternative to radiolabelling is western blotting with a phospho-LckY505 specific antiserum. Such a reagent does not currently exist; however, a commercial vendor has recently generated antisera specific for tyrosine phosphorylation sites in Src which is highly homologous to Lck.

Phospho-specific anti-Src antisera recognize Lck Y394 and Y505

Figure 5: Lck, but not CD4-LckY394F, is in GEMs

Glycolipid enriched membranes (GEMs) were prepared from $50x10^6$ CD45-deficient T cells stably transfected with both EGFR-CD45 and CD4-LckY394F by ultracentrifugation over a sucrose gradient. Fractions from this gradient were prepared, and a portion of each was analyzed by SDS-PAGE followed by western blotting with anti-Lck. The relative mobilities of endogenous Lck and transfected CD4-LckY394F are indicated on the right. A significant proportion of Lck, but no CD4-LckY394F was detected in the GEMs (fractions 2-4). Molecular mass markers are indicated on the left.

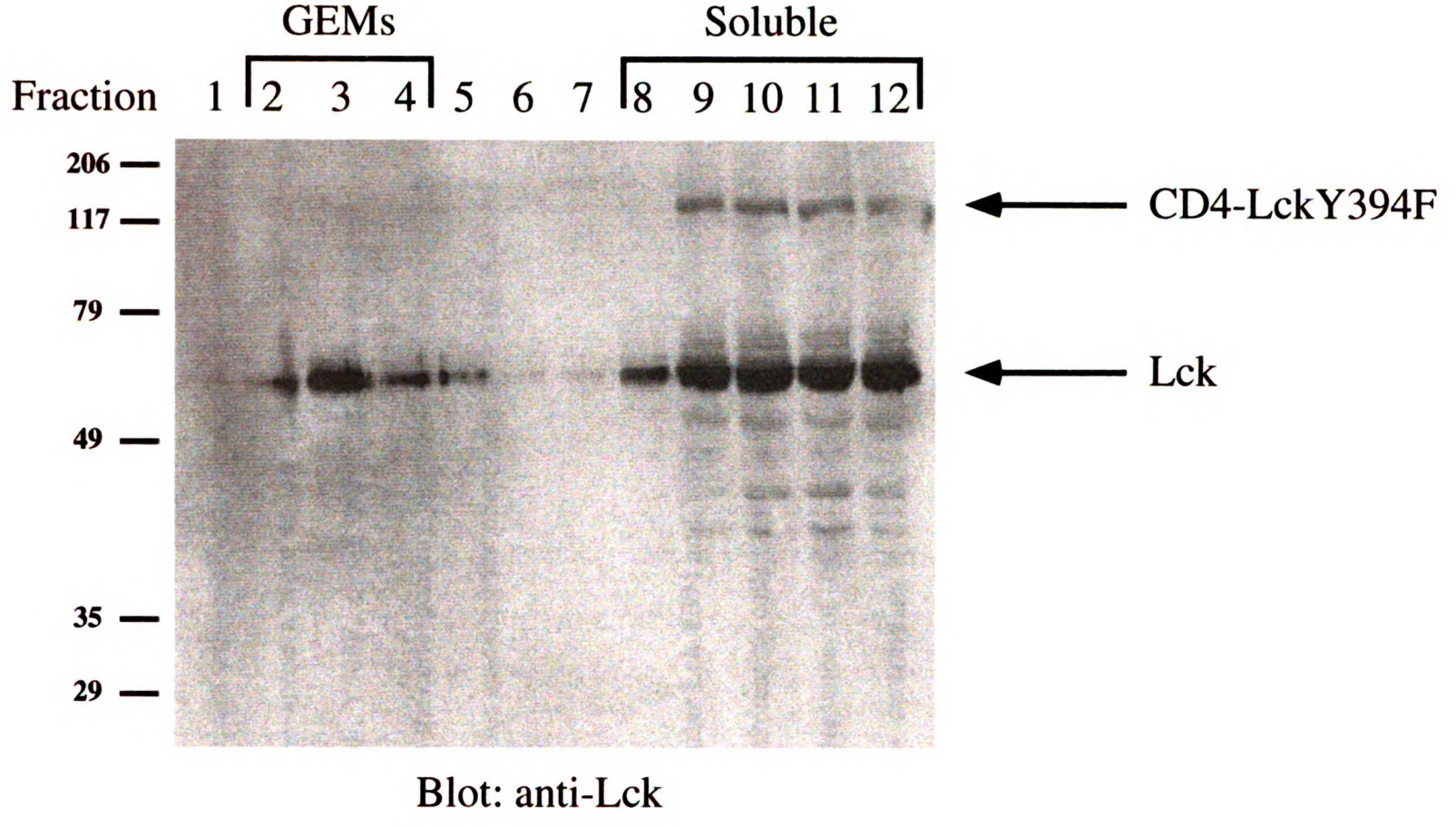

Blot: anti-Lck

A commericial vendor has generated two antisera that recognize phospho-SrcY418 and phospho-SrcY529, respectively, which are analogous to LckY394 and LckY505; furthermore, the primary sequences surrounding these residues are highly conserved in the case of SrcY418 and somewhat conserved for SrcY529. Thus, it is possible that these antisera will specifically recognize the corresponding phosphorylated forms of Lck. These antisera were tested against the panel of CD4-Lck chimeric molecules (wt, Y394F, Y505F, and Y394F/Y505F) by western blotting and found to specifically recognize the corresponding phosphorylated forms of Lck (Figure 6). These reagents can be used for assessing the phosphorylation status of individual tyrosines in Lck.

Analysis of total cellular Lck Y394 and Y505 phosphorylation in stimulated cells

EGFR-CD45 expressing cells were either unstimulated, TCR-stimulated, or TCR-stimulated in the presence of EGF. Lck was immunoprecipitated and Y394 phosphorylation was determined by blotting with anti-SrcY418 (Figure 7A); no differences were detected. The blot was stripped and reprobed with anti-SrcY529; again, no differences were detected (Figure 7A). Anti-phosphotyrosine blotting of whole cell lysates demonstrated inhibition of TCR signals by EGF (Figure 7B). Thus, no differences in Lck Y394 or Y505 phosphorylation were detected in analysis of total cellular Lck. If T cell signal transduction machinery translocates to the GEMs, perhaps GEM Lck should be analyzed under these stimulation conditions.

Conclusion

Figure 6: Phospho-specific anti-Src antisera recognize Lck Y394 and Y505

The same blot used for the analysis of CD4-Lck tyrosine mutants in Figure 1 was stripped and re-probed with anti-SrcY418 (top) and again stripped and re-probed with anti-SrcY529 (bottom). These phospho-specific anti-Src antisera specifically recognized CD4-Lck tyrosine phosphorylated at Y394 (top) and Y505 (bottom). These reagents can be used for assessing the phosphorylation status of individual tyrosines in Lck.

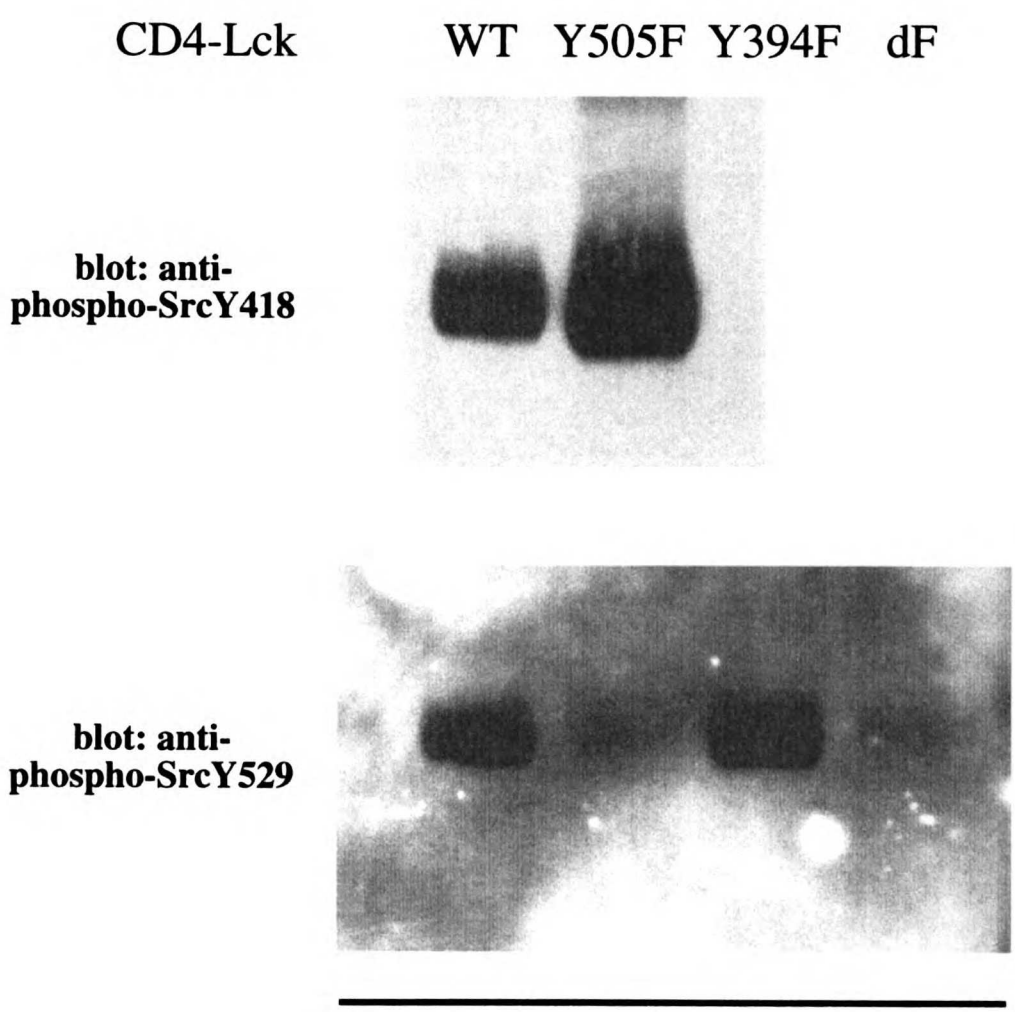
CD4-Lck
WT
Y505F
Y394F
dF
blot: anti-phospho-SrcY418
blot: anti-phospho-SrcY529
IP: anti-CD4

Figure 7: Analysis of total cellular Lck Y394 and Y505 phosphorylation in stimulated cells

A CD45-deficient T cell line stably reconstituted with EGFR-CD45, was either unstimulated, stimulated with anti-TCR for 2 minutes, or stimulated with anti-TCR in the presence of EGF for 2 minutes.

(**A**) Lysates were immunoprecipiated with anti-Lck, resolved by SDS-PAGE, and western blotted with anti-phospho-SrcY418 (top). The same blot was stripped and re-probed with anti-phospho-SrcY529 (middle), and again stripped and re-probed with anti-Lck (bottom). No differences in Lck Y394 or Y505 phosphorylation were detected in this analysis of total cellular Lck.

(**B**) Lysates were directly resolved by SDS-PAGE, and western blotted with anti-phosphotyrosine. Treatment with EGF resulted in inhibition of inducible tyrosine phosphorylation indicating inhibition of CD45 function by EGF. Molecular mass markers are indicated on the left.

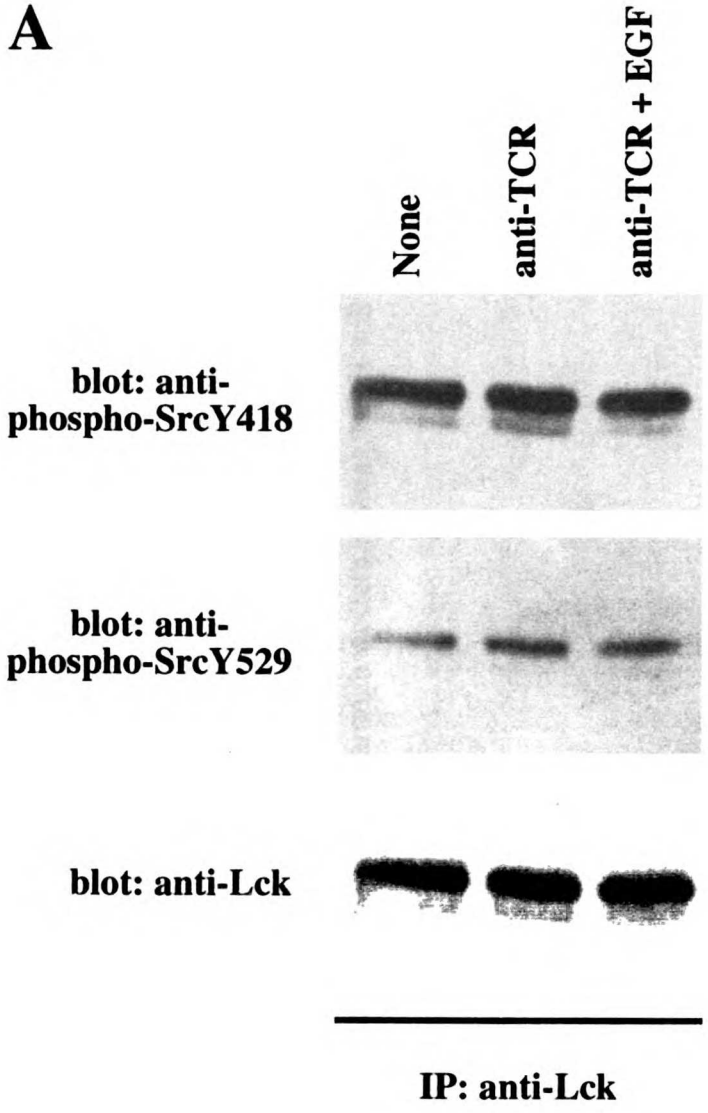
A
None
anti-TCR
anti-TCR + EGF
blot: anti-phospho-SrcY418
blot: anti-phospho-SrcY529
blot: anti-Lck
IP: anti-Lck

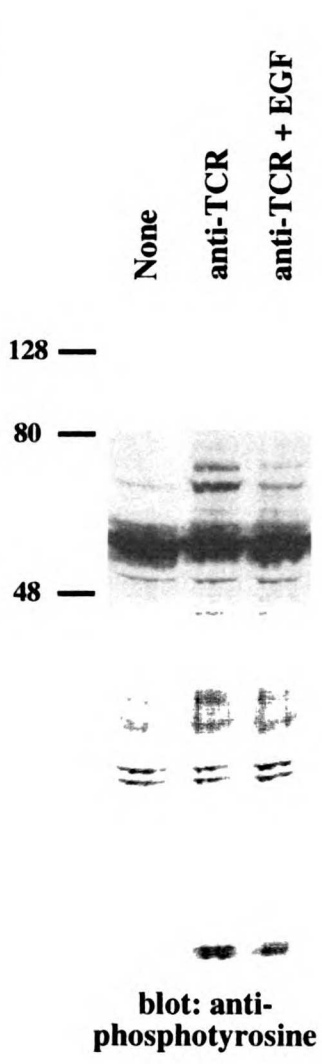
B
None
anti-TCR
anti-TCR + EGF
128
80
48
blot: anti-phosphotyrosine

Unfortunately, none of the experiments presented in this appendix demonstrated dimerization-induced inhibition of CD45 phosphatase activity. However, cotransfection of CD45 with CD4-LckY394F is an easy assay for rapid analysis of CD45 phosphatase activity in vivo. Clearly, the interaction between CD45 and Lck is much more complicated than early models suggested. It is tempting to speculate that CD45 dimerization modulates the phosphorylation status of GEM-associated Lck and not other cellular pools of Lck. With the new phospho-specific Lck antisera available, it is possible to test this directly through western blotting. This will certainly be an exciting experiment for the future.

Experimental Procedures

Reagents and cell lines

Expression constructs for the panel of CD4-Lck tyrosine mutants have been described (*110,111*). pEF:CD45 and pEF:LCAX were used for transient expression of CD45 and EGFR-CD45 respectively. For generation of "double stables" CD4-LckY394F was subloned into pCEP-4 (Invitrogen). This vector was transfected into H45XL2 and selected for hygromycin resistance as described (*36*). Individual clones were screened for expression of CD4-LckY394F by flow cytometry as described (*70*); two clones with moderate expression were selected for further analysis. Cell lines used in this study included: 293T, H45XL2 (EGFR-CD45), and H45XL2.CtmlY394F.1 and H45XL2.CtmlY394F.2 (double stables). Antibodies used included: 4G10 (anti-phosphotyrosine), 1F6 (anti-Lck), GK1.5 (anti-CD4), 235 (anti-CD3), anti-phospho-SrcY418 (Biosource), and anti-phospho-SrcY529 (Biosource).

CD4-Lck analysis in transiently transfected 293 cells

293T cells were transfected with the indicated amount of expression plasmid using the calcium phosphate method. In all samples, 10 μg of CD4-Lck expression construct was used. Briefly, 293T cells from a confluent 10 cm plate were split into 4 6-well plates and left overnight. On day 2, cells were fed with 4.5 mL fresh media per well approximately one hour prior to transfection. 20-30 μg total DNA was used per transfection in a final volume of 218.5 μL. 31.5 μL of 2 M $CaCl_2$ was added to a volume of 250 μL. 250 μL of 2x HBS was added, mixed well, and left at room temperature for

30 minutes. The total mix of 500 μL was added dropwise to the cells and left overnight. On day 3, the media was aspirated and the cells were refed fresh media and left overnight. On day 4, the cells were washed once with PBS and harvested in 1 mL PBS. Cells were either directly lysed or split in half and treated with EGF (500 ng/ml final) for 3 minutes and then lysed. Lysis buffer, immunoprecipitation, and western blotting was described previously (*70*). 500 μL of GK1.5 culture supernatant was used per immunoprecipitation. For western blotting: 4G10 was used at 1/1000, 1F6 ascites was used at 1/10,000, anti-phospho-Src antibodies were used at 1/1000.

Preparation of glycolipid-enriched membranes (GEMs)

GEMs from $50x10^6$ H45XL2.CtmlY394F.1 cells were prepared by ultracentrifugation within a sucrose gradient as described (*112*). 20 μL of each fraction was mixed with 20 μL 2xSDS sample buffer, resolved by SDS-PAGE, and western blotted with anti-Lck (1F6 at 1/10,000) as described (*70*).

Simulation and analysis of stable cell lines

H45XL2, H45XL2.CtmlY394F.1, and H45XL2.CtmlY394F.2 were stimulated as described (*70*). CD4-LckY394F was assayed as described above. Lck was immunoprecipitated with 1F6-coupled protein A beads. Lysis, immunoprecipitation, and western blotting was described above and previously (*70*).

REFERENCES

1. Weiss, A. and Littman, D.R. (1994). Signal transduction by lymphocyte antigen receptors. Cell. 76: 263-274.

2. Goldsmith, M.A. and Weiss, A. (1987). Isolation and characterization of a T-lymphocyte somatic mutant with altered signal transduction by the antigen receptor. Proc. Natl. Acad. Sci. USA. 84: 6879-6883.

3. Straus, D. and Weiss, A. (1992). Genetic evidence for the involvement of the Lck tyrosine kinase in signal transduction throught the T cell antigen receptor. Cell. 70: 585-593.

4. Molina, T.J., Kishihara, K., Siderovski, D.P., van Ewijk, W., Narendran, A., Timms, E., Wakeham, A., Paige, C.J., Hartmann, K.U., Veillette, A. and et al. (1992). Profound block in thymocyte development in mice lacking p56lck [see comments]. Nature. 357: 161-164.

5. Sefton, B.M. (1991). The lck tyrosine protein kinase. Oncogene. 6: 683-686.

6. Chan, A.C., Desai, D.M. and Weiss, A. (1994). The role of protein tyrosine kinases and protein tyrosine phosphatases in T cell antigen receptor signal transduction. Annu Rev Immunol. 12: 555-592.

7. D'Oro, U., Sakaguchi, K., Appella, E. and Ashwell, J.D. (1996). Mutational analysis of Lck in CD45-negative T cells: dominant role of tyrosine 394 phosphorylation in kinase activity. Molecular and Cellular Biology. 16: 4996-5003.

8. Chow, L.M., Fournel, M., Davidson, D. and Veillette, A. (1993). Negative regulation of T-cell receptor signalling by tyrosine protein kinase p50csk. Nature. 365: 156-160.

9. Chow, L.M. and Veillette, A. (1995). The Src and Csk families of tyrosine protein kinases in hemopoietic cells. Semin Immunol. 7: 207-226.

10. Cloutier, J.F. and Veillette, A. (1999). Cooperative inhibition of T-cell antigen receptor signaling by a complex between a kinase and a phosphatase. Journal of Experimental Medicine. 189: 111-121.

11. D'Oro, U. and Ashwell, J.D. (1999). The CD45 tyrosine phosphatase is an inhibitor of Lck activity in thymocytes. Journal of Immunology. 162: 1879-1883.

12. Ashwell, J.D. and D'Oro, U. (1999). CD45 and Src-family kinases: and now for something completely different. Immunology Today. 20: 412-416.

13. Thomas, M.L. and Brown, E.J. (1999). Positive and negative regulation of Src-family membrane kinases by CD45. Immunology Today. 20: 406-411.

14. Abraham, K.M., Levin, S.D., Marth, J.D., Forbush, K.A. and Perlmutter, R.M. (1991). Thymic tumorigenesis induced by overexpression of p56lck. Proceedings of the National Academy of Sciences of the United States of America. 88: 3977-3981.

15. Superti-Furga, G. and Courtneidge, S.A. (1995). Structure-function relationships in Src family and related protein tyrosine kinases. Bioessays. 17: 321-330.

16. Brown, M.T. and Cooper, J.A. (1996). Regulation, substrates and functions of src. Biochimica et Biophysica Acta. 1287: 121-149.

17. Frearson, J.A. and Alexander, D.R. (1996). Protein tyrosine phosphatases in T-cell development, apoptosis and signalling. Immunology Today. 17: 385-391.

18. Trowbridge, I.S. and Thomas, M.L. (1994). CD45: an emerging role as a protein tyrosine phosphatase required for lymphocyte activation and development. Annu Rev Immunol. 12: 85-116.

19. Thomas, M.L. (1989). The leukocyte common antigen family. Annual Review of Immunology. 7: 339-369.

20. Neel, B.G. (1997). Role of phosphatases in lymphocyte activation. Current Opinion in Immunology. 9: 405-420.

21. Pingel, J.T. and Thomas, M.L. (1989). Evidence that the leukocyte-common antigen is required for antigen-induced T lymphocyte proliferation. Cell. 58: 1055-1065.

22. Koretzky, G.A., Picus, J., Thomas, M.L. and Weiss, A. (1990). Tyrosine phosphatase CD45 is essential for coupling T-cell antigen receptor to the phosphatidyl inositol pathway. Nature. 346: 66-68.

23. Weaver, C.T., Pingel, J.T., Nelson, J.O. and Thomas, M.L. (1991). CD8+ T-cell clones deficient in the expression of the CD45 protein tyrosine phosphatase have impaired responses to T-cell receptor stimuli. Mol Cell Biol. 11: 4415-4422.

24. Justement, L.B., Campbell, K.S., Chien, N.C. and Cambier, J.C. (1991). Regulation of B cell antigen receptor signal transduction and phosphorylation by CD45. Science. 252: 1839-1842.

25. Kishihara, K., Penninger, J., Wallace, V.A., Kundig, T.M., Kawai, K., Wakeham, A., Timms, E., Pfeffer, K., Ohashi, P.S., Thomas, M.L. and et al. (1993). Normal B lymphocyte development but impaired T cell maturation in CD45-exon6 protein tyrosine phosphatase-deficient mice. Cell. 74: 143-156.

26. Byth, K.F., Conroy, L.A., Howlett, S., Smith, A.J., May, J., Alexander, D.R. and Holmes, N. (1996). CD45-null transgenic mice reveal a positive regulatory role for CD45

in early thymocyte development, in the selection of CD4+CD8+ thymocytes, and B cell maturation. J Exp Med. 183: 1707-1718.

27. Cale, C.M., Klein, N.J., Novelli, V., Veys, P., Jones, A.M. and Morgan, G. (1997). Severe combined immunodeficiency with abnormalities in expression of the common leucocyte antigen, CD45. Archives of Disease in Childhood. 76: 163-164.

28. Kung, C., Pingel, J.T., Heikinheimo, M., Klemola, T., Varkila, K., Yoo, L.I., Vuopala, K., Poyhonen, M., Uhari, M., Rogers, M., Speck, S.H., Chatila, T. and Thomas, M.L. (2000). Mutations in the tyrosine phosphatase CD45 gene in a child with severe combined immunodeficiency disease. Nature Medicine. 6: 343-345.

29. Mustelin, T., Coggeshall, K.M. and Altman, A. (1989). Rapid activation of the T-cell tyrosine protein kinase pp56lck by the CD45 phosphotyrosine phosphatase. Proc Natl Acad Sci U S A. 86: 6302-6306.

30. Hurley, T.R., Hyman, R. and Sefton, B.M. (1993). Differential effects of expression of the CD45 tyrosine protein phosphatase on the tyrosine phosphorylation of the *lck*, *fyn*, and c-*src* tyrosine protein kinases. Mol. Cell. Biol. 13: 1651-1656.

31. Shiroo, M., Goff, L., Biffen, M., Shivnan, E. and Alexander, D. (1992). CD45 tyrosine phosphatase-activated p59fyn couples the T cell antigen receptor to pathways of

diacylglycerol production, protein kinase C activation and calcium influx. Embo J. 11: 4887-4897.

32. McFarland, E.D., Hurley, T.R., Pingel, J.T., Sefton, B.M., Shaw, A. and Thomas, M.L. (1993). Correlation between Src family member regulation by the protein-tyrosine-phosphatase CD45 and transmembrane signaling through the T-cell receptor. Proc Natl Acad Sci U S A. 90: 1402-1406.

33. Sieh, M., Bolen, J.B. and Weiss, A. (1993). CD45 specifically modulates binding of Lck to a phosphopeptide encompassing the negative regulatory tyrosine of Lck. Embo J. 12: 315-321.

34. Seavitt, J.R., White, L.S., Murphy, K.M., Loh, D.Y., Perlmutter, R.M. and Thomas, M.L. (1999). Expression of the p56(Lck) Y505F mutation in CD45-deficient mice rescues thymocyte development. Molecular and Cellular Biology. 19: 4200-4208.

35. Volarevic, S., Niklinska, B.B., Burns, C.M., June, C.H., Weissman, A.M. and Ashwell, J.D. (1993). Regulation of TCR signaling by CD45 lacking transmembrane and extracellular domains. Science. 260: 541-544.

36. Desai, D.M., Sap, J., Schlessinger, J. and Weiss, A. (1993). Ligand-mediated negative regulation of a chimeric transmembrane receptor tyrosine phosphatase. Cell. 73: 541-554.

37. Hovis, R.R., Donovan, J.A., Musci, M.A., Motto, D.G., Goldman, F.D., Ross, S.E. and Koretzky, G.A. (1993). Rescue of signaling by a chimeric protein containing the cytoplasmic domain of CD45. Science. 260: 544-546.

38. Denu, J.M., Stuckey, J.A., Saper, M.A. and Dixon, J.E. (1996). Form and function in protein dephosphorylation [comment]. Cell. 87: 361-364.

39. Zhang, Z.Y. (1998). Protein-tyrosine phosphatases: biological function, structural characteristics, and mechanism of catalysis. Critical Reviews in Biochemistry and Molecular Biology. 33: 1-52.

40. Johnson, P., Ostergaard, H.L., Wasden, C. and Trowbridge, I.S. (1992). Mutational analysis of CD45: A leukocyte-specific protein tyrosine phosphatase. J. Biol. Chem. 12: 8035-8041.

41. Streuli, M., Krueger, N.X., Thai, T., Tang, M. and Saito, H. (1990). Distinct functional roles of the two intracellular phosphatase like domains of the receptor-linked protein tyrosine phosphatases LCA and LAR. Embo Journal. 9: 2399-2407.

42. Felberg, J. and Johnson, P. (1998). Characterization of recombinant CD45 cytoplasmic domain proteins. Evidence for intramolecular and intermolecular interactions. Journal of Biological Chemistry. 273: 17839-17845.

43. Desai, D.M., Sap, J., Silvennoinen, O., Schlessinger, J. and Weiss, A. (1994). The catalytic activity of the CD45 membrane-proximal phosphatase domain is required for TCR signaling and regulation. Embo J. 13: 4002-4010.

44. McCall, M.N., Shotton, D.M. and Barclay, A.N. (1992). Expression of soluble isoforms of rat CD45. Analysis by electron microscopy and use in epitope mapping of anti-CD45R monoclonal antibodies. Immunology. 76: 310-317.

45. Novak, T.J., Farber, D., Leitenberg, D., Hong, S.C., Johnson, P. and Bottomly, K. (1994). Isoforms of the transmembrane tyrosine phosphatase CD45 differentially affect T cell recognition. Immunity. 1: 109-119.

46. Leitenberg, D., Boutin, Y., Lu, D.D. and Bottomly, K. (1999). Biochemical association of CD45 with the T cell receptor complex: regulation by CD45 isoform and during T cell activation. Immunity. 10: 701-711.

47. Kozieradzki, I., Kündig, T., Kishihara, K., Ong, C.J., Chiu, D., Wallace, V.A., Kawai, K., Timms, E., Ionescu, J., Ohashi, P., Marth, J.D., Mak, T.W. and Penninger, J.M. (1997). T cell development in mice expressing splice variants of the protein tyrosine phosphatase CD45. Journal of Immunology. 158: 3130-3139.

48. Schlessinger, J. and Ullrich, A. (1992). Growth factor signaling by receptor tyrosine kinases. Neuron. 9: 383-391.

49. Weiss, A. and Schlessinger, J. (1998). Switching signals on or off by receptor dimerization. Cell. 94: 277-280.

50. Neel, B.G. and Tonks, N.K. (1997). Protein tyrosine phosphatases in signal transduction. Curr Opin Cell Biol. 9: 193-204.

51. Schaapveld, R., Wieringa, B. and Hendriks, W. (1997). Receptor-like protein tyrosine phosphatases: alike and yet so different. Molecular Biology Reports. 24: 247-262.

52. Ledbetter, J.A., Schieven, G.L., Uckun, F.M. and Imboden, J.B. (1991). CD45 cross-linking regulates phospholipase C activation and tyrosine phosphorylation of specific substrates in CD3/Ti-stimulated T cells. Journal of Immunology. 146: 1577-1583.

53. Mittler, R.S., Schieven, G.L., Dubois, P.M., Klussman, K., O'Connell, M.P., Kiener, P.A. and Herndon, V. (1994). CD45-mediated regulation of extracellular calcium influx in a CD4-transfected human T cell line. Journal of Immunology. 153: 84-96.

54. Marvel, J., Rimon, G., Tatham, P. and Cockcroft, S. (1991). Evidence that the CD45 phosphatase regulates the activity of the phospholipase C in mouse T lymphocytes. European Journal of Immunology. 21: 195-201.

55. Takeda, A., Wu, J.J. and Maizel, A.L. (1992). Evidence for monomeric and dimeric forms of CD45 associated with a 30-kDa phosphorylated protein. J. Biol. Chem. 267: 16651-16659.

56. Cochet, C., Kashles, O., Chambaz, E.M., Borrello, I., King, C.R. and Schlessinger, J. (1988). Demonstration of epidermal growth factor-induced receptor dimerization in living cells using a chemical covalent cross-linking agent. Journal of Biological Chemistry. 263: 3290-3295.

57. Lemmon, M.A., Bu, Z., Ladbury, J.E., Zhou, M., Pinchasi, D., Lax, I., Engelman, D.M. and Schlessinger, J. (1997). Two EGF molecules contribute additively to stabilization of the EGFR dimer. Embo Journal. 16: 281-294.

58. Lemmon, M.A. and Schlessinger, J. (1998). Transmembrane signaling by receptor oligomerization. Methods in Molecular Biology. 84: 49-71.

59. Bilwes, A.M., den Hertog, J., Hunter, T. and Noel, J.P. (1996). Structural basis for inhibition of receptor protein-tyrosine phosphatase-alpha by dimerization. Nature. 382: 555-559.

60. Mourey, R.J. and Dixon, J.E. (1994). Protein tyrosine phosphatases: characterization of extracellular and intracellular domains. Curr Opin Genet Dev. 4: 31-39.

61. Ostergaard, H.L., Shackelford, D.A., Hurley, T.R., Johnson, P., Hyman, R., Sefton, B.M. and Trowbridge, I.S. (1989). Expression of CD45 alters phosphorylation of the lck-encoded tyrosine protein kinase in murine lymphoma T-cell lines. Proc Natl Acad Sci U S A. 86: 8959-8963.

62. Grynkiewicz, G., Poenie, M. and Tsien, R.Y. (1985). A new generation of Ca2+ indicators with greatly improved fluorescence properties. J Biol Chem. 260: 3440-3450.

63. Qian, D., Lev, S., van Oers, N.S., Dikic, I., Schlessinger, J. and Weiss, A. (1997). Tyrosine phosphorylation of Pyk2 is selectively regulated by Fyn during TCR signaling. J Exp Med. 185: 1253-1259.

64. Sicheri, F., Moarefi, I. and Kuriyan, J. (1997). Crystal structure of the Src family tyrosine kinase Hck [see comments]. Nature. 385: 602-609.

65. Xu, W., Harrison, S.C. and Eck, M.J. (1997). Three-dimensional structure of the tyrosine kinase c-Src [see comments]. Nature. 385: 595-602.

66. Okumura, M., Matthews, R.J., Robb, B., Litman, G.W., Bork, P. and Thomas, M.L. (1996). Comparison of CD45 extracellular domain sequences from divergent vertebrate species suggests the conservation of three fibronectin type III domains. Journal of Immunology. 157: 1569-1575.

67. Akbar, A.N., Terry, L., Timms, A., Beverley, P.C. and Janossy, G. (1988). Loss of CD45R and gain of UCHL1 reactivity is a feature of primed T cells. Journal of Immunology. 140: 2171-2178.

68. Birkeland, M.L., Johnson, P., Trowbridge, I.S. and Puré, E. (1989). Changes in CD45 isoform expression accompany antigen-induced murine T-cell activation. Proceedings of the National Academy of Sciences of the United States of America. 86: 6734-6738.

69. Jiang, G., den Hertog, J., Su, J., Noel, J., Sap, J. and Hunter, T. (1999). Dimerization inhibits the activity of receptor-like protein-tyrosine phosphatase-alpha. Nature. 401: 606-610.

70. Majeti, R., Bilwes, A.M., Noel, J.P., Hunter, T. and Weiss, A. (1998). Dimerization-induced inhibition of receptor protein tyrosine phosphatase function through an inhibitory wedge. Science. 279: 88-91.

71. Hoffmann, K.M., Tonks, N.K. and Barford, D. (1997). The crystal structure of domain 1 of receptor protein-tyrosine phosphatase mu. Journal of Biological Chemistry. 272: 27505-27508.

72. Nam, H.J., Poy, F., Krueger, N.X., Saito, H. and Frederick, C.A. (1999). Crystal structure of the tandem phosphatase domains of RPTP LAR. Cell. 97: 449-457.

73. Andrews, B.S., Eisenberg, R.A., Theofilopoulos, A.N., Izui, S., Wilson, C.B., McConahey, P.J., Murphy, E.D., Roths, J.B. and Dixon, F.J. (1978). Spontaneous murine lupus-like syndromes. Clinical and immunopathological manifestations in several strains. Journal of Experimental Medicine. 148: 1198-1215.

74. Steinberg, A.D., Raveché, E.S., Laskin, C.A., Smith, H.R., Santoro, T., Miller, M.L. and Plotz, P.H. (1984). NIH conference. Systemic lupus erythematosus: insights from animal models. Annals of Internal Medicine. 100: 714-727.

75. Roths, J.B., Murphy, E.D. and Eicher, E.M. (1984). A new mutation, gld, that produces lymphoproliferation and autoimmunity in C3H/HeJ mice. Journal of Experimental Medicine. 159: 1-20.

76. Tsao, B.P., Cantor, R.M., Kalunian, K.C., Chen, C.J., Badsha, H., Singh, R., Wallace, D.J., Kitridou, R.C., Chen, S.L., Shen, N., Song, Y.W., Isenberg, D.A., Yu, C.L., Hahn, B.H. and Rotter, J.I. (1997). Evidence for linkage of a candidate

chromosome 1 region to human systemic lupus erythematosus. Journal of Clinical Investigation. 99: 725-731.

77. Moser, K.L., Neas, B.R., Salmon, J.E., Yu, H., Gray-McGuire, C., Asundi, N., Bruner, G.R., Fox, J., Kelly, J., Henshall, S., Bacino, D., Dietz, M., Hogue, R., Koelsch, G., Nightingale, L., Shaver, T., Abdou, N.I., Albert, D.A., Carson, C., Petri, M., Treadwell, E.L., James, J.A. and Harley, J.B. (1998). Genome scan of human systemic lupus erythematosus: evidence for linkage on chromosome 1q in African-American pedigrees. Proceedings of the National Academy of Sciences of the United States of America. 95: 14869-14874.

78. Gaffney, P.M., Kearns, G.M., Shark, K.B., Ortmann, W.A., Selby, S.A., Malmgren, M.L., Rohlf, K.E., Ockenden, T.C., Messner, R.P., King, R.A., Rich, S.S. and Behrens, T.W. (1998). A genome-wide search for susceptibility genes in human systemic lupus erythematosus sib-pair families. Proceedings of the National Academy of Sciences of the United States of America. 95: 14875-14879.

79. Harley, J.B., Moser, K.L., Gaffney, P.M. and Behrens, T.W. (1998). The genetics of human systemic lupus erythematosus. Current Opinion in Immunology. 10: 690-696.

80. Gu, H., Zou, Y.R. and Rajewsky, K. (1993). Independent control of immunoglobulin switch recombination at individual switch regions evidenced through Cre-loxP-mediated gene targeting. Cell. 73: 1155-1164.

81. Mansour, S.L., Thomas, K.R. and Capecchi, M.R. (1988). Disruption of the proto-oncogene int-2 in mouse embryo-derived stem cells: a general strategy for targeting mutations to non-selectable genes. Nature. 336: 348-352.

82. Ramírez-Solis, R., Davis, A.C. and Bradley, A. (1993). Gene targeting in embryonic stem cells. Methods in Enzymology. 225: 855-878.

83. Hogan, B. 1994. Manipulating the mouse embryo : a laboratory manual. 2nd ed. [Plainview, N.Y.]: Cold Spring Harbor Laboratory Press.

84. Lewandoski, M. and Martin, G.R. (1997). Cre-mediated chromosome loss in mice. Nature Genetics. 17: 223-225.

85. Wofsy, D. and Seaman, W.E. (1985). Successful treatment of autoimmunity in NZB/NZW F1 mice with monoclonal antibody to L3T4. Journal of Experimental Medicine. 161: 378-391.

86. Thude, H., Hundrieser, J., Wonigeit, K. and Schwinzer, R. (1995). A point mutation in the human CD45 gene associated with defective splicing of exon A. European Journal of Immunology. 25: 2101-2106.

87. Zilch, C.F., Walker, A.M., Timón, M., Goff, L.K., Wallace, D.L. and Beverley, P.C. (1998). A point mutation within CD45 exon A is the cause of variant CD45RA splicing in humans. European Journal of Immunology. 28: 22-29.

88. den Hertog, J., Blanchetot, C., Buist, A., Overvoorde, J., van der Sar, A. and Tertoolen, L.G. (1999). Receptor protein-tyrosine phosphatase signalling in development. International Journal of Developmental Biology. 43: 723-733.

89. Desai, C.J., Gindhart, J.G., Jr., Goldstein, L.S. and Zinn, K. (1996). Receptor tyrosine phosphatases are required for motor axon guidance in the Drosophila embryo. Cell. 84: 599-609.

90. Desai, C.J., Krueger, N.X., Saito, H. and Zinn, K. (1997). Competition and cooperation among receptor tyrosine phosphatases control motoneuron growth cone guidance in Drosophila. Development. 124: 1941-1952.

91. Krueger, N.X., Van Vactor, D., Wan, H.I., Gelbart, W.M., Goodman, C.S. and Saito, H. (1996). The transmembrane tyrosine phosphatase DLAR controls motor axon guidance in Drosophila. Cell. 84: 611-622.

92. Garrity, P.A., Lee, C.H., Salecker, I., Robertson, H.C., Desai, C.J., Zinn, K. and Zipursky, S.L. (1999). Retinal axon target selection in Drosophila is regulated by a receptor protein tyrosine phosphatase. Neuron. 22: 707-717.

93. Brady-Kalnay, S.M., Flint, A.J. and Tonks, N.K. (1993). Homophilic binding of PTP mu, a receptor-type protein tyrosine phosphatase, can mediate cell-cell aggregation. Journal of Cell Biology. 122: 961-972.

94. Gebbink, M.F., Zondag, G.C., Wubbolts, R.W., Beijersbergen, R.L., van Etten, I. and Moolenaar, W.H. (1993). Cell-cell adhesion mediated by a receptor-like protein tyrosine phosphatase. Journal of Biological Chemistry. 268: 16101-16104.

95. Sap, J., Jiang, Y.P., Friedlander, D., Grumet, M. and Schlessinger, J. (1994). Receptor tyrosine phosphatase R-PTP-kappa mediates homophilic binding. Molecular and Cellular Biology. 14: 1-9.

96. Peles, E., Schlessinger, J. and Grumet, M. (1998). Multi-ligand interactions with receptor-like protein tyrosine phosphatase beta: implications for intercellular signaling. Trends in Biochemical Sciences. 23: 121-124.

97. Peles, E., Nativ, M., Campbell, P.L., Sakurai, T., Martinez, R., Lev, S., Clary, D.O., Schilling, J., Barnea, G., Plowman, G.D. and et al. (1995). The carbonic anhydrase domain of receptor tyrosine phosphatase beta is a functional ligand for the axonal cell recognition molecule contactin. Cell. 82: 251-260.

98. Meng, K., Rodriguez-Peña, A., Dimitrov, T., Chen, W., Yamin, M., Noda, M. and Deuel, T.F. (2000). Pleiotrophin signals increased tyrosine phosphorylation of beta beta-catenin through inactivation of the intrinsic catalytic activity of the receptor-type protein tyrosine phosphatase beta/zeta. Proceedings of the National Academy of Sciences of the United States of America. 97: 2603-2608.

99. Blakely, B.T., Rossi, F.M., Tillotson, B., Palmer, M., Estelles, A. and Blau, H.M. (2000). Epidermal growth factor receptor dimerization monitored in live cells. Nature Biotechnology. 18: 218-222.

100. Maxwell, A. (1993). The interaction between coumarin drugs and DNA gyrase. Molecular Microbiology. 9: 681-686.

101. Farrar, M.A., Alberol, I. and Perlmutter, R.M. (1996). Activation of the Raf-1 kinase cascade by coumermycin-induced dimerization [see comments]. Nature. 383: 178-181.

102. Ley, S.C., Marsh, M., Bebbington, C.R., Proudfoot, K. and Jordan, P. (1994). Distinct intracellular localization of Lck and Fyn protein tyrosine kinases in human T lymphocytes. Journal of Cell Biology. 125: 639-649.

103. Minami, Y., Stafford, F.J., Lippincott-Schwartz, J., Yuan, L.C. and Klausner, R.D. (1991). Novel redistribution of an intracellular pool of CD45 accompanies T cell activation. Journal of Biological Chemistry. 266: 9222-9230.

104. Carrera, A.C., Li, P. and Roberts, T.M. (1991). Characterization of an active, non-myristylated, cytoplasmic form of the lymphoid protein tyrosine kinase pp56lck. International Immunology. 3: 673-682.

105. Simons, K. and Ikonen, E. (1997). Functional rafts in cell membranes. Nature. 387: 569-572.

106. Xavier, R., Brennan, T., Li, Q., McCormack, C. and Seed, B. (1998). Membrane compartmentation is required for efficient T cell activation. Immunity. 8: 723-732.

107. Lin, J., Weiss, A. and Finco, T.S. (1999). Localization of LAT in glycolipid-enriched microdomains is required for T cell activation. Journal of Biological Chemistry. 274: 28861-28864.

108. Kabouridis, P.S., Magee, A.I. and Ley, S.C. (1997). S-acylation of LCK protein tyrosine kinase is essential for its signalling function in T lymphocytes. Embo Journal. 16: 4983-4998.

109. Rodgers, W. and Rose, J.K. (1996). Exclusion of CD45 inhibits activity of p56lck associated with glycolipid-enriched membrane domains. Journal of Cell Biology. 135: 1515-1523.

110. Xu, H. and Littman, D.R. (1993). A kinase-independent function of Lck in potentiating antigen-specific T cell activation. Cell. 74: 633-643.

111. Xu, H. and Littman, D.R. (1995). The kinase-dependent function of Lck in T-cell activation requires an intact site for tyrosine autophosphorylation. Annals of the New York Academy of Sciences. 766: 99-116.

112. Zhang, W., Trible, R.P. and Samelson, L.E. (1998). LAT palmitoylation: its essential role in membrane microdomain targeting and tyrosine phosphorylation during T cell activation. Immunity. 9: 239-246.